A Differential Requirement for Cdc48/p97 and Protein Chaperones in Nuclear Protein Quality Control Degradation

Pamela Sue Gallagher

A dissertation
submitted in partial fulfillment of the
requirements for the degree of

Doctor of Philosophy

University of Washington
2013

Reading Committee:
Richard Gardner, Chair
Maitreya Dunham
Chris Hague

Program Authorized to Offer Degree:
Pharmacology

University of Washington

Abstract

A Differential Requirement for Cdc48/p97 and Protein Chaperones in Nuclear Protein Quality Control Degradation

Pamela Sue Gallagher

Chair of Supervisory Committee:

Assistant Professor Richard Gardner

Department of Pharmacology

The ubiquitin-proteasome system is one of the principal means for the destruction of misfolded proteins in the cell. In addition to the core enzymes within the ubiquitination cascade and the 26S proteasome, many ancillary factors function to maintain protein homeostasis. For example, Cdc48/p97 is an abundant AAA-ATPase essential for many critical ubiquitin-dependent processes. One well-documented role for Cdc48 is facilitating the delivery of ubiquitinated misfolded endoplasmic-reticulum proteins to the proteasome for degradation. By contrast, Cdc48's participation in misfolded nuclear protein degradation is unknown. In yeast, degradation of misfolded nuclear proteins is mediated by the ubiquitin-protein ligase San1. The results presented here reveal that although Cdc48 and cofactors are involved in the degradation of some San1 substrates, they are not universally required for all San1 substrates. The differential Cdc48 requirement correlates with San1 substrate insolubility: the more insoluble the substrate, the more its degradation requires Cdc48. Expression of Cdc48-dependent insoluble San1 substrates in mutant *cdc48* cells results in increased substrate insolubility, greater inclusion formation, and reduced cell viability. We propose that Cdc48 functions to maintain ubiquitinated substrate solubility en route to the proteasome, preventing toxic aggregation from occurring post-ubiquitination. Additionally, the requirement for protein chaperones for San1-mediated degradation also correlates with substrate insolubility. This work illuminates insolubility as a key determinant for Cdc48 and chaperone involvement in the San1 degradation pathway.

TABLE OF CONTENTS

LIST OF ABBREVIATIONS

PQC Protein quality control

HECT Homologous to the E6-AP carboxyl terminus

RING Really interesting new gene

ER Endoplasmic reticulum

NLS Nuclear localization signal

AAA-ATPase ATPase associated with a variety of cellular activities

IBMPFD Inclusion body myopathy associated with Paget's disease of bone and frontotemporal dementia

ALS Amyotrophic lateral sclerosis

GFP Green fluorescent protein

GAD Gal4 activation domain

UBX Ubiquitin regulatory X

ERAD ER-associated degradation

UPR Unfolded protein response

LIST OF FIGURES

Figure Number

PREFACE

A large portion of the data and text in Chapters II, III and IV of this dissertation is derived from the following publications:

Gallagher PS and Gardner RG. Requirement for Cdc48/p97 in nuclear protein quality control degradation correlates with misfolded substrate insolubility. *Manuscript submitted for review*.

Fredrickson EK, Gallagher PS, Clowes Candadai SV, Gardner RG. Chaperone involvement in nuclear protein quality control degradation is substrate dependent. *Manuscript submitted for review.*

Fredrickson EK, Gallagher PS, Clowes Candadai SV, Gardner RG. Substrate recognition in nuclear protein quality control degradation is governed by exposed hydrophobicity that correlates with aggregation and insolubility. *J Biol Chem*. 2013 Jan 18.

ACKNOWLEDGEMENTS

I would first like to thank Dr. Richard Gardner for being an extremely dedicated and compassionate mentor. His guidance throughout my graduate career has helped me to become an independent thinker and enthusiastic scientist. I greatly appreciate him challenging me over the years to think carefully about each experiment, yet never lose sight of the "big picture." I thank Dr. Richard Gardner, Dr. Maitreya Dunham, Dr. Chris Hague, Dr. Matt Kaeberlein, Dr. Debra Schwinn, and Dr. Ning Zheng for their scientific input and support as my supervisory committee. I would like to acknowledge the past and present members of the Gardner lab for creating an incredibly fun and creative work environment. In particular, a special thanks goes out to my fellow graduate students Eric Fredrickson, Michelle Oeser, Ben Reed, Joel Rosenbaum, and Lauren Richardson, as well as lab managers Sarah Clowes and Melissa Locke. Finally, I would like to thank my friends and family for their encouragement and unconditional love. I cannot explain how much they mean to me.

DEDICATION

To my loving and supportive parents, Bishop and Sue.

CHAPTER I: BACKGROUND AND SIGNIFICANCE

It is essential for the viability of all organisms that individual proteins accomplish particular tasks in the cell. In order for proteins to function properly, they must acquire specific three-dimensional confirmations. However, proteins are vulnerable to misfolding events triggered by genetic mutations, translational errors, or environmental stressors. The cell continuously encounters abnormal proteins but is equipped with quality control mechanisms to protect itself from the potentially deleterious consequences of protein misfolding. If not properly managed, abnormal or misfolded proteins can accumulate and possibly aggregate, leading to cellular toxicity. The importance of correct protein folding in the cell is evidenced by the identification of over thirty-five age-dependent neurodegenerative disorders in humans characterized pathologically by the aggregation of misfolded proteins. Prominent examples of protein aggregation diseases include Parkinson's, Alzheimer's, and Huntington's diseases (Wang et al., 2008).

When the cell encounters a defective protein, it can employ a number of protein quality control (PQC) systems to either repair or degrade the misfolded substrate. Protein chaperones are the principal components that refold or sequester misfolded substrates (Stirling et al., 2003). If the misfolding is severe, the cell may eradicate the damaged protein rather than attempting to repair it (Goldberg, 2003). This may be accomplished by autophagy, lysosomal degradation, or ubiquitin-mediated proteolysis. In the following chapters, I will

focus primarily on the ubiquitin-proteasome pathway for PQC degradation, though I will present some data on chaperone involvement in PQC in Chapter IV.

Ubiquitination enzymatic cascade

Ubiquitin is a highly conserved 8.5 kDa protein that received its name for being ubiquitously expressed in all eukaryotic cells (Goldstein et al., 1975). Ubiquitination, the process of attaching ubiquitin to target proteins, is a posttranslational modification that regulates a myriad of cellular processes. Covalent attachment of ubiquitin to a target protein can affect a substrate's stability, localization, activity, or interactions with other proteins in the cell. Ubiquitin is typically attached to lysine residues in its target protein as a single unit or as polyubiquitin chains. A ubiquitin molecule contains seven lysine residues, which allows for numerous types of linkages between ubiquitin moieties within a chain (Glickman and Ciechanover, 2002).

Ubiquitin is covalently attached to its target substrates via a conserved enzymatic cascade. First, ubiquitin is activated by a ubiquitin-activating enzyme (or E1) in an ATP-dependent reaction. The E1 forms a high-energy thioester linkage with a single ubiquitin molecule. Following activation, ubiquitin is transferred to a ubiquitin conjugating enzyme (or E2). The E2 partners with a specific ubiquitin-protein ligase (or E3) to facilitate transfer of the charged ubiquitin to the substrate. Depending on the E3 involved, ubiquitin can be transferred onto its target substrate in one of two ways. If the

E3 contains a HECT domain (Homologous to the E6-AP carboxyl terminus), an E3-ubiquitin intermediate is formed with the ligase before ubiquitin is attached to the substrate. However, if the E3 possesses a RING (really interesting new gene) domain, the E3 mediates direct transfer from the E2.

The E3 is thought to confer substrate specificity via intrinsic interaction domains or recruitment of ancillary factors. Importantly, ubiquitin can be removed from a protein via the action of deubiquitinating enzymes. Thus, ubiquitination is a highly dynamic, reversible process within the cell (Glickman and Ciechanover, 2002).

The types of linkages within polyubiquitin chains can determine the physiological fate of a protein. For example, linkages originating at lysine 63 (K63) in ubiquitin chains can affect the localization of the target protein and regulate DNA repair (Spence et al., 1995). Lysine 11 (K11) linkages are suggested to play a critical role in cell cycle control in the degradation of cyclins and other key cell-cycle control proteins (Matsumoto et al., 2010). One of the more thoroughly studied ubiquitin linkages occurs at lysine 48 (K48), which targets proteins for degradation by the 26S proteasome (Thrower et al., 2000).

Ubiquitin-proteasome system

Polyubiquitination of at least four K48-linked ubiquitin moieties shuttles proteins to the 26S proteasome, a multisubunit proteolytic apparatus responsible for degrading proteins. The ubiquitin chain functions as a recognition signal for

the barrel-shaped proteasome (Thrower et al., 2000). Following ubiquitin chain cleavage, the substrate is threaded into the core of the 26S proteasome where it is degraded by peptidases into small peptides. Once released from the degradation machinery, the peptides can be further degraded into amino acids and recycled for *de novo* synthesis of new proteins (Finley et al., 2012).

The proteasome is highly enriched in the nucleus and the cytosol (Wojcik and DeMartino, 2003). The cytoplasm is the location of protein synthesis, and it is estimated that nearly one-third of nascent polypeptides are defective and immediately destroyed (Schubert et al., 2000). This suggests that cytosolic quality control degradation and protein synthesis may be intimately connected. Because postproduction damage can occur anywhere in the cell, additional subcellular compartments are equipped with PQC machinery to combat protein misfolding. For example, misfolded proteins in the endoplasmic reticulum (ER) are targeted for ubiquitination by ER-localized E3s and subsequently delivered to cytosolic proteasomes to be degraded (Hampton, 2002). Similarly, misfolded mitochondrial proteins are ubiquitinated by E3s associated with the outer mitochondrial membrane, then sent to the degradation machinery in the cytoplasm (Taylor and Rutter, 2011).

The nucleus and the challenges it faces

In contrast to the cytosol, ER, and mitochondria, far less is known about the quality control systems that maintain protein homeostasis within the nucleus. We now know the nucleus contains PQC mechanisms, though the mechanisms

involved remain poorly understood. Because the nucleus is where the DNA is harbored and packaged as chromatin, PQC mechanisms may be necessary to protect the chromatin environment.

In addition to housing the genetic material, the nucleus is home to many subcellular compartments. The nucleolus is localized within the cell nucleus, and is the hub of ribosome biogenesis. Cajal bodies are also implicated in many RNA-related functions, including snRNP biogenesis, mRNA processing, and telomere maintenance (Gall et al., 1999; Zhao et al., 2011). PML bodies, or nuclear dots, are punctate structures that are associated with transcriptional activation (Xie et al., 1993). Nuclear lamins provide the architecture of the nucleus and are involved in an array of nuclear functions, including transcription, DNA replication, and DNA repair (Dittmer and Misteli, 2011). Taken together, the nucleus is presented with a unique set of challenges to maintain the integrity of many distinct subcellular compartments that are vital to every cell.

Misfolded proteins may appear in the cell nucleus from a couple of different routes. Nuclear localization sequence (NLS) containing proteins synthesized in the cytosol are trafficked to the nucleus, where they can become damaged. On the other hand, nuclear pores can break down as a consequence of aging, and thus become more permissive to cytosolic damaged proteins leaking in to the nucleus (D'Angelo et al., 2009). Importantly, the nucleus appears particularly sensitive to protein misfolding, as many protein aggregation diseases correlate with abnormal proteins accumulating in the nucleus (Woulfe, 2007).

San1-mediated nuclear protein quality control degradation

Recently, San1 has been characterized as a principal E3 targeting misfolded nuclear proteins in *Saccharomyces cerevisiae* for destruction via the ubiquitin-proteasome system (Gardner et al., 2005). San1 was initially identified for its ability to suppress two independent temperature-sensitive phenotypes (Schnell et al., 1989; Xu et al., 1993). These findings led to the discovery that San1 is the major E3 for quality control degradation in the nucleus (Gardner et al., 2005). San1 is a RING domain E3 that recognizes a variety of misfolded nuclear proteins. Interestingly, San1 is an intrinsically disordered protein, which may enable recognition of many abnormal protein confirmations in the nuclear environment (Rosenbaum et al., 2011). The unifying characteristic among San1's substrates was determined to be exposed hydrophobicity (Fredrickson et al., 2011). Because exposed hydrophobicity can promote aggregation associated with cellular toxicity, this underscores the value of San1 function.

San1 partners with the E2s Cdc34 and Ubc1 (Gardner et al., 2005), however, it was not known if any ancillary factors facilitated nuclear PQC degradation. Additional components that function in the pathway for nuclear quality control degradation remained yet to be discovered. In contrast to other E3s, San1 does not require protein chaperones to function *in vitro* (Rosenbaum et al., 2011). We were interested in determining if any auxiliary factors functioned in the San1 pathway *in vivo*. I focused on an AAA-ATPase (ATPase associated with a variety of cellular activities) called Cdc48/p97. The data in the

following chapters demonstrate a surprising differential involvement of Cdc48 in the San1 degradation pathway, and characterize several adaptors that associate with the Cdc48 complex to facilitate nuclear PQC. We also establish differential chaperone involvement in San1-mediated degradation, which parallels our findings for Cdc48's role in the proteolysis of misfolded substrates in the nucleus.

CHAPTER II: CDC48 IS DIFFERENTIALLY INVOLVED IN SAN1-MEDIATED DEGRADATION

Introduction on Cdc48/p97

In the pathway for destruction via the ubiquitin-proteasome, a key AAA-ATPase, known as p97/VCP in mammals and Cdc48 in budding yeast, often acts between the E3 and the proteasome to facilitate ubiquitinated-substrate delivery to the proteasome (Meyer et al., 2012; Yamanaka et al., 2012). In yeast, Cdc48 was first discovered in a genetic analysis to identify proteins required for cell-cycle progression (Moir et al., 1982), and was later found to be homologous to human p97 (Frohlich et al., 1991). In the three decades since Cdc48's discovery, its function in eukaryotes has been extended well beyond regulating the cell cycle to a multitude of ubiquitin-dependent pathways including protein degradation, membrane fusion, and chromatin-associated processes (Dantuma and Hoppe, 2012; Meyer et al., 2012; Ye, 2006).

Cdc48's involvement in many crucial cellular functions underscores its importance in the cell. The human relevance of Cdc48/p97 is highlighted by pathologies caused by or correlated with mutations in p97 (Nalbandian et al., 2012). For example, autosomal-dominant mutations in p97 cause the devastating, age-dependent, degenerative disorder termed inclusion body myopathy associated with Paget's disease of bone and frontotemporal dementia (IBMPFD) (Watts et al., 2004). A subset of mutations in p97 also account for 1-

2% of familial amyotrophic lateral sclerosis (ALS) cases (Johnson et al., 2010). More recently, it has been suggested that augmented levels of p97 are correlated with several human cancers and associated with poor prognoses (Lague et al., 2012; Yamamoto et al., 2004; Yamamoto et al., 2005).

Cdc48's main cellular role is thought to be a segregase (Braun et al., 2002). In this capacity, Cdc48 segregrates ubiquitinated proteins from protein complexes, chromatin, or membranes (Jentsch and Rumpf, 2007). The best-studied segregase function of Cdc48 is its key role in PQC degradation in the ER (Wolf and Stolz, 2012). Following the ubiquitination of misfolded ER proteins, Cdc48 extracts ubiquitinated proteins from the ER membrane and targets them for degradation by cytoplasmic proteasomes (Bays et al., 2001; Elkabetz et al., 2004; Huyer et al., 2004; Jarosch et al., 2002; Rabinovich et al., 2002; Richly et al., 2005; Schuberth and Buchberger, 2005; Taxis et al., 2003; Ye et al., 2001). The PQC degradation role of Cdc48 has also been extended to the mitochondria (Taylor and Rutter, 2011). Following oxidative stress, Cdc48 acts at the outer mitochondrial membrane to assist in removing ubiquitinated mitochondrial proteins for presentation to cytoplasmic proteasomes (Heo et al., 2010). While the cellular pool of proteasomes is cytoplasmic and nuclear in large part (Wojcik and DeMartino, 2003), Cdc48's involvement in mediating the PQC degradation of misfolded proteins in the cytoplasm and nucleus is poorly understood.

Background on substrate selection

In our previous studies (Fredrickson et al., 2011; Gardner et al., 2005; Rosenbaum et al., 2011), we identified >40 substrates of San1 representing a broad variety of misfolded nuclear proteins likely to be encountered by San1 in the nucleus. The first San1 substrates we identified are proteins that carry single missense mutations that lead to their San1-dependent degradation and loss of function (Gardner et al., 2005). Later, through a yeast 2-hybrid analysis, we discovered proteins with truncations that are San1 substrates due to their truncation-induced misfolding (Rosenbaum et al., 2011). Through similar yeast 2-hybrid analyses, we identified small hydrophobic peptides that act as degrons and lead to the San1-mediated degradation of the reporter proteins to which they are fused (Fredrickson et al., 2011). Using these different classes of San1 substrates, we could thoroughly explore if Cdc48 is universally required for San1-mediated nuclear PQC degradation.

To do this, I examined the degradation of representative examples of each class of San1 substrate in cells deficient for Cdc48 function. For truncated proteins, I used GFP^{NLS}-Tef2*, which contains residues 190-458 of the translation elongation factor Tef2 fused to GFP carrying an NLS, and GFP^{NLS}-Bgl2*, which contains residues 20-313 of the endo-beta-1,3-glucanase Bgl2 fused to GFP^{NLS} (Rosenbaum et al., 2011). For the hydrophobic peptide degrons, I used Peptide 6 (RDILVYTYILVYVYI) and Peptide I (RETGWRVLLVVVGVVGIP) fused to GFP^{NLS} (Fredrickson et al., 2011). For missense mutant proteins, I used constructs carrying the self-contained N-terminal domains of Cdc68-1, which has

the point mutation G132D (Evans et al., 1998), and Cdc13-1, which has the point mutation P371S (Nugent et al., 1996), fused to the Gal4 activation domain (GAD) (Rosenbaum et al., 2011). Both of these mimic the San1-dependent degradation seen with unaltered Cdc13-1 and Cdc68-1 proteins (Gardner et al., 2005; Rosenbaum et al., 2011).

Cdc48 is differentially involved in the degradation of San1 substrates

If Cdc48 were a general San1 pathway factor, we expected it would be required for the degradation of all San1 substrates. I found this was not the case, and that there was wide variability for Cdc48 involvement within the San1 pathway. For some substrates, I found that Cdc48 was essential for San1-mediated degradation, as was seen by the stabilization of GFP^{NLS}-Tef2* and GFP^{NLS}-Bgl2* in *cdc48-3* mutant cells that was as great as the stabilization seen in *san1*Δ cells. In other cases, I found that Cdc48 was partially involved in San1-mediated degradation, as was seen by the incomplete stabilization of GFP^{NLS}-Peptide 6, GFP^{NLS}-Peptide I, and GAD-Cdc68-1 in *cdc48-3* cells compared with *san1*Δ cells. Lastly, I found that some San1 substrates did not utilize Cdc48 for their San1-mediated degradation, as was seen by the lack of stabilization of GAD-Cdc13-1 in *cdc48-3* cells compared with *san1*Δ cells (Figure 2.1). Taken together, these data indicated that the requirement for Cdc48 in the degradation of San1 substrates is not universal but exists on a spectrum that depends upon some feature of the substrate.

We realized a couple of potential caveats to these studies that needed to be examined in order to rule out confounding effects. First, the substrates that showed complete dependency on Cdc48 for degradation, GFP^{NLS}-Tef2* and GFP^{NLS}-Bgl2*, were highly expressed from the galactose-inducible *GAL1* promoter, which is one of the strongest promoters in yeast. I needed to express these substrates from an inducible promoter due to the fact that they are toxic in *san1*Δ cells (Rosenbaum et al., 2011) and *cdc48-3* cells (see Figure 2.14), and thus cannot be expressed from a constitutive promoter in these genetic backgrounds. It is therefore possible that the high expression of these substrates forced a dependency on Cdc48 that wouldn't be observed under lower expression conditions. We didn't think this likely due to the fact that other substrates, GFP^{NLS}-Peptide 6 and GFP^{NLS}-Peptide I, were also expressed from the *GAL1* promoter and did not show complete dependency on Cdc48. Nevertheless, I did examine if reduced expression of GFP^{NLS}-Tef2* and GFP^{NLS}-Bgl2* altered their Cdc48 dependency. In both cases, I found that the Cdc48 dependency under lower expression conditions (using decreased amounts of galactose for induction) was similar to the dependency under the greater expression conditions (Figure 2.2), ruling out this possibility. Secondly, it is possible that the GFP^{NLS} fusion protein is degraded in a Cdc48-dependent manner and it imposes this requirement on the misfolded protein to which it is fused. However, I verified that GFP^{NLS} is a stable protein (Figure 2.3), eliminating this possibility. Thus, the Cdc48 dependency of each San1 substrate depends upon some defining feature of the misfolded protein fusion itself.

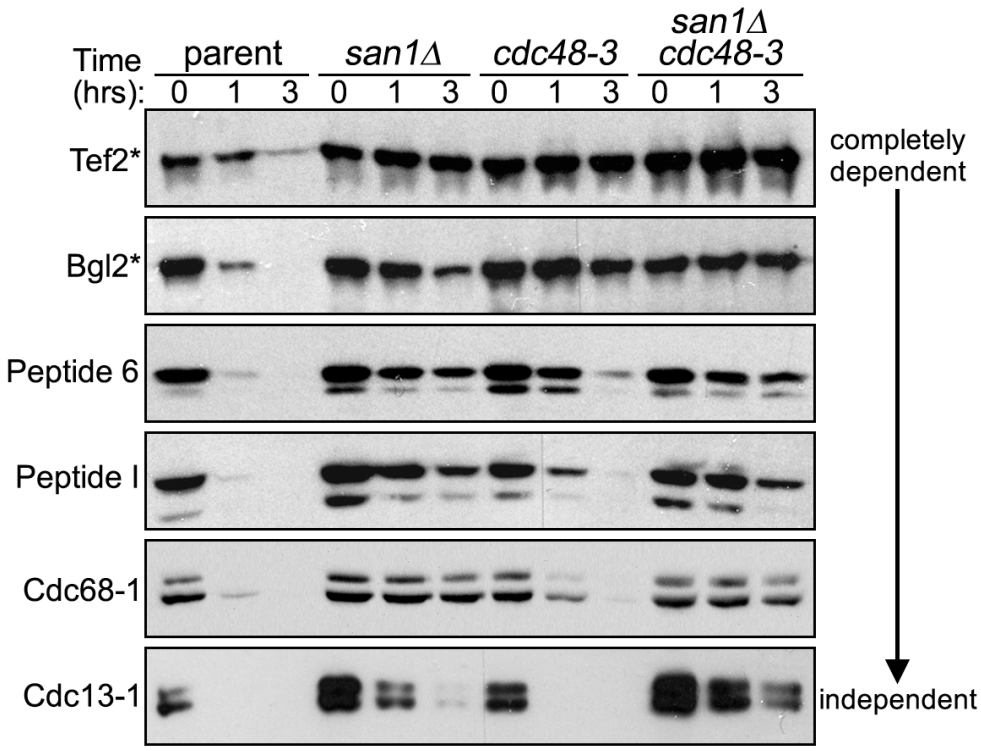

Figure 2.1: Cdc48 is differentially involved in the degradation of San1 substrates. Cycloheximide-chase degradation assays were performed on parent, *san1*Δ, *cdc48-3*, and *san1*Δ*cdc48-3* cells to assess the stability of GFP^{NLS}-Tef2*, GFP^{NLS}-Bgl2*, GFP^{NLS}-Peptide 6, GFP^{NLS}-Peptide I, GAD-Cdc68-1, and GAD-Cdc68-1. For the GFP^{NLS}-substrates expressed from the *GAL1* promoter, expression was induced by addition of galactose for 2 hours prior to cycloheximide addition. For the GAD-substrates, expression from the *ADH1* promoter was constitutive. Cell cultures were shifted from 25˚C to 37˚C after cycloheximide addition to inactivate *cdc48-3*. Time after cycloheximide addition is indicated above each lane. Anti-GFP or anti-GAD antibodies were used to detect each appropriate substrate.

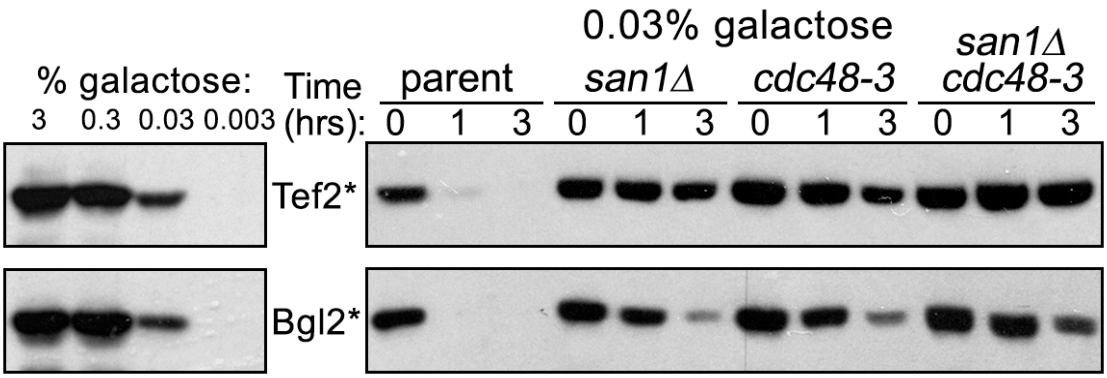

Figure 2.2: Cdc48 dependency is not altered under low substrate expression conditions. Cycloheximide-chase degradation assays were performed on parent, *san1*Δ, *cdc48-3*, and *san1*Δ*cdc48-3* cells to assess the stability of GFP^{NLS}-Tef2* and GFP^{NLS}-Bgl2* under reduced expression conditions. Left panels are the expression of each substrate after 2 hours of induction using the indicated final concentration of galactose. Right panel is the degradation assays performed using 0.03% galactose to induce expression for 2 hours prior to cycloheximide addition. Cell cultures were shifted from 25˚C to 37˚C after cycloheximide addition to inactivate *cdc48-3*. Time after cycloheximide addition is indicated above each lane. Anti-GFP antibodies were used to detect each substrate.

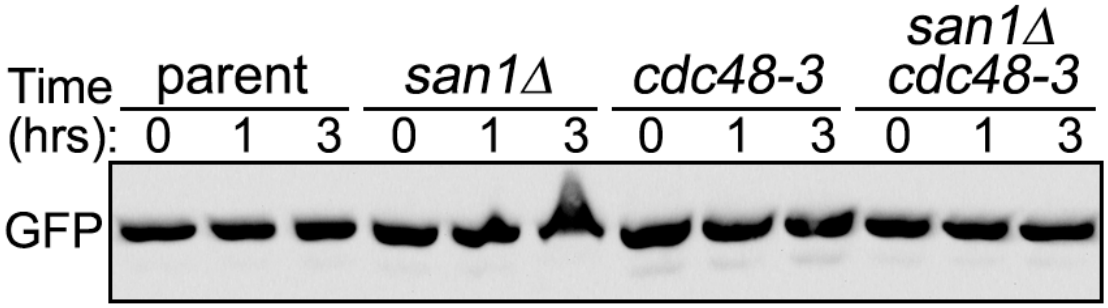

Figure 2.3: GFP^{NLS} is a stable protein. Cycloheximide-chase degradation assays were performed on parent, *san1*Δ, *cdc48-3*, and *san1*Δ*cdc48-3* cells to assess the stability of GFP^{NLS}. Anti-GFP antibodies were used to detect GFP^{NLS}.

Loss of Cdc48 function leads to increased substrate ubiquitination

After establishing that a subset of San1 substrates depends upon Cdc48 for degradation, we wanted to understand whether Cdc48 functions prior to or after San1-mediated degradation. If prior, we expected to see a decrease in substrate ubiquitination in *cdc48-3* cells. If after, we anticipated an increase in substrate ubiquitination in *cdc48-3* cells. I performed assays to assess the levels of GFP^{NLS}-Tef2* and GFP^{NLS}-Peptide 6 ubiquitination in parent, *san1*Δ, and *cdc48-3* strains to examine this feature of Cdc48 action. As expected from San1's E3 activity, we observed decreased levels of GFP^{NLS}-Tef2* and GFP^{NLS}-Peptide 6 ubiquitination in *san1*Δ cells compared with parent cells (Figure 2.4). On the other hand, we observed enhanced levels of GFP^{NLS}-Tef2* and GFP^{NLS}-Peptide 6 ubiquitination in mutant *cdc48-3* cells compared with parent cells (Figure 2.4). These results indicated that Cdc48 likely acts at a step prior to the proteasome and presumably after San1 ubiquitination. To see if this were the case, I focused on GFP^{NLS}-Tef2* and performed the assay again this time after inhibiting the proteasome with the addition of MG132. Proteasome inhibition led to greater levels of ubiquitinated substrate in parent cells as expected and this increase in ubiquitination was comparable to what was observed in *cdc48-3* cells without proteasome inhibition (Figure 2.5). We did not observe any increase in substrate ubiquitination in *cdc48-3* cells with MG132 (Figure 2.5). Interestingly, the overall size of the ubiquitin conjugates observed in parent cells after proteasome inhibition appeared smaller than the size of the ubiquitin conjugates in *cdc48-3* cells with or without proteasome inhibition (Figure 2.5). These

observations suggest that Cdc48 could be acting in a ubiquitin-chain editing capacity prior to delivery of the substrate to the proteasome.

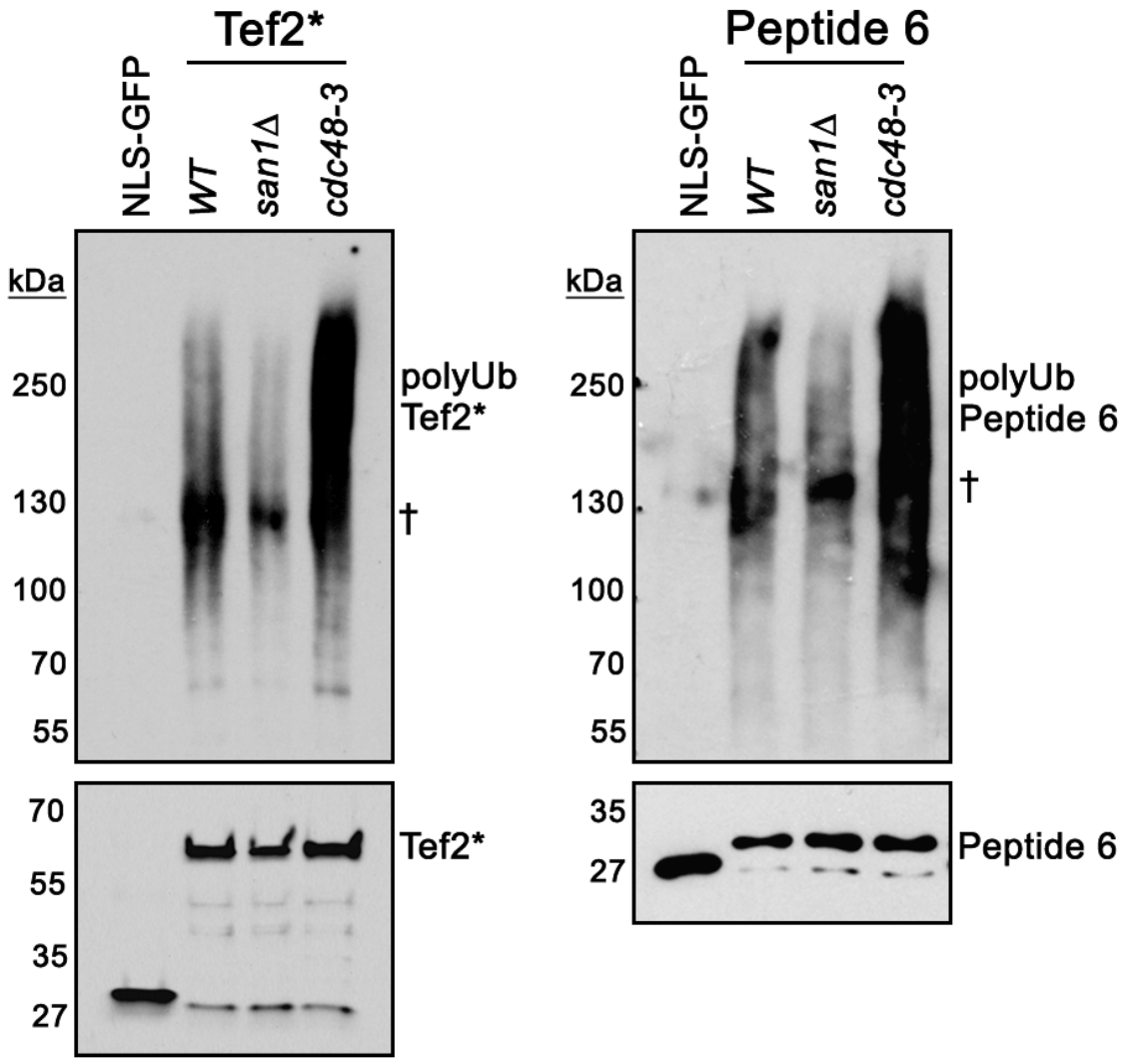

Figure 2.4: Substrate ubiquitination is increased in *cdc48* mutant cells. Ubiquitination assays were performed to examine levels of ubiquitinated GFP^{NLS}-Tef2* or GFP^{NLS}-Peptide 6 in parent, *san1*Δ, and *cdc48-3* cells expressing 3HA-ubiquitin. GFP^{NLS}-Tef2* and GFP^{NLS}-Peptide 6 expression was induced by addition of galactose for 2 hours in log phase. Cells were shifted to 37˚C 1 hour prior to lysis to inactivate *cdc48-3*. GFP^{NLS}, GFP^{NLS}-Tef2*, or GFP^{NLS}-Peptide 6 was immunoprecipitated from cell lysates using anti-GFP antibodies. Blots of the immunoprecipitates were probed with anti-HA antibodies to detect ubiquitin (top panels) or anti-GFP antibodies to assess GFP^{NLS}, GFP^{NLS}-Tef2*, or GFP^{NLS}-Peptide 6 levels (bottom panels). "†" indicates cross-reacting antibody band.

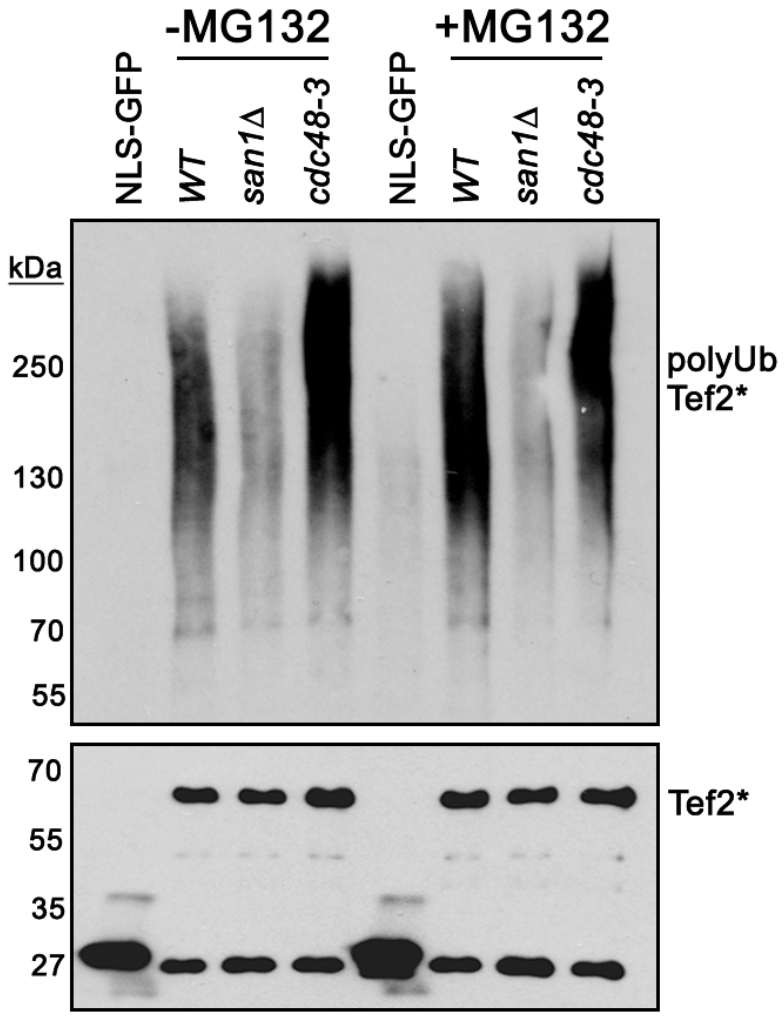

Figure 2.5: Substrate ubiquitination is increased in parent cells but not in *cdc48* mutant cells with proteasome inhibition. Ubiquitination assays were performed to assess levels of ubiquitinated GFP^{NLS}-Tef2* in parent, *san1*Δ, and *cdc48-3* cells in the presence or absence of MG132. GFP^{NLS}-Tef2* expression was induced by addition of galactose for 2 hours in log phase. Cells were shifted to 37˚C 1 hour prior to lysis to inactivate *cdc48-3*. Cells were treated with 50 µg/ml MG132 for 1 hour prior to lysis. GFP^{NLS} or GFP^{NLS}-Tef2* was immunoprecipitated from cell lysates using anti-GFP antibodies. Blots of the immunoprecipitates were probed with anti-HA antibodies to detect ubiquitin (top panels) or anti-GFP antibodies to assess GFP^{NLS} or GFP^{NLS}-Tef2* levels (bottom panels).

Differential solubility of substrates correlates with Cdc48 dependency

Because the Cdc48 requirement for San1 substrate degradation was variable, we wanted to explore the underlying reason for this variability. Unlike PQC degradation in the ER, which requires Cdc48 as a means to extract ubiquitinated ER proteins from the ER membrane (Bays et al., 2001; Elkabetz et al., 2004; Huyer et al., 2004; Jarosch et al., 2002; Rabinovich et al., 2002; Richly et al., 2005; Schuberth and Buchberger, 2005; Taxis et al., 2003; Ye et al., 2001), San1 functions primarily in the nucleoplasm and nuclear substrate delivery to the proteasome would not have to contend with membrane extraction. Furthermore, the San1 substrates used in this study that require Cdc48, GFP^{NLS}-Tef2* and GFP^{NLS}-Bgl2*, are not chromatin-associated proteins and would not require extraction from chromatin as seen with RNA polymerase II or the transcriptional repressor alpha2 (Verma et al., 2011; Wilcox and Laney, 2009). Cdc48/p97 does have chaperone activity *in vitro* and can prevent the aggregation of denatured luciferase (Song et al., 2007). We surmised that Cdc48's role in San1-mediated degradation might be to prevent or reverse the aggregation of San1 substrates in transit to the proteasome. If true, we suspected that the requirement for Cdc48 in San1-mediated degradation might correlate with the intrinsic insolubility of the San1 substrate. That is, the more insoluble the substrate the greater the need for Cdc48.

To examine substrate solubility, I performed sedimentation assays on San1 substrates to determine how they partitioned between soluble and insoluble fractions in parent cells. Substrates that were strongly dependent on Cdc48 for

their degradation, GFP^{NLS}-Tef2* and GFP^{NLS}-Bgl2*, were predominantly insoluble as measured by their partitioning primarily into the insoluble fraction (Figure 2.6). This was independent of expression levels as GFP^{NLS}-Tef2* and GFP^{NLS}-Bgl2* expressed at lower levels also predominantly partitioned into the soluble fraction (Figure 2.7). Substrates that had a moderate dependency on Cdc48 for their degradation, GFP^{NLS}-Peptide 6 and GFP^{NLS}-Peptide I, exhibited an intermediate level of insolubility, as indicated by modest, but observable partitioning into the insoluble fraction (Figure 2.6). Lastly, substrates that had little, if any requirement for Cdc48 in their degradation, GAD-Cdc68-1 and GAD-Cdc13-1, had little, if any observable partitioning into the insoluble fraction (Figure 2.6). I also verified that GFP^{NLS} is predominantly a soluble protein (Figure 2.8). Thus, the requirement for Cdc48 in San1-mediated degradation strongly correlated with substrate insolubility.

If Cdc48's function were to maintain the solubility of ubiquitinated San1 substrates prior to their proteasomal degradation, we expected that a reduction in Cdc48 function would result in an increase in the level of the San1 substrate in the insoluble fraction compared to parent cells. When we examined the insolubility of GFP^{NLS}-Tef2* and GFP^{NLS}-Bgl2* in *cdc48-3* cells after inactivation of Cdc48, which is accomplished by shifting *cdc48-3* cells to the restrictive temperature of 37˚C, we did observe that the proportion of each substrate increased in the insoluble fraction in *cdc48-3* cells compared to parent cells (Figure 2.9). This indicates that Cdc48 function is important for maintaining the solubility of Cdc48-dependent San1 substrates.

A major caution to these studies is that both GFP^{NLS}-Tef2* and GFP^{NLS}-Bgl2* were more soluble in parent cells grown at 37˚C compared to 30˚C (Figure 2.10). This result was initially surprising and unexpected. But, after reading the literature, we think the effect is likely due to the upregulation of heat shock proteins and chaperones that occurs at 37˚C (Gasch et al., 2000; Lindquist and Kim, 1996). Increased expression of heat shock proteins and chaperones has been shown to increase the solubility of prions and other aggregation-prone proteins *in vivo* (Duennwald et al., 2012; Newnam et al., 1999). Despite this change in solubility at the higher temperature, direct comparison of GFP^{NLS}-Tef2* and GFP^{NLS}-Bgl2* solubility between parent and *cdc48-3* cells at 37˚C revealed that the Cdc48-dependent substrates are more insoluble in the absence of Cdc48 function.

To control for this possibility, I also examined the insolubility of GFP^{NLS}-Tef2* and GFP^{NLS}-Bgl2* in parent and *cdc48-3* cells at the semi-restrictive temperature of 30˚C. At 30˚C, we observed considerable insolubility in parent cells and increased insolubility in *cdc48-3* cells (Figure 2.11). Thus, at both restrictive and semi-restrictive temperatures that impair Cdc48-3 function, we observed increased insolubility of the substrates in *cdc48-3* cells relative to parent cells.

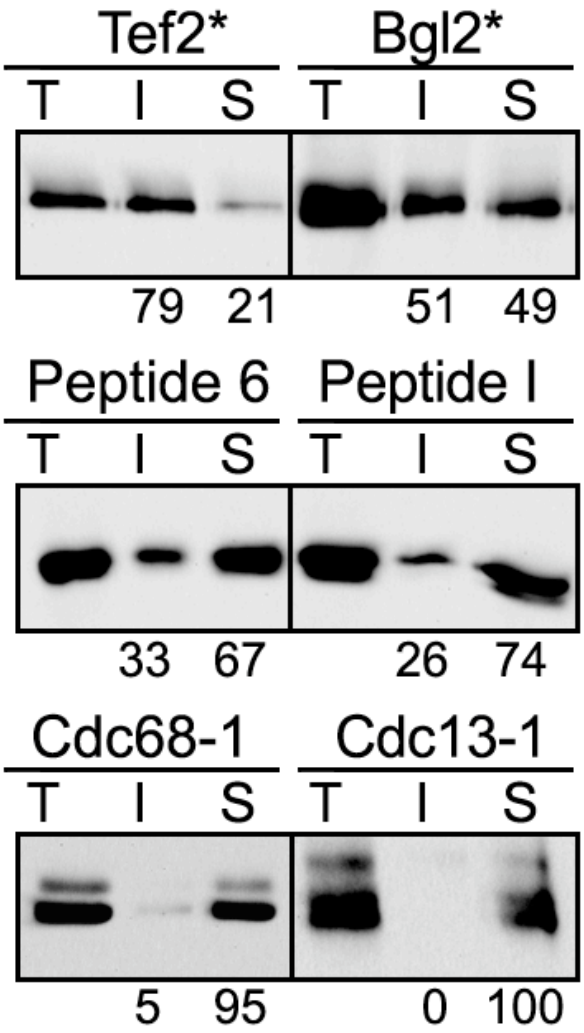

Figure 2.6: Cdc48 dependency correlates with substrate insolubility. Sedimentation assays were performed to determine how GFP^{NLS}-Tef2*, GFP^{NLS}-Bgl2*, GFP^{NLS}-Peptide 6, GFP^{NLS}-Peptide I, GAD-Cdc13-1, and GAD-Cdc68-1 partition between the insoluble pellet fraction (I) and the soluble supernatant fraction (S). Total lysate (T) indicates the total amount of GFP^{NLS}-Tef2*, GFP^{NLS}-Bgl2*, GFP^{NLS}-Peptide 6, GFP^{NLS}-Peptide I, GAD-Cdc68-1, and GAD-Cdc13-1 in cell lysates. Anti-GFP or anti-GAD antibodies were used to detect each substrate. Numbers below each blot indicate the percentage of substrate in each fraction. Relative levels of the insoluble and soluble fractions were determined using ImageJ.

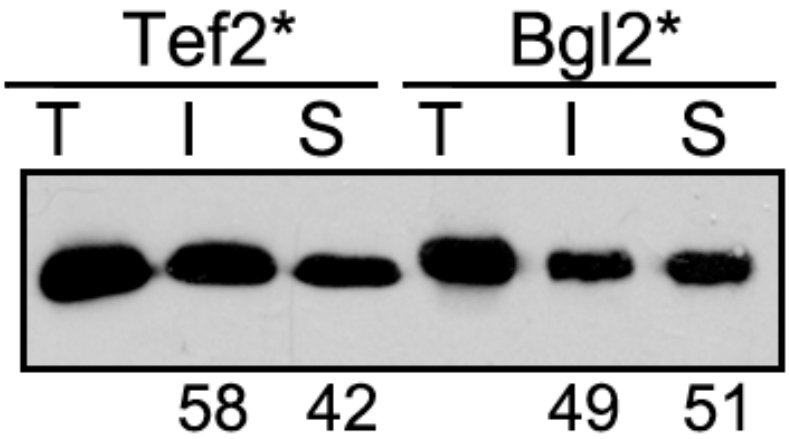

Figure 2.7: Substrate solubility is not altered under low substrate expression conditions. Sedimentation assays were performed to determine how GFP^{NLS}-Tef2* and GFP^{NLS}-Bgl2* partition between the insoluble pellet fraction (I) and the soluble supernatant fraction (S). Substrate expression was induced by 0.03% galactose addition 2 hours prior to harvesting cells. Total lysate (T) indicates the total amount of GFP^{NLS}-Tef2* and GFP^{NLS}-Bgl2* in cell lysates. Anti-GFP antibodies were used to detect each substrate. Numbers below each blot indicate the percentage of substrate in each fraction. Relative levels of the insoluble and soluble fractions were determined using ImageJ.

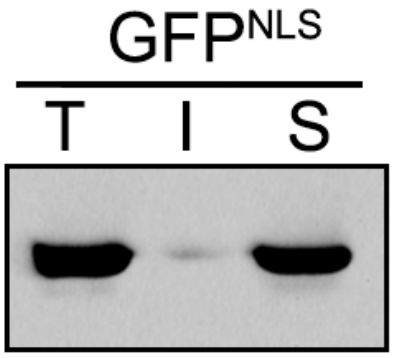

Figure 2.8: GFP is predominantly a soluble protein. Sedimentation assays were performed to determine how GFP^{NLS} partitions between the insoluble pellet fraction (I) and the soluble supernatant (S). Total lysate (T) indicates the total amount of GFP^{NLS} in cell lysates. Anti-GFP antibodies were used to detect GFP^{NLS}.

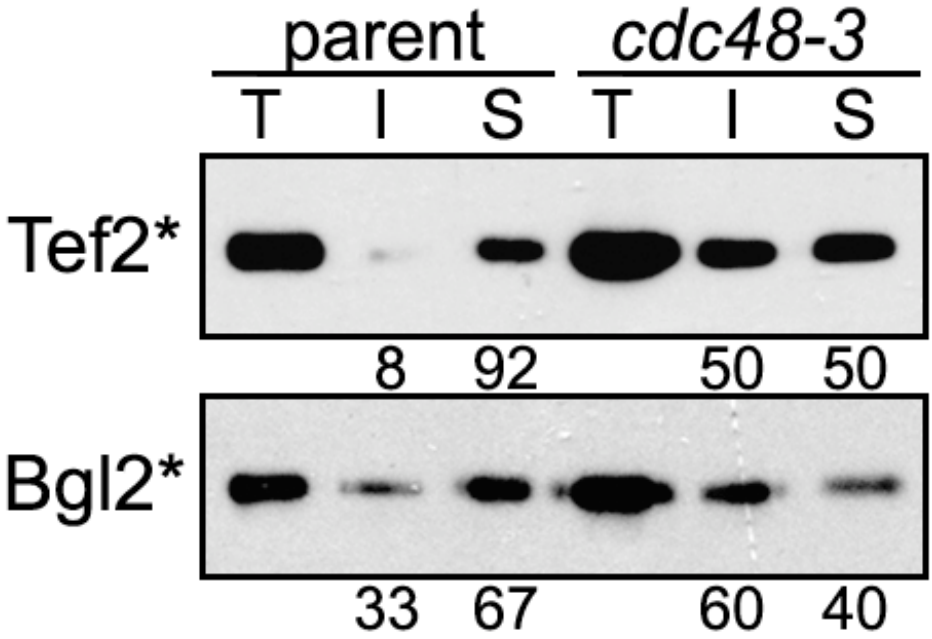

Figure 2.9: Insolubility increases with loss of Cdc48 function.
Sedimentation assays were performed to determine how GFP^{NLS}-Tef2* and GFP^{NLS}-Bgl2* partition between the insoluble pellet fraction (I) and the soluble supernatant fraction (S) in parent and *cdc48-3* cells. Cells were grown at 25˚C and shifted to 37˚C 1 hour prior to lysis to inactivate *cdc48-3*. Total lysate (T) indicates the total amount of GFP^{NLS}-Tef2* or GFP^{NLS}-Bgl2* in cell lysates. Anti-GFP antibodies were used to detect each substrate. Percentage of protein in the insoluble versus soluble fractions is listed below each appropriate lane. Relative levels of the insoluble and soluble fractions were determined using ImageJ.

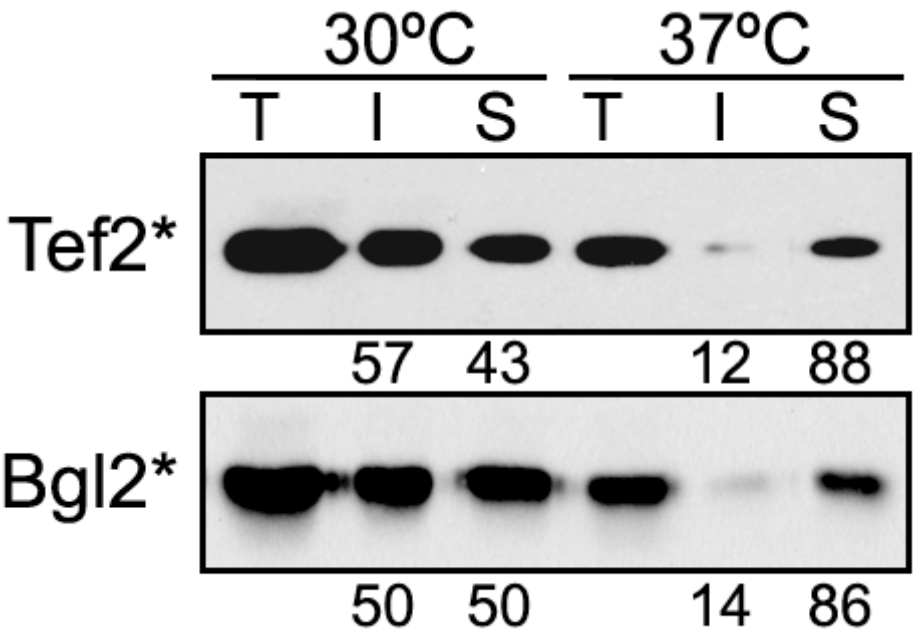

Figure 2.10: Solubility increases at higher temperatures. Sedimentation assays were performed to determine how GFP^{NLS}-Tef2* and GFP^{NLS}-Bgl2* partition between the insoluble pellet fraction (I) and the soluble supernatant fraction (S) at 30˚C or 37˚C. Total lysate (T) indicates the total amount of GFP^{NLS}-Tef2* or GFP^{NLS}-Bgl2* in cell lysates. Anti-GFP antibodies were used to detect each substrate. Percentage of protein in the insoluble versus soluble fractions is listed below each appropriate lane. Relative levels of the insoluble and soluble fractions were determined using ImageJ.

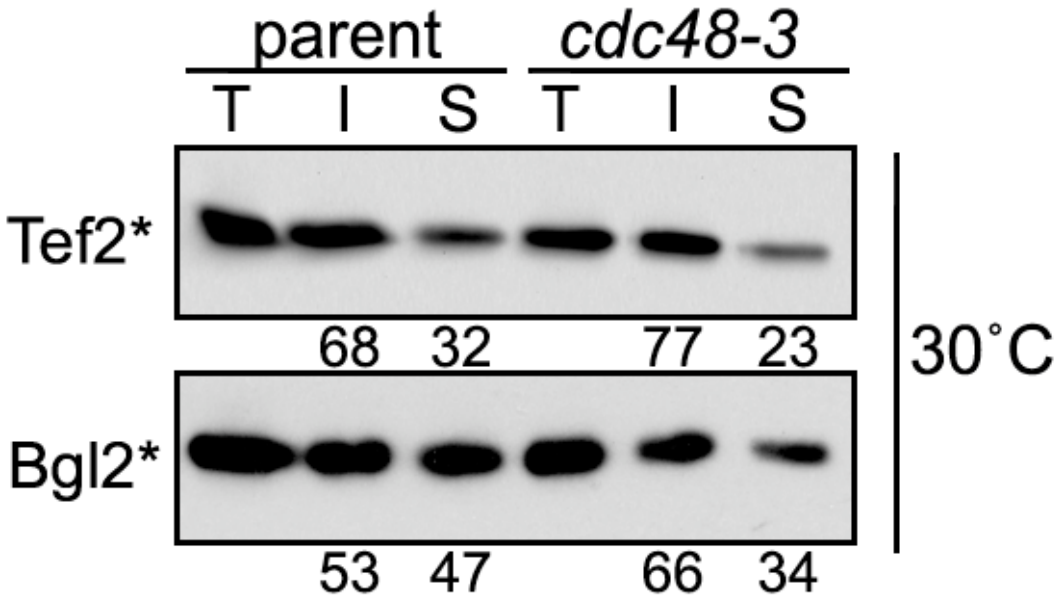

Figure 2.11: Insolubility increases with a reduction in Cdc48 function. Sedimentation assays were performed to determine how GFP^{NLS}-Tef2* and GFP^{NLS}-Bgl2* partition between the insoluble pellet fraction (I) and the soluble supernatant fraction (S) in parent and *cdc48-3* cells. Cells were grown at 25˚C and shifted to 30˚C 1 hour prior to lysis to inactivate *cdc48-3*. Total lysate (T) indicates the total amount of GFP^{NLS}-Tef2* or GFP^{NLS}-Bgl2* in cell lysates. Anti-GFP antibodies were used to detect each substrate. Percentage of protein in the insoluble versus soluble fractions is listed below each appropriate lane. Relative levels of the insoluble and soluble fractions were determined using ImageJ.

Loss of Cdc48 function is associated with increased inclusion formation and cell inviability upon expression of insoluble, misfolded nuclear proteins

Because GFP^{NLS}-Tef2* and GFP^{NLS}-Bgl2* were more insoluble in *cdc48-3* cells compared to parent cells (Figure 2.9), we wanted to determine if there was increased cellular inclusion formation of these substrates in *cdc48-3* cells at the restrictive temperature. Using fluorescence microscopy, I found that both GFP^{NLS}-Tef2* and GFP^{NLS}-Bgl2* formed cellular inclusions in parent cells, and there was an increase in both the size and frequency of the inclusions in *cdc48-3* cells (Figure 2.12). By comparison, GFP^{NLS}, which is predominantly a soluble protein (Figure 2.8), localized diffusely throughout the cell in parent and *cdc48-3* mutant cells (Figure 2.13). We note that GFP^{NLS} does not show as much nuclear enrichment as expected from possessing an NLS due to the fact that it is ~27 kDa in size and thus has a monomeric molecular weight below the passive <40kDa diffusion limit of the yeast nuclear pore (Shulga and Goldfarb, 2003; Shulga et al., 2000). Altogether, one cellular consequence for losing Cdc48 function is the increased accumulation and aggregation of insoluble nuclear PQC degradation substrates.

We previously found that expression of many misfolded San1 substrates resulted in cellular toxicity in the absence of San1 function, including Tef2* and Bgl2* (Rosenbaum et al., 2011). From these observations, we expected that loss of Cdc48 function would also result in toxicity upon expression of San1 substrates that require Cdc48 for their degradation. I examined the growth of

parent and *cdc48-3* cells expressing either GFP^{NLS}-Tef2* or GFP^{NLS}-Bgl2* from the galactose-inducible *GAL1* promoter at semi-restrictive temperatures that normally allow growth of *cdc48-3* cells but restrict Cdc48-3 function. Under these conditions, I found that expression of both substrates significantly impaired cell viability in *cdc48-3* cells at both 25˚C and 32˚C compared to parent cells (Figure 2.14). I also tested growth of parent and *cdc48-3* cells expressing GFP^{NLS} alone and did not observe any cellular toxicity (Figure 2.15). Our findings indicate that the reduction or loss of Cdc48 function results in cell inviability when insoluble, inclusion-forming, misfolded nuclear proteins consequently accumulate in the cell.

The observations thus far suggest that Cdc48 is likely interacting with aggregation-prone, misfolded proteins en route from San1 to the proteasome. To support this, I wanted to establish a direct interaction with Cdc48 and GFP^{NLS}-Tef2* or GFP^{NLS}-Bgl2* using co-precipitation experiments. Unfortunately, I found that the substrates are exceptionally aggregation-prone without the use of solubilizing detergents, which disrupt protein-protein interactions if included in the lysis and co-precipitation buffers. This aggregation characteristic resulted in a large proportion of the substrates accumulating on the beads used for the co-precipitation experiments, confounding my ability to determine if GFP^{NLS}-Tef2* and GFP^{NLS}-Bgl2* could co-precipitate with Cdc48. Because I was unable to perform co-precipitation experiments due to this technical aggregation issue, I instead sought to explore if a fraction of Cdc48 colocalizes with GFP^{NLS}-Tef2* and GFP^{NLS}-Bgl2* *in vivo.* Using fluorescence microscopy and an mCherry

tagged version of Cdc48, I found that Cdc48 was uniformly localized throughout the cell when GFP^{NLS} was expressed (Figure 2.16). By contrast, in ~20% of cells expressing GFP^{NLS}-Tef2* or GFP^{NLS}-Bgl2*, we observed Cdc48 forming inclusions that colocalized with the GFP^{NLS}-Tef2* or GFP^{NLS}-Bgl2* inclusions (representative examples in Figure 2.17). These results indicate that at least in a subset of cells, Cdc48 is recruited to nuclear inclusions.

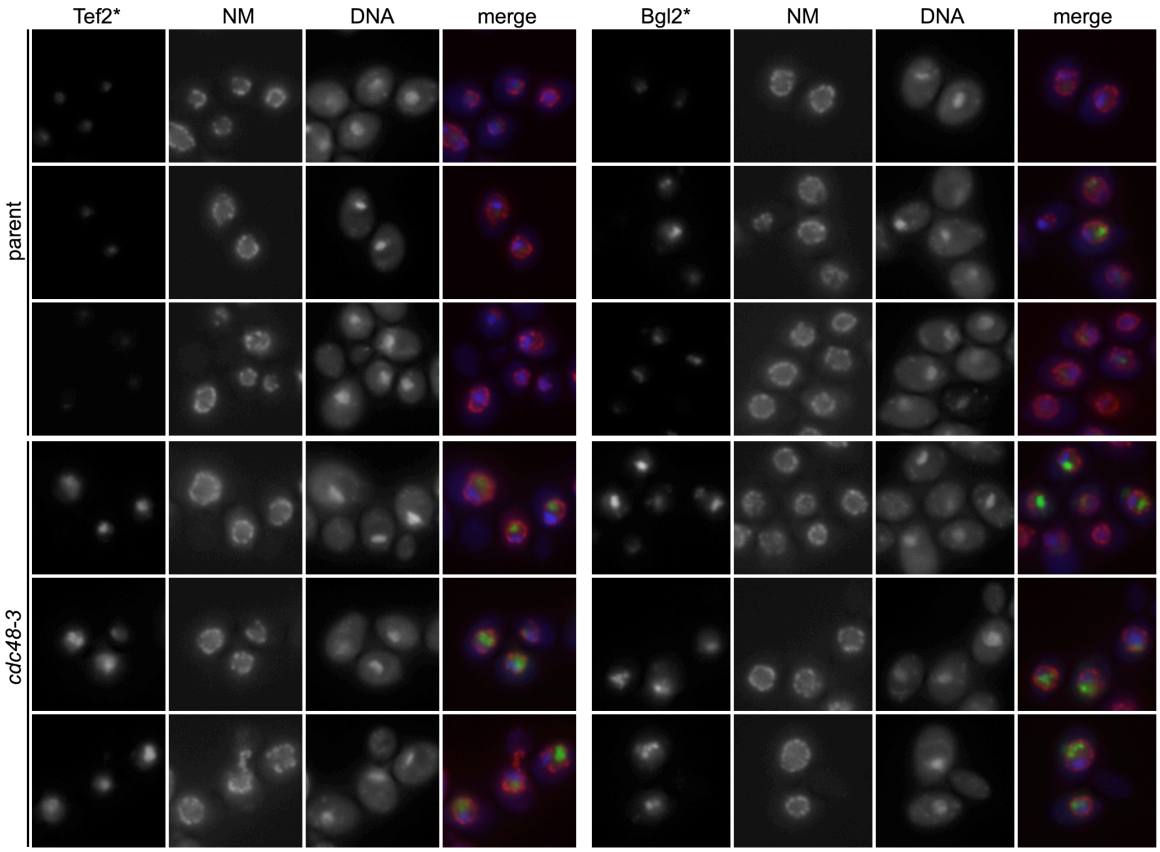

Figure 2.12: Loss of Cdc48 function results in increased inclusion formation. Expression of GFP^{NLS}-Tef2* and GFP^{NLS}-Bgl2* was induced in parent and *cdc48-3* cells by addition of galactose for 6 hours in log phase. Cells were shifted to 37˚C 1 hour prior to fixation. Cells were fixed in 4% paraformaldehyde, stained with DAPI, and examined by fluorescence microscopy.

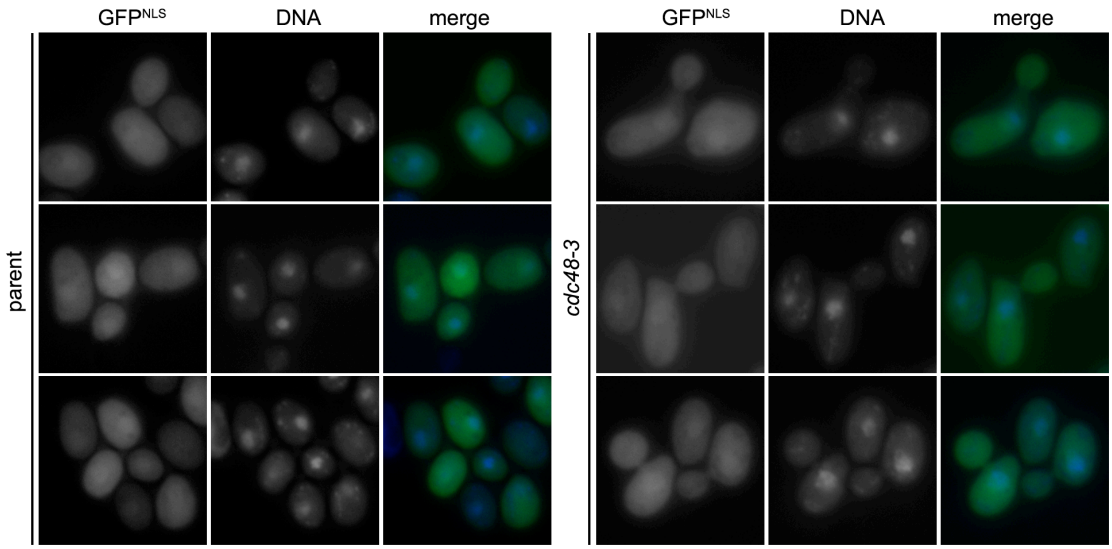

Figure 2.13: GFP^{NLS} localizes diffusely throughout parent and *cdc48-3* mutant cells. Expression of GFP^{NLS} was induced in parent and *cdc48-3* cells by addition of galactose for 6 hours in log phase. Cells were shifted to 37˚C 1 hour prior to fixation. Cells were fixed in 4% paraformaldehyde, stained with DAPI, and examined by fluorescence microscopy.

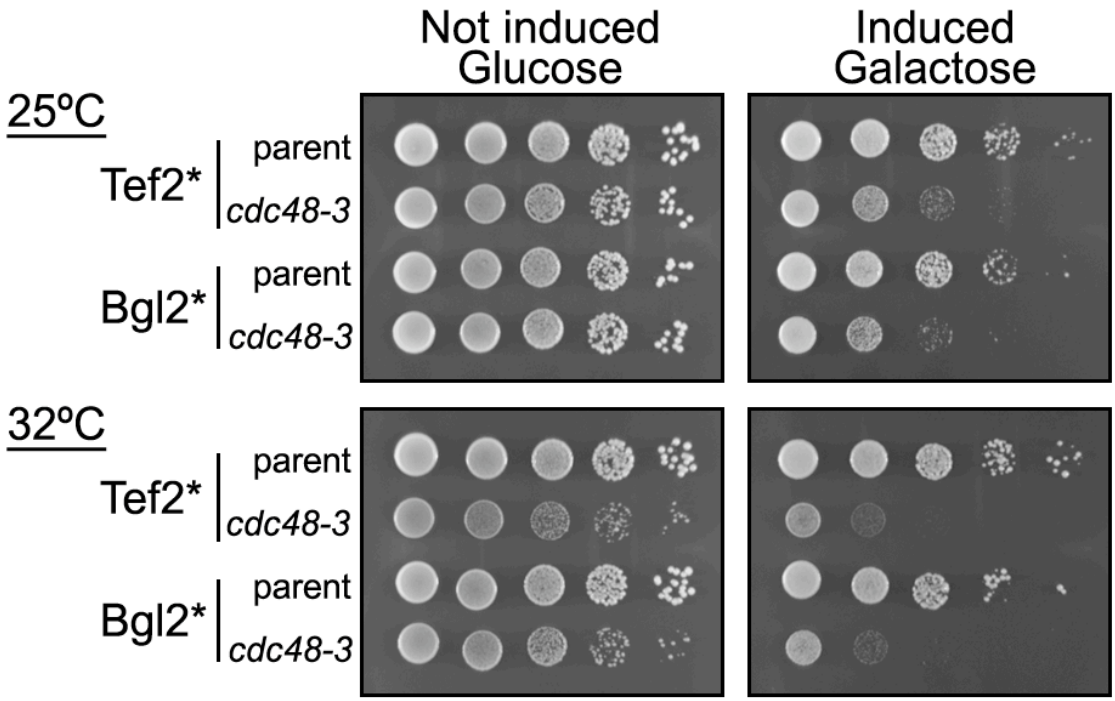

Figure 2.14: Reduction in Cdc48 function results in cell inviability upon expression of insoluble, misfolded nuclear proteins. Parent or *cdc48-3* cells expressing GFP^{NLS}-Tef2* or GFP^{NLS}-Bgl2* were spotted at 10-fold serial dilutions onto media containing glucose to measure spotting efficiency or galactose to induce expression at 25˚C and 32˚C.

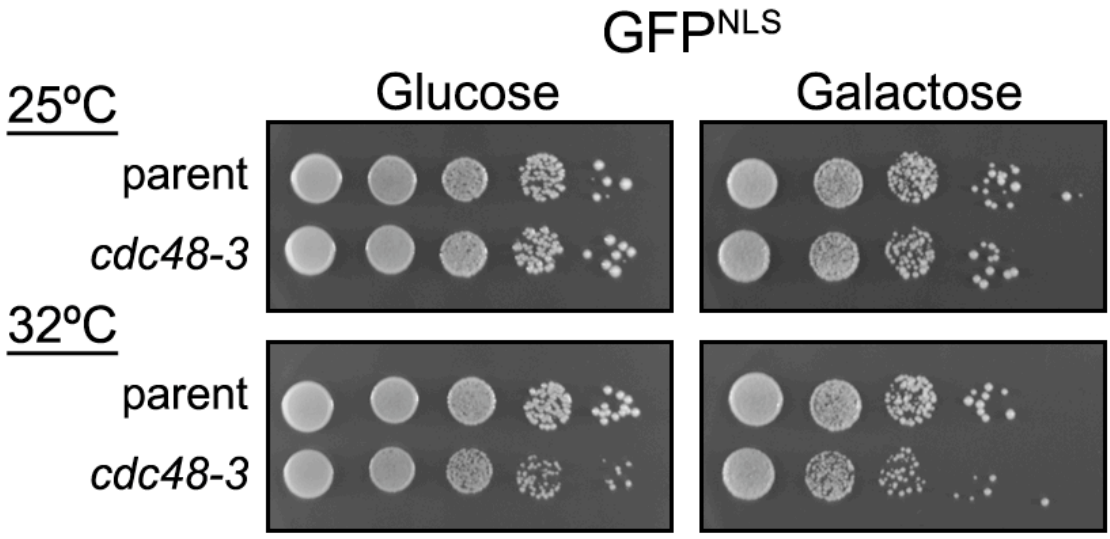

Figure 2.15: Expression of GFP^{NLS} is not toxic in parent or *cdc48-3* cells. Parent or *cdc48-3* cells expressing GFP^{NLS} were spotted at 10-fold serial dilutions onto media containing glucose to measure spotting efficiency or galactose to induce expression at 25˚C and 32˚C.

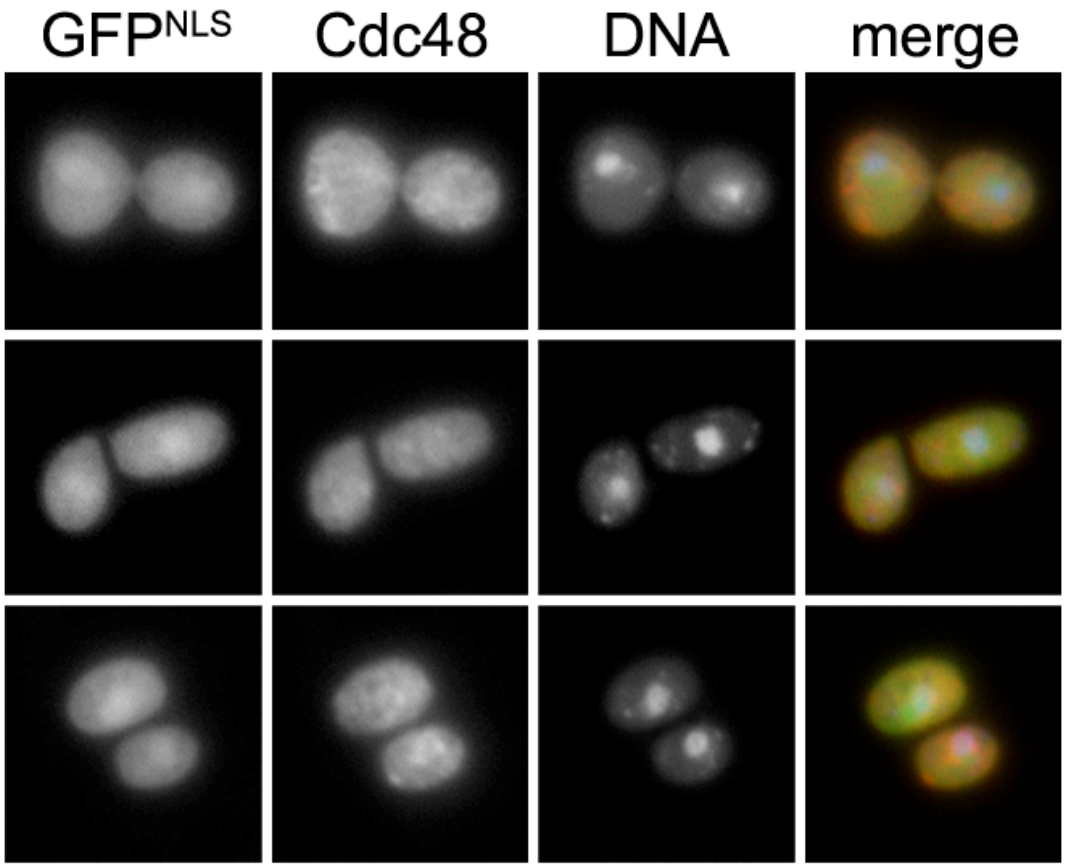

Figure 2.16: Cdc48 is localized uniformly throughout the cell when GFP^{NLS} is expressed. Expression of GFP^{NLS} was induced by addition of galactose for 6 hours in log phase. Cells were fixed in 4% paraformaldehyde, stained with DAPI, and examined by fluorescence microscopy.

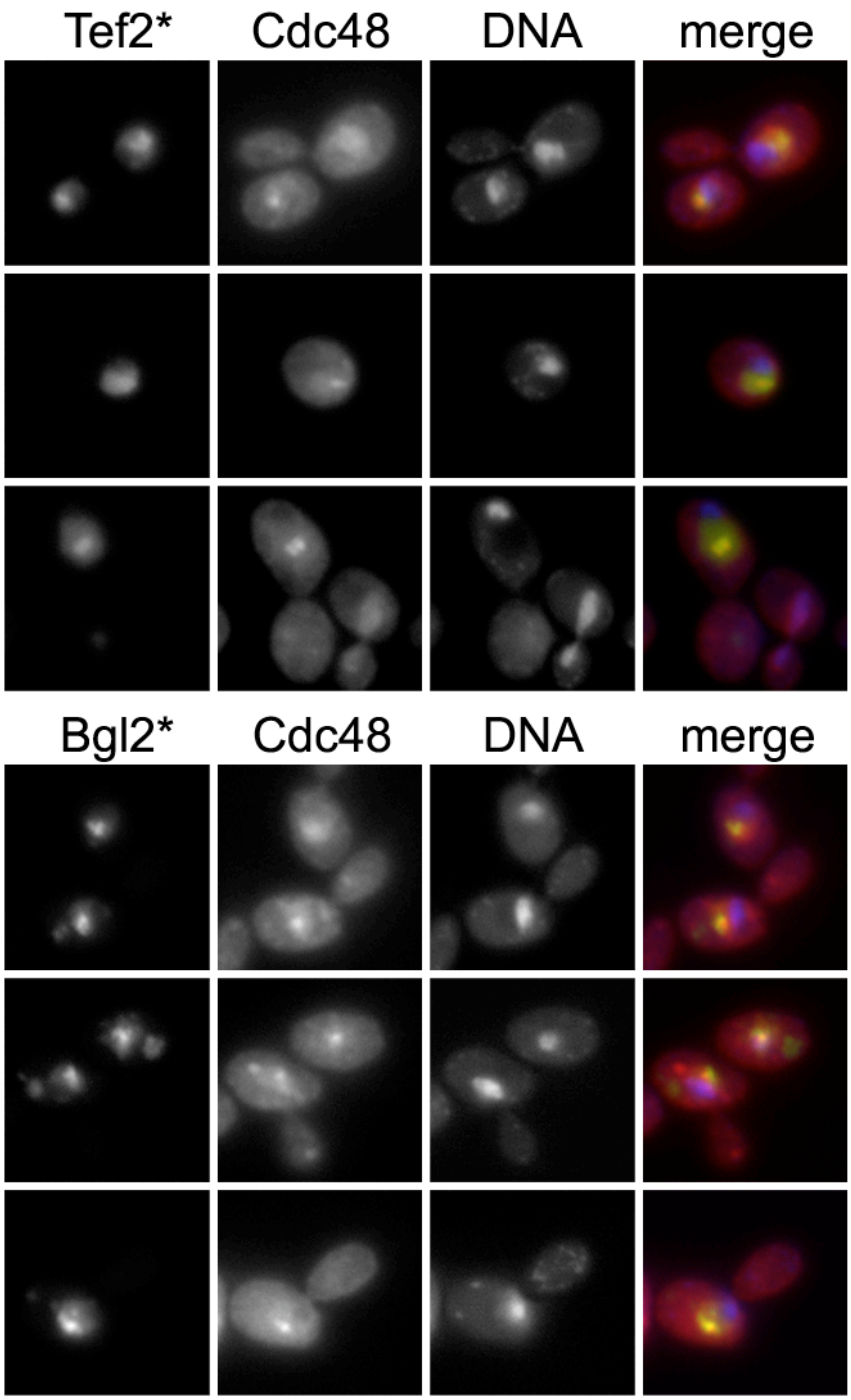

Figure 2.17: Cdc48 colocalizes with nuclear inclusions. Expression of GFP^{NLS}-Tef2* and GFP^{NLS}-Bgl2* proteins was induced by addition of galactose for 6 hours in log phase. Cells were fixed in 4% paraformaldehyde, stained with DAPI, and examined by fluorescence microscopy.

Cdc48 dependency can be changed by altering substrate solubility

The model emerging from our observations thus far is that the requirement for Cdc48 in San1-mediated degradation correlates with the degree of misfolded substrate insolubility; the greater the substrate insolubility, the greater the need for Cdc48. A key test of this model would be to create a means to increase or decrease the solubility of a San1 substrate without affecting its San1 dependency, and then query how the changes in solubility alter the substrate's dependency on Cdc48. I predicted that as the solubility of a substrate is increased, its dependency on Cdc48 would decrease. Conversely, as the solubility of a substrate is decreased, its dependency on Cdc48 would increase.

We reasoned this test could be accomplished through the use of the GFP^{NLS} and GAD reporter proteins that we already used in this study. It has been previously shown that the folding of GFP is negatively affected by its fusion to proteins that fold poorly or misfold (Waldo et al., 1999). Accordingly, fusion to GFP might be expected to increase the insolubility of a misfolded substrate. On the other hand, transcriptional activation domains like the GAD are often intrinsically disordered when not bound to their protein targets (Dyson and Wright, 2005). In this case, a misfolded fusion protein cannot alter the folding of the GAD because it already lacks structure due to its inherent disorder. Furthermore, intrinsically disordered proteins are exceptionally soluble because they lack sufficient hydrophobicity to form hydrophobic cores (Tompa, 2002), and their fusion to proteins improves solubility in bacterial expression systems

(Santner et al., 2012). As a result, fusion of the GAD to a misfolded protein might be expected to increase the solubility of the GAD-misfolded protein fusion.

To test the insolubility hypothesis further, I focused on GFP^{NLS}-Tef2*, GFP^{NLS}-Bgl2*, GAD-Cdc68-1, and GAD-Cdc13-1. I switched the fusion proteins to create the new substrates GAD-Tef2*, GAD-Bgl2*, GFP^{NLS}-Cdc68-1, and GFP^{NLS}-Cdc13-1. An important parameter of the swap strategy is whether the swaps altered San1-dependent degradation. Deletion of *SAN1* stabilized GAD-Tef2*, GAD-Bgl2*, GFP^{NLS}-Cdc68-1, and GFP^{NLS}-Cdc13-1 (Figure 2.18) to the identical extent as GFP^{NLS}-Tef2*, GFP^{NLS}-Bgl2*, GAD-Cdc68-1, and GAD-Cdc13-1 (Figure 2.1). Thus, swapping the fusion reporter did not alter San1-mediated degradation in any way.

On the other hand, the fusion reporter swap did alter the Cdc48 dependency for Tef2*, Bgl2*, and Cdc68-1 as anticipated based on solubility of the GAD and GFP^{NLS} reporter proteins. The degradation of GAD-Tef2* and GAD-Bgl2* was now less dependent on Cdc48 (Figure 2.18) than the degradation of GFP^{NLS}-Tef2* and GFP^{NLS}-Bgl2* (Figure 2.1). By contrast, the degradation of GFP^{NLS}-Cdc68-1 was now more dependent on Cdc48 (Figure 2.18) than the degradation of GAD-Cdc68-1 (Figure 2.1). The degradation of GFP^{NLS}-Cdc13-1 remained independent of Cdc48 (Figure 2.18), as was the degradation of GAD-Cdc13-1 (Figure 2.1). This is a key result because it means that GFP^{NLS} itself does not dictate Cdc48 dependency.

If the hypothesis that Cdc48 dependency correlates with substrate insolubility is correct, then we expected appropriate changes in the solubility of

GAD-Tef2*, GAD-Bgl2*, and GFP^{NLS}-Cdc68-1 that match their altered Cdc48 dependency. Consistent with their reduced dependency on Cdc48, GAD-Tef2* and GAD-Bgl2* were much more soluble (Figure 2.19) than GFP^{NLS}-Tef2* and GFP^{NLS}-Bgl2* (Figure 2.6). Consistent with an increased dependency on Cdc48, GFP^{NLS}-Cdc68-1 was more insoluble (Figure 2.19) than GAD-Cdc68-1 (Figure 2.6). The solubility of GFP^{NLS}-Cdc13-1 remained unchanged (Figure 2.19) from GAD-Cdc13-1 (Figure 2.6), mirroring its Cdc48 independence. Taken together, the fusion reporter swap data provide important evidence supporting the hypothesis that the requirement for Cdc48 in the degradation of misfolded nuclear substrates correlates with substrate insolubility.

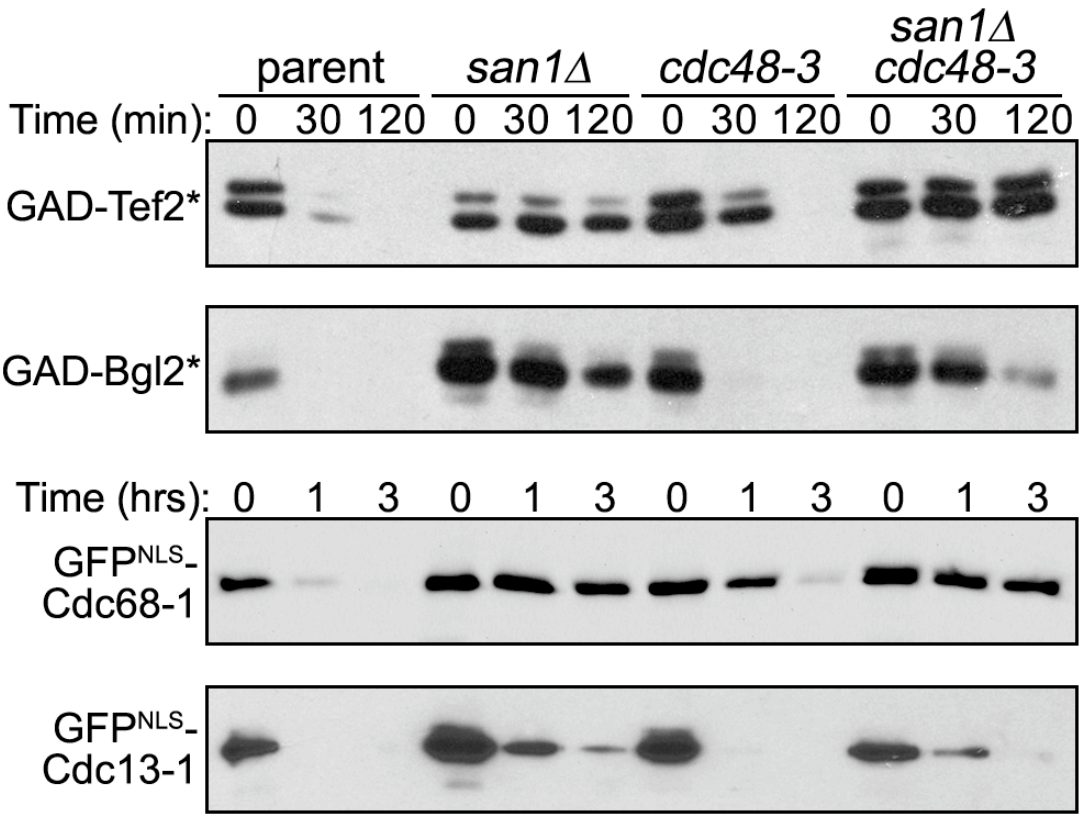

Figure 2.18: Fusion reporter swap alters Cdc48 dependency.
Cycloheximide-chase degradation assays were performed on parent, *san1*Δ, *cdc48-3*, and *san1*Δ*cdc48-3* cells to assess the stability of GAD-Tef2*, GAD-Bgl2*, GFP^{NLS}-Cdc68-1, and GFP^{NLS}-Cdc13-1. For the GFP^{NLS}-substrates expressed from the *GAL1* promoter, expression was induced by addition of galactose for 2 hours prior to cycloheximide addition. For the GAD-substrates, expression from the *ADH1* promoter was constitutive. Cell cultures were shifted from 25˚C to 37˚C after cycloheximide addition to inactivate *cdc48-3*. Time after cycloheximide addition is indicated above each lane. Anti-GFP or anti-GAD antibodies were used to detect each substrate.

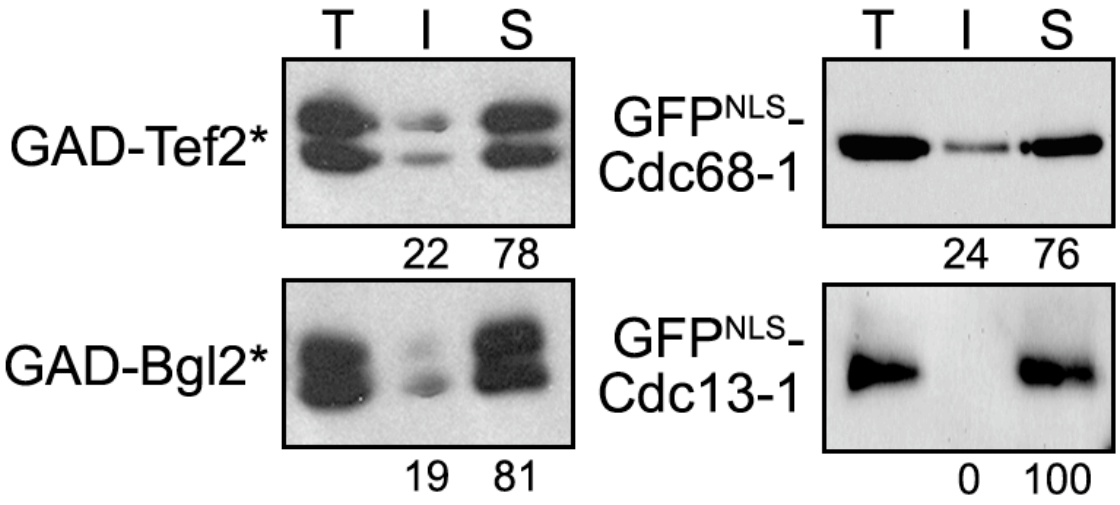

Figure 2.19: Fusion reporter swap alters substrate solubility. Sedimentation assays were performed to determine how GAD-Tef2*, GAD-Bgl2*, GFP^{NLS}-Cdc68-1, and GFP^{NLS}-Cdc13-1partition between the insoluble pellet fraction (I) and the soluble supernatant fraction (S) (right panels). Total lysate (T) indicates the total amount of GFP^{NLS}-Tef2*, GFP^{NLS}-Bgl2*, GFP^{NLS}-Peptide 6, GFP^{NLS}-Peptide I, GAD-Cdc86-1, and GAD-Cdc13-1 in cell lysates. Anti-GFP or anti-GAD antibodies were used to detect each substrate. Numbers below each blot indicate the percentage of substrate in each fraction. Relative levels of the insoluble and soluble fractions were determined using ImageJ.

Cdc48 function in the San1 pathway

We predicted that San1 substrates would all follow the same linear pathway to the proteasome. Contrary to our prediction, we discovered that this wasn't the case and some San1 substrates take different Cdc48-dependent and -independent routes correlated with their degree of solubility (Figure 2.20). We found only one other example where substrates for the same E3 show differential involvement of Cdc48 for their degradation, the yeast ER E3 Doa10 (Ravid et al., 2006). In the Doa10 degradation pathway, Cdc48 facilitates turnover of ER membrane substrates but is not required for degradation of cytoplasmic Doa10 substrates (Ravid et al., 2006). Perhaps insoluble San1 substrates require similar extraction from an aggregate as do Doa10 substrates from the ER membrane, thus their dependence on Cdc48. Alternatively, Cdc48 could be using a chaperone activity to maintain protein solubility for San1 substrates thereby preventing aggregation prior to proteasome delivery. Cdc48/p97 has been shown to prevent the aggregation of denaturated luciferase *in vitro* and *in vivo* (Song et al., 2007). Furthermore, Cdc48/p97 has been demonstrated to re-solubilize heat denatured luciferase from insoluble aggregates as well as facilitate the clearance of pre-formed polyglutamine inclusions (Kobayashi et al., 2007). Based on these observations, both scenarios for Cdc48 in San1-mediated nuclear PQC degradation could be operative. Because the proteasome has difficulty degrading aggregated proteins (Holmberg et al., 2004; Snyder et al., 2003; Verhoef et al., 2002), maintenance of protein solubility

upstream of the proteasome but downstream of the E3 would be a crucial function for Cdc48 in a PQC degradation pathway.

We found that the insolubility of San1 substrates GFP^{NLS}-Tef2* and GFP^{NLS}-Bgl2* was increased in *cdc48-3* cells compared to parent cells at the restrictive temperature of 37˚C, supporting the hypothesis that Cdc48 helps maintain the solubility of these San1 substrates. However, the intrinsic insolubility of GFP^{NLS}-Tef2* and GFP^{NLS}-Bgl2* decreased in parent cells at 37˚C compared with 30˚C, which we ascribed to an upegulation of heat shock proteins and chaperones that occurs at this temperature (Gasch et al., 2000; Lindquist and Kim, 1996). This explanation at first appears counterintuitive when thinking about Cdc48 and a role in maintaining misfolded protein solubility. Why would Cdc48 be required to maintain misfolded protein solubility if heat shock proteins and chaperones have been upregulated and are acting to increase misfolded protein solubility themselves? To explain this, we think it is important to consider where in the San1 pathway chaperones and Cdc48 act on the substrate. It has been found that the Hsp70 chaperones Ssa1/Ssa2, the Hsp110 chaperone Sse1, and the Hsp40 chaperone Ydj1 facilitate the degradation of some San1 substrates by acting upstream of San1 ubiquitination (Guerriero et al., 2013; Heck et al., 2010; Prasad et al., 2010, 2012). Here, I show that Cdc48 facilitates the degradation of some San1 substrates by acting downstream of San1 ubiquitination. It is therefore probable that chaperones and Cdc48 act on different pools of a San1 substrate: not yet ubiquitinated versus ubiquitinated. Because the sedimentation assay cannot distinguish between these pools (due

to the unconstrained activities of deubiquitinating enzymes after cell lysis), the amount of the protein in the insoluble pellet will be a function of total chaperone activity upstream of San1 and total Cdc48 activity downstream of San1. Whether Ssa1/Ssa2 or other chaperones also collaborate with Cdc48 to maintain substrate solubility after San1 ubiquitination is not known.

In examining the ubiquitination of San1 substrates that require Cdc48, we observed the accumulation of high-molecular weight ubiquitinated conjugates in *cdc48-3* mutant cells. By contrast, while I found increased levels of ubiquitinated substrate in parent cells after inhibition of the proteasome, we did not observe a shift in the molecular weight of ubiquitinated conjugates. One explanation for the accumulation of high-molecular weight ubiquitinated conjugates in *cdc48-3* cells could be due to unconstrained ubiquitin chain extension and/or branching. It has been shown that Cdc48 prevents the formation of excessive multiubiquitin chains *in vitro* (Richly et al., 2005), supporting this possibility. Another explanation for the presence of high-molecular weight conjugates is that when insoluble substrates are allowed to accumulate in the absence of Cdc48, they aggregate. We did observe increased substrate insolubility and inclusion formation in *cdc48-3* cells. However, in the assay assessing substrate ubiquitination, I lysed cells under heavy denaturing conditions and these conditions should have solubilized aggregates. Thus, we favor the model that the higher molecular weight ubiquitin conjugates in the ubiquitination assays are a function of unconstrained ubiquitin chain extension and/or branching rather than aggregated forms of the substrate.

Implications for aggregation disorders

Over thirty-five age-dependent neurodegenerative disorders in humans are characterized by the aggregation of misfolded proteins in neurons (Wang et al., 2008). Human p97 has been reported to colocalize with ubiquitinated aggregates in neurons taken from patients affected by neurodegenerative disorders including Alzheimer's, Parkinson's, Huntington's, and ALS (Hirabayashi et al., 2001; Ishigaki et al., 2004; Mizuno et al., 2003). Additionally, missense mutations in human p97 underlie the etiology of IBMPFD (Watts et al., 2004), and may also be causative in some cases of ALS (Johnson et al., 2010). Loss of p97 function in IBMPFD leads to the accumulation of ubiquitinated protein aggregates in affected cells (Hubbers et al., 2007; Janiesch et al., 2007; Ju et al., 2008; Weihl et al., 2006; Weihl et al., 2007). I identified Cdc48/p97 as a critical factor for the proteolysis of insoluble misfolded substrates in the nucleus. Furthermore, I revealed that the loss of Cdc48/p97 function led to increased misfolded protein insolubility, *in vivo* inclusion formation, and cell inviability when misfolded, insoluble, nuclear proteins were expressed. Cdc48 also localized to cellular inclusions. Further work will be required to determine if possible failures of Cdc48/p97 to clear insoluble misfolded proteins significantly contribute to the age-dependent pathology of neurodegenerative disorders associated with nuclear protein aggregation.

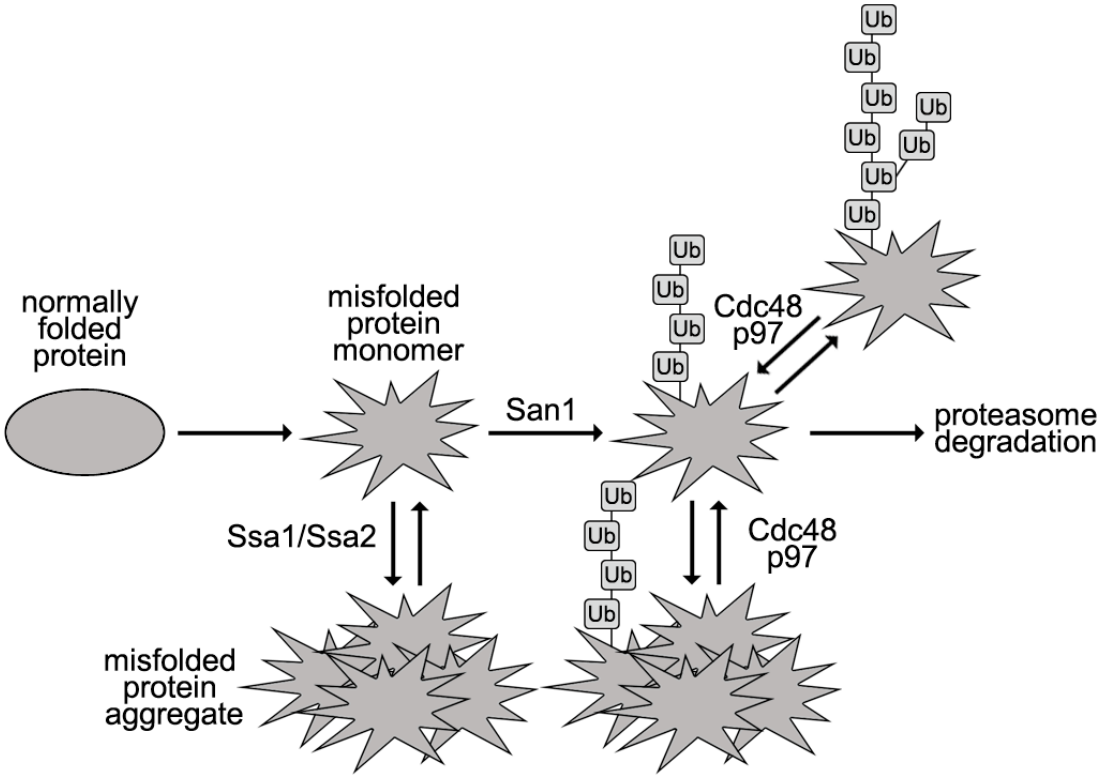

Figure 2.20: Model for Cdc48 function in nuclear PQC degradation. Cdc48 functions upstream of the proteasome to maintain ubiquitinated substrate solubility.

CHAPTER III: CDC48 ADAPTORS INVOLVED IN NUCLEAR PQC DEGRADATION

Npl4-Ufd1 heterodimer

Cdc48 has a flexible N-terminal domain that allows for interaction with a wide variety of cellular cofactors (Yeung et al., 2008). Recruitment of diverse adaptors is thought to confer functional versatility of the AAA-ATPase. Of these, the Npl4-Ufd1 heterodimer cofactor has been implicated in a majority of Cdc48-dependent cellular processes including ER degradation (Ye et al., 2001), and several chromatin-associated degradative events (Franz et al., 2011; Meerang et al., 2011; Verma et al., 2011; Wilcox and Laney, 2009). One Npl4-Ufd1 heterodimer interacts with one Cdc48 hexamer to form a functional complex, and Npl4-Ufd1 facilitates substrate recruitment to Cdc48 via intrinsic ubiquitin binding. Loss of function mutations in either Npl4 or Ufd1 significantly impairs Cdc48-dependent processes, underscoring their individual value within the complex (Wolf and Stolz, 2012).

Npl4 is required for Cdc48-dependent, San1-mediated degradation

I evaluated if Npl4 and Ufd1 were involved in the degradation of San1 substrates that showed either complete or partial dependency on Cdc48 (Figure 2.1). For GFP^{NLS}-Tef2* and GFP^{NLS}-Bgl2*, whose degradation showed complete dependence on Cdc48, I found their degradation also showed a partial dependence on Npl4 as indicated by the stabilization of these substrates in *npl4-*

1 mutant cells compared with parent cells (Figure 3.1). For the substrates GFP^{NLS}-Peptide 6 and GFP^{NLS}-Peptide I, whose degradation showed partial dependence on Cdc48, I found their degradation also showed a partial dependence on Npl4 as indicated by their modest stabilization in *npl4-1* mutant cells (Figure 3.1). Unexpectedly, I found that degradation of San1 substrates tested demonstrated weak dependency on Ufd1 as was indicated by slight stability in *ufd1-1* mutant cells (Figure 3.2).

Vms1 is not involved in nuclear PQC

It has been recently demonstrated that Vms1 also forms a heterodimer with Npl4 and associates with Cdc48 to mediate the degradation of mitochondrial proteins in response to oxidative stress (Heo et al., 2010), and regulate the proteolysis of Cdc13 (Baek et al., 2012). Therefore, I examined the potential involvement of Vms1 in the degradation of San1 substrates. In no case did we observe stabilization of San1 substrates in *vms1*Δ cells, indicating that Vms1 is not involved in the degradation of Cdc48-dependent, San1 substrates (Figure 3.3). Perhaps Npl4 has another, as yet unidentified cofactor that functions in Cdc48-dependent, San1-mediated nuclear PQC degradation.

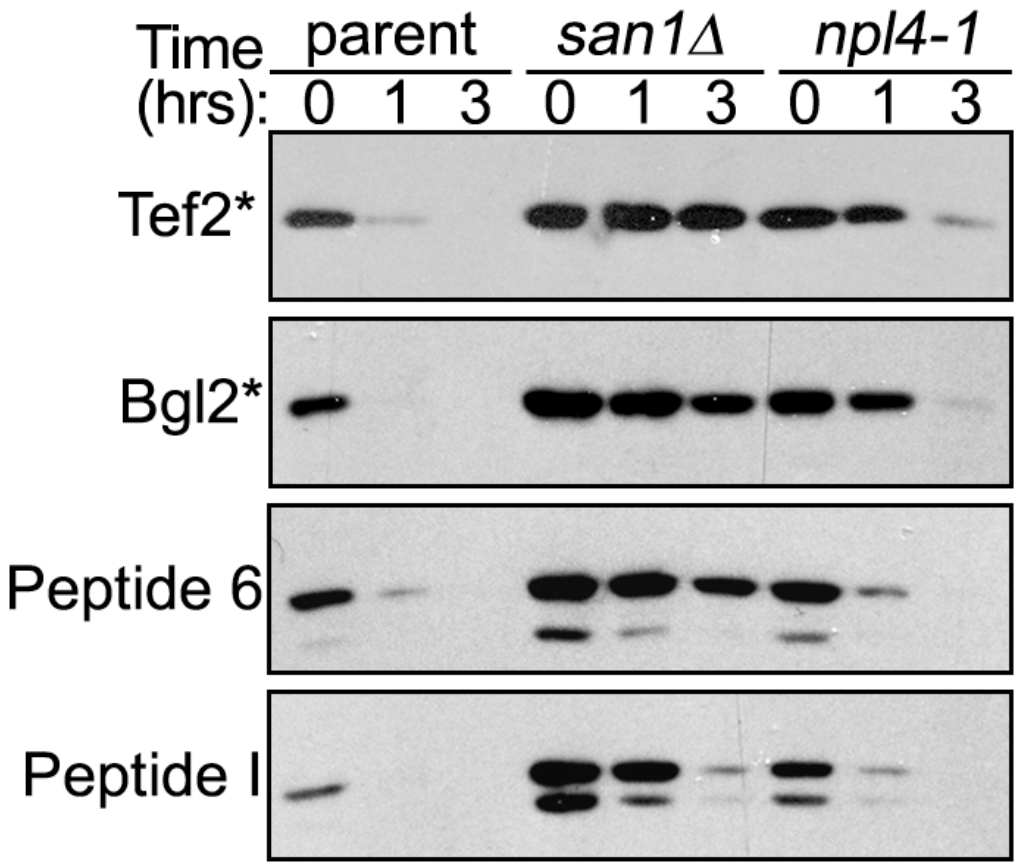

Figure 3.1: Npl4 is involved in Cdc48-dependent San1-mediated degradation. Cycloheximide-chase degradation assays were performed to assess the stability of GFP^{NLS}-Tef2*, and GFP^{NLS}-Bgl2*, GFP^{NLS}-Peptide 6, and GFP^{NLS}-Peptide I in parent, *san1*Δ, and *npl4-1* cells. San1 substrate expression was induced by addition of galactose for 2 hours prior to cycloheximide addition. Cell cultures were shifted from 25˚C to 37˚C after cycloheximide addition to inactivate *npl4-1*. Time after cycloheximide addition is indicated above each lane. Anti-GFP antibodies were used to detect each substrate.

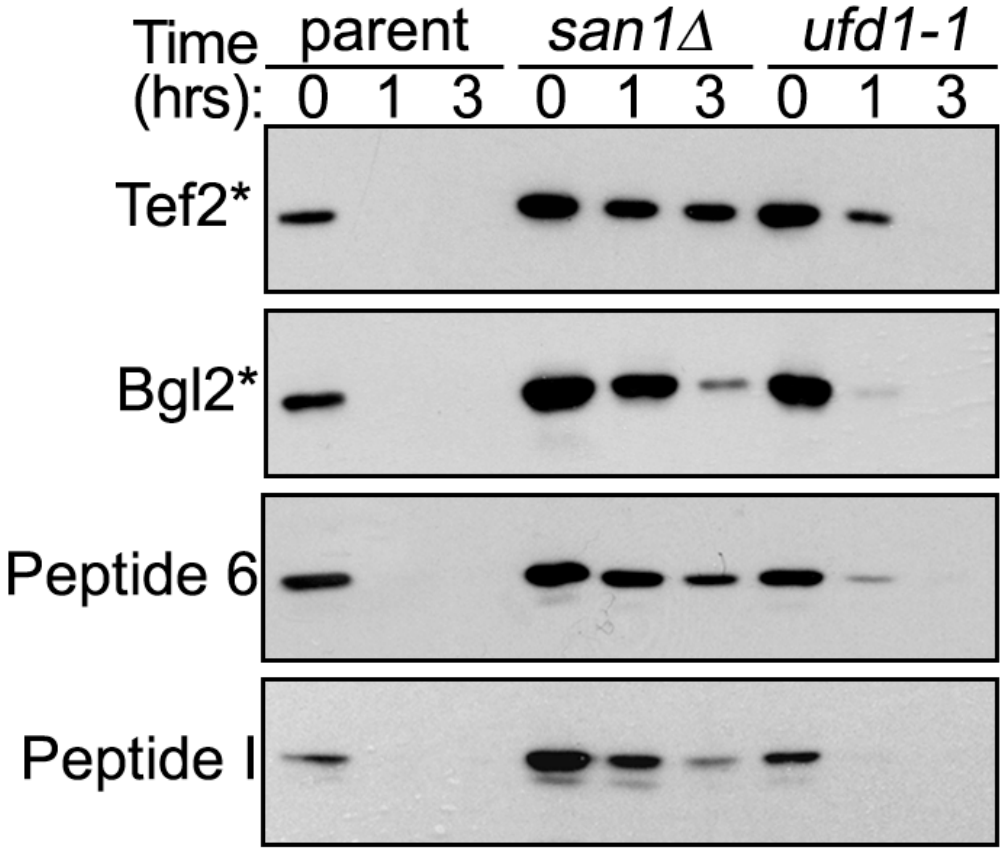

Figure 3.2: Ufd1 is modestly involved in Cdc48-dependent San1-mediated degradation. Cycloheximide-chase degradation assays were performed to assess the stability of GFP^{NLS}-Tef2*, and GFP^{NLS}-Bgl2*, GFP^{NLS}-Peptide 6, and GFP^{NLS}-Peptide I in parent, *san1*Δ, and *ufd1-1* cells. San1 substrate expression was induced by addition of galactose for 2 hours prior to cycloheximide addition. Cell cultures were shifted from 25˚C to 37˚C after cycloheximide addition to inactivate *ufd1-1*. Time after cycloheximide addition is indicated above each lane. Anti-GFP antibodies were used to detect each substrate.

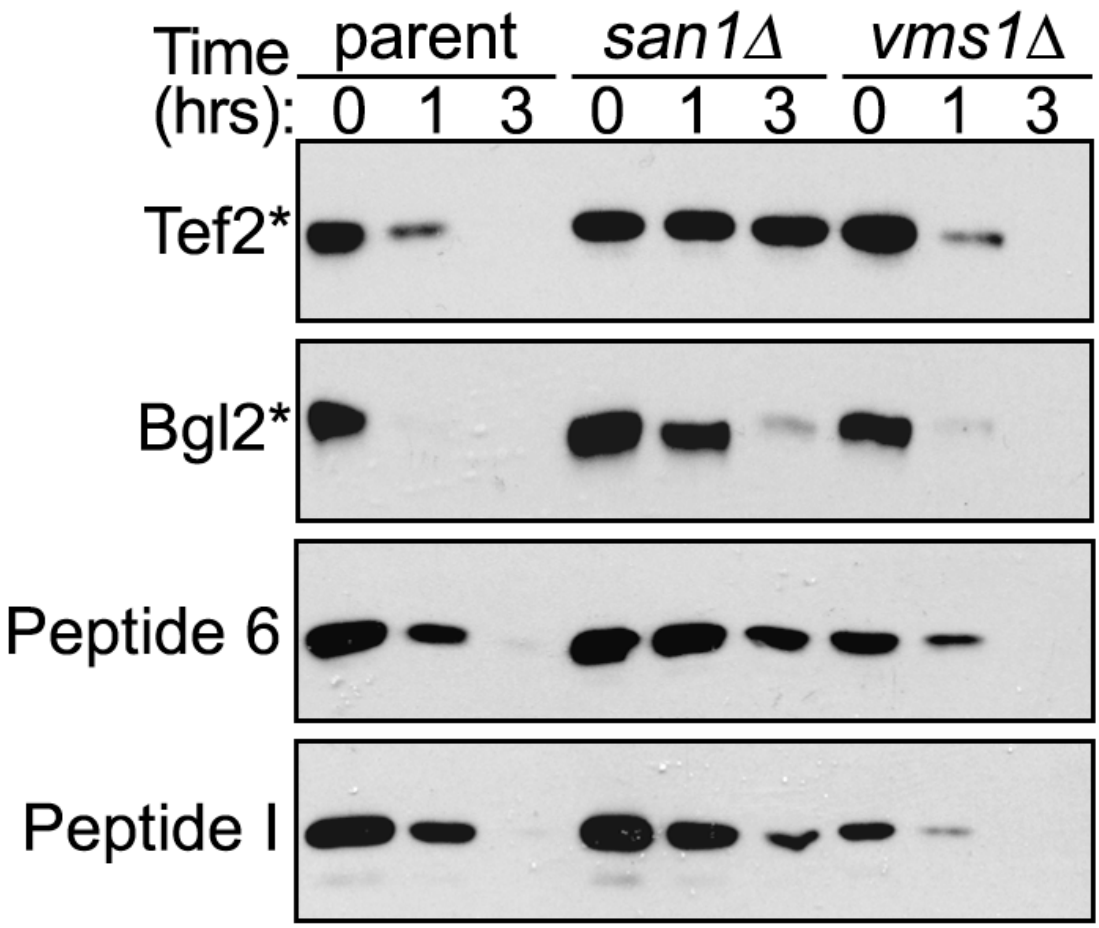

Figure 3.3: Vms1 is not involved in Cdc48-dependent San1-mediated degradation. Cycloheximide-chase degradation assays were performed to assess the stability of GFP^{NLS}-Tef2*, and GFP^{NLS}-Bgl2*, GFP^{NLS}-Peptide 6, and GFP^{NLS}-Peptide I in parent, *san1*Δ, and *vms1*Δ cells. San1 substrate expression was induced by addition of galactose for 2 hours prior to cycloheximide addition. Time after cycloheximide addition is indicated above each lane. Anti-GFP antibodies were used to detect each substrate.

UBX domain proteins

Members of the largest family of known Cdc48 cofactors each contain a ubiquitin regulatory X (UBX) domain (Schuberth and Buchberger, 2008). There are seven UBX domain proteins in yeast that have all been shown to directly interact with Cdc48. In addition to having a UBX domain, Ubx1, Ubx2, and Ubx5 each contain a UBA domain and can bind ubiquitinated proteins *in vivo* (Schuberth et al., 2004).

Ubx2 has been the best characterized of the UBX proteins for its function in coordinating degradation of misfolded ER proteins. Ubx2 is an integral ER membrane protein and has been found to assist Cdc48 in ER-associated degradation (ERAD). Ubx2 recruits Cdc48 to the ER membrane and mediates the interaction between the Cdc48 complex and the ER membrane E3s, Hrd1 and Doa10 (Alberts et al., 2009; Neuber et al., 2005; Schuberth and Buchberger, 2005). It has also been shown that Ubx4 is crucial for efficient ERAD, yet is not found in a complex with Ubx2 (Alberts et al., 2009). This suggests that individual UBX proteins are recruited to Cdc48 at distinct steps to regulate Cdc48 activity in the same pathway. Furthermore, Ubx1, Ubx4, and Ubx5 have been shown to modulate Cdc48-dependent degradation of the largest subunit of RNA polymerase II (Verma et al., 2011). Although a number of roles of many UBX proteins have been documented, the complete breadth of UBX protein functions in the cell remains to be elucidated.

Ubx1, Ubx4, and Ubx5 facilitate Cdc48-dependent, San1-mediated degradation

Of the seven UBX domain proteins in yeast, GFP-tagged Ubx1, Ubx4, and Ubx5 localize predominantly to the nucleus (http://yeastgfp.yeastgenome.org/). I therefore focused my analyses on these particular UBX proteins to determine if any function in Cdc48-dependent, San1-mediated degradation. I found that Ubx1, Ubx4, and Ubx5 were each required for the degradation of GFP^{NLS}-Tef2* and GFP^{NLS}-Bgl2*, with each substrate stabilized in mutant *ubx1*Δ, *ubx4*Δ, and *ubx5*Δ cells nearly to the same extent as in *san1*Δ cells (Figure 3.4, 3.5, 3.6). I found that the degradation of GFP^{NLS}-Peptide 6 and GFP^{NLS}-Peptide I was partially stabilized in *ubx1*Δ, *ubx4*Δ, and *ubx5*Δ strains (Figure 3.4, 3.5, 3.6). I did not observe additional stabilization of any substrates in *san1*Δ*ubx1*Δ, *san1*Δ*ubx4*Δ, or *san1*Δ*ubx5* strains, indicating that Ubx1, Ubx4, and Ubx5 are functioning in the San1 degradation pathway.

I also evaluated whether the other known UBX proteins participated in Cdc48-dependent, San1 mediated nuclear PQC. I did not observe stabilization of any San1 substrates in *ubx2*Δ, *ubx3*Δ, *ubx6*Δ, or *ubx7*Δ cells (Figure 3.7).

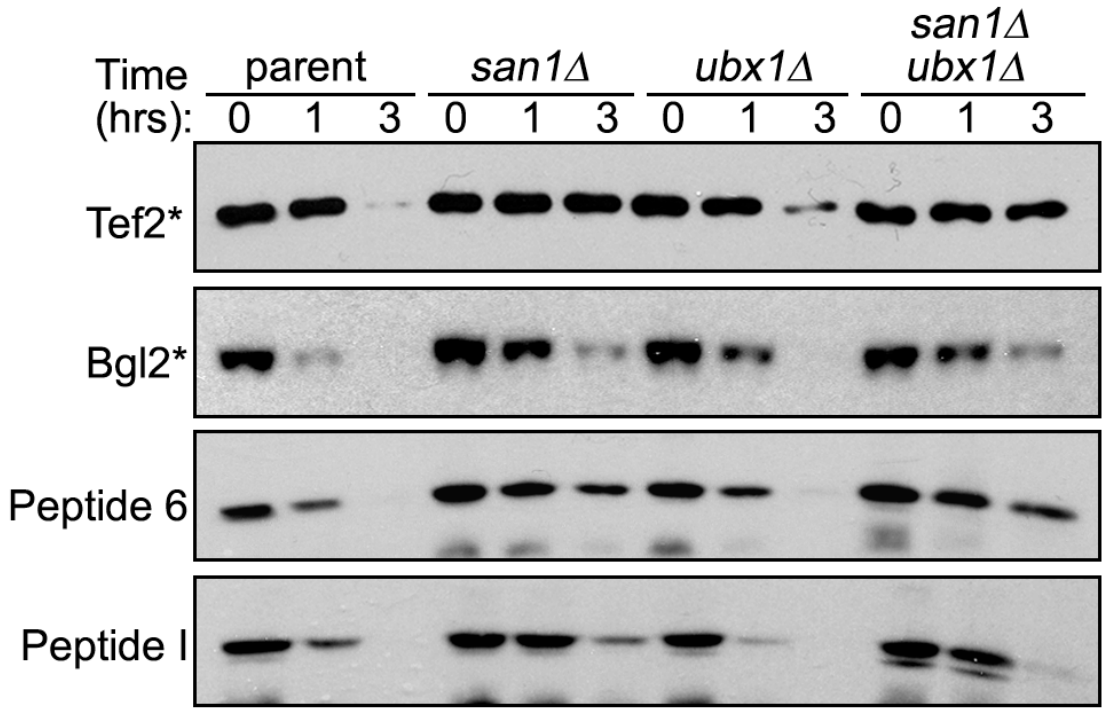

Figure 3.4: Ubx1 is involved in Cdc48-dependent San1-mediated degradation. Cycloheximide-chase degradation assays were performed to assess the stability of GFP^{NLS}-Tef2*, and GFP^{NLS}-Bgl2*, GFP^{NLS}-Peptide 6, and GFP^{NLS}-Peptide I in parent, *san1*Δ, *ubx1*Δ, and *san1*Δ*ubx1*Δ cells. San1 substrate expression was induced by addition of galactose for 2 hours prior to cycloheximide addition. Time after cycloheximide addition is indicated above each lane. Anti-GFP antibodies were used to detect each substrate.

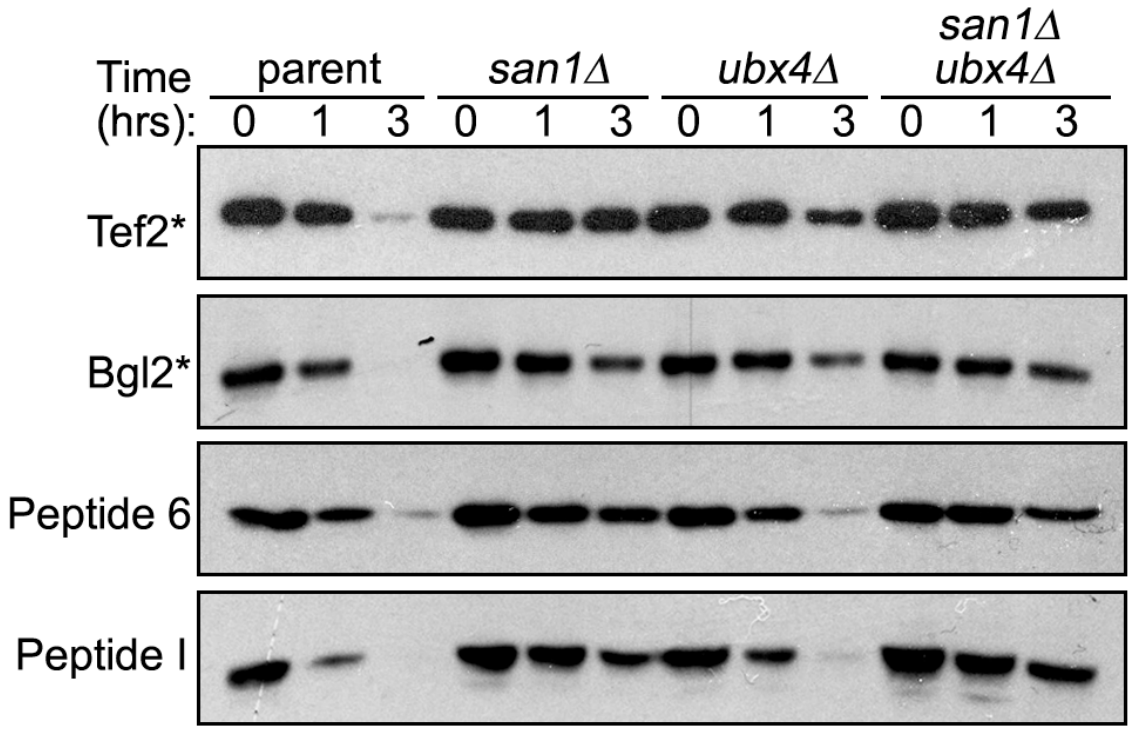

Figure 3.5: Ubx4 is involved in Cdc48-dependent San1-mediated degradation. Cycloheximide-chase degradation assays were performed to assess the stability of GFP^{NLS}-Tef2*, and GFP^{NLS}-Bgl2*, GFP^{NLS}-Peptide 6, and GFP^{NLS}-Peptide I in parent, *san1*Δ, *ubx4*Δ, and *san1*Δ*ubx4*Δ cells. San1 substrate expression was induced by addition of galactose for 2 hours prior to cycloheximide addition. Time after cycloheximide addition is indicated above each lane. Anti-GFP antibodies were used to detect each substrate.

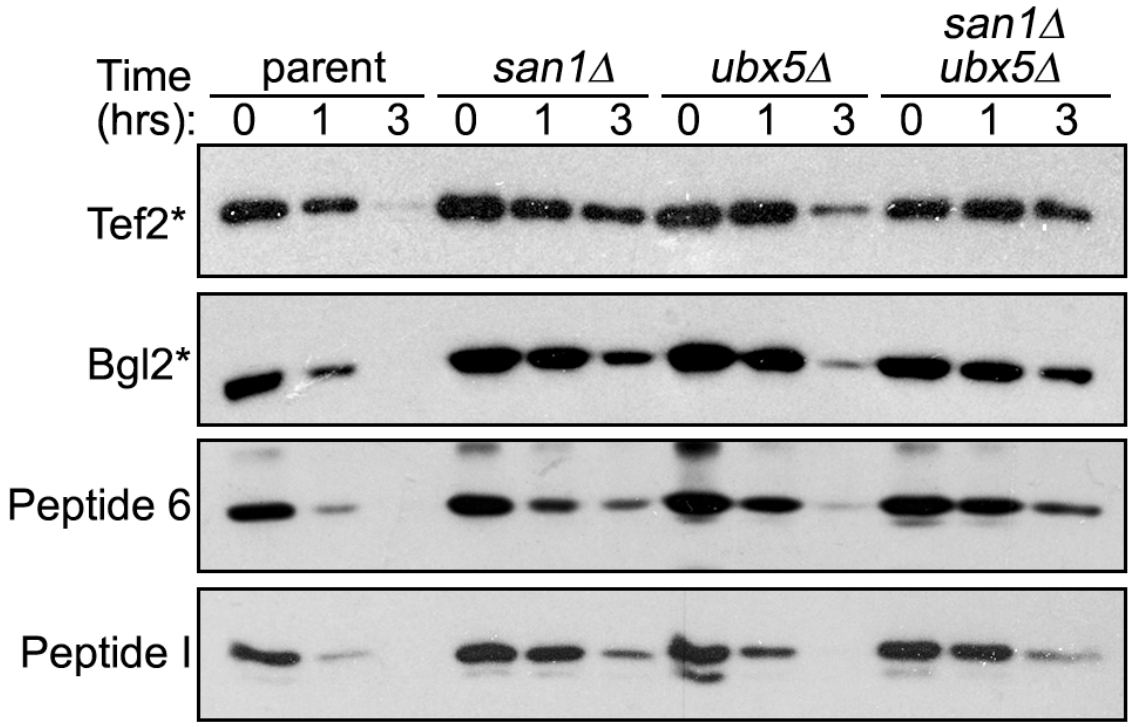

Figure 3.6: Ubx5 is involved in Cdc48-dependent San1-mediated degradation. Cycloheximide-chase degradation assays were performed to assess the stability of GFP^{NLS}-Tef2*, and GFP^{NLS}-Bgl2*, GFP^{NLS}-Peptide 6, and GFP^{NLS}-Peptide I in parent, *san1*Δ, *ubx5*Δ, and *san1*Δ*ubx5*Δ cells. San1 substrate expression was induced by addition of galactose for 2 hours prior to cycloheximide addition. Time after cycloheximide addition is indicated above each lane. Anti-GFP antibodies were used to detect each substrate.

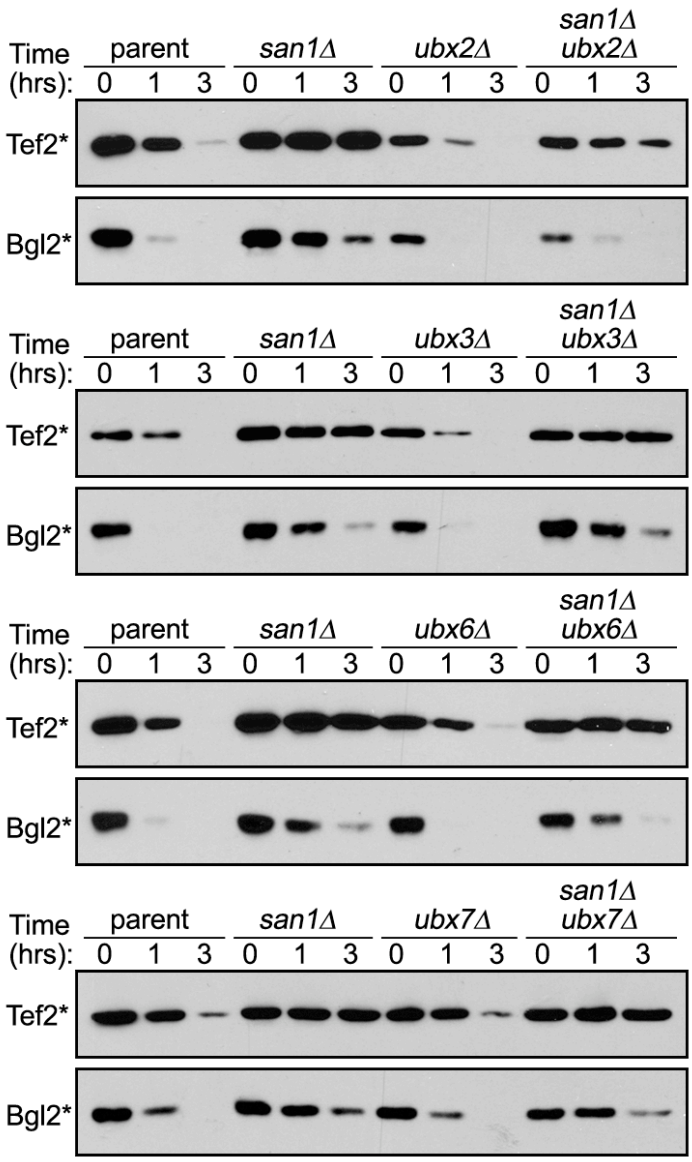

Figure 3.7: Ubx2, Ubx3, Ubx6 and Ubx7 are not involved in Cdc48-dependent San1-mediated degradation. Cycloheximide-chase degradation assays were performed to assess the stability of GFP^{NLS}-Tef2*, and GFP^{NLS}-Bgl2* in parent, *san1*Δ, *ubx2*Δ, *san1*Δ*ubx2*Δ, *ubx3*Δ, *san1*Δ*ubx3*Δ, *ubx6*Δ, *san1*Δ*ubx6*Δ, *ubx7*Δ, and *san1*Δ*ubx7*Δ cells. San1 substrate expression was induced by addition of galactose for 2 hours prior to cycloheximide addition. Time after cycloheximide addition is indicated above each lane. Anti-GFP antibodies were used to detect each substrate.

Ubx1, Ubx4, and Ubx5 operate in the same pathway

Because the data indicated that multiple UBX proteins were important in facilitating Cdc48-dependent, San1-mediated nuclear PQC degradation, I wanted to ascertain if the UBX proteins were functioning sequentially or in parallel pathways. I found that deletion of both *UBX1* and *UBX4* resulted in synthetic lethality (Figure 3.8), which prevented me from querying the double mutant. The double *ubx1*Δ*ubx5*Δ and double *ubx4*Δ*ubx5*Δ mutant cells were viable and we did not observe significant enhancement in the stabilization of GFP^{NLS}-Tef2* or GFP^{NLS}-Bgl2* compared to the single deletion mutants (Figure 3.9, 3.10). Thus, we think it is likely that Ubx1, Ubx4, and Ubx5 are operating in the same pathway to facilitate degradation of San1 substrates.

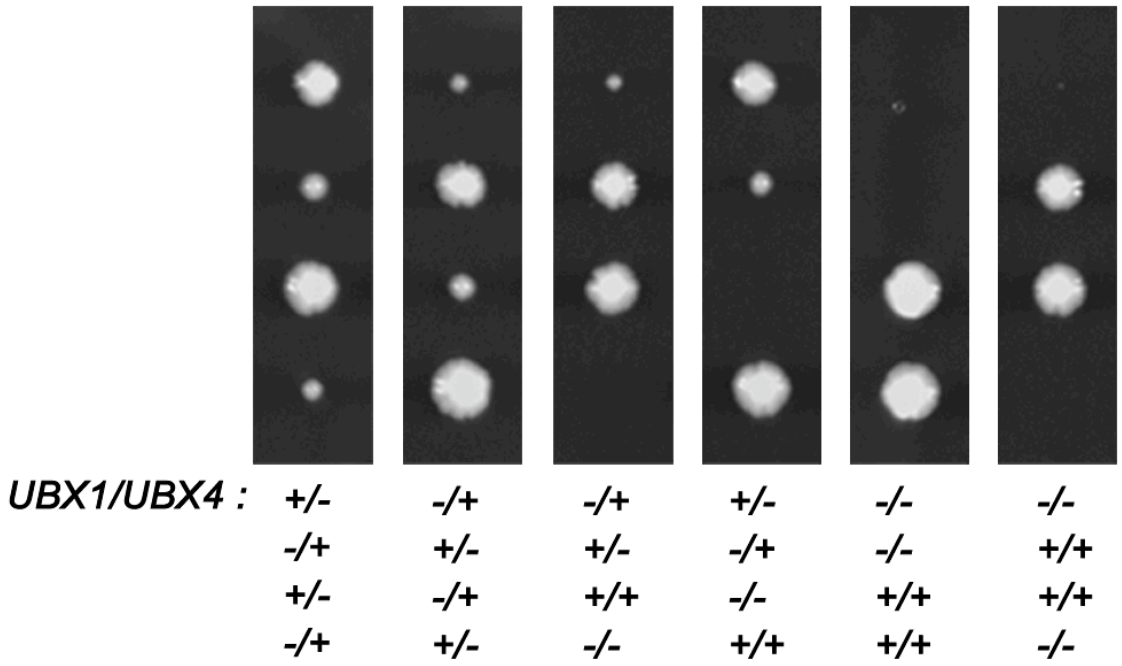

Figure 3.8: Deletion of *UBX1* and *UBX4* is synthetically lethal. Tetrads were dissected to show synthetic lethality upon double *UBX1* and *UBX4* deletions. Growth of spores from individual tetrads on rich media is shown on vertical strips. The genotype for each spore is indicated underneath each tetrad.

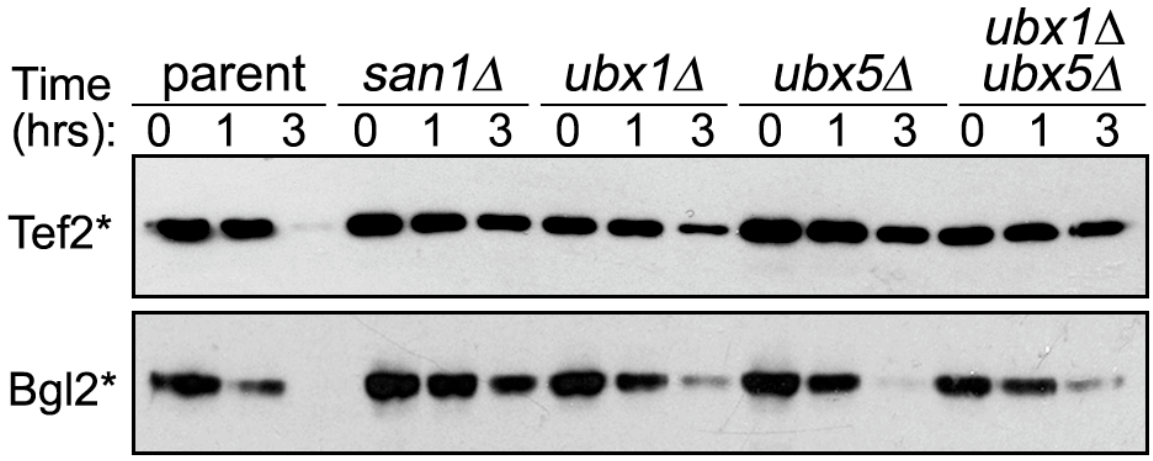

Figure 3.9: Ubx1 and Ubx5 operate in the same pathway. Cycloheximide-chase degradation assays were performed to assess the stability of GFP^{NLS}-Tef2* and GFP^{NLS}-Bgl2* in parent, *san1*Δ, *ubx1*Δ, *ubx5*Δ, and *ubx1*Δ*ubx5*Δ cells. San1 substrate expression was induced by addition of galactose for 2 hours prior to cycloheximide addition. Time after cycloheximide addition is indicated above each lane. Anti-GFP antibodies were used to detect each substrate.

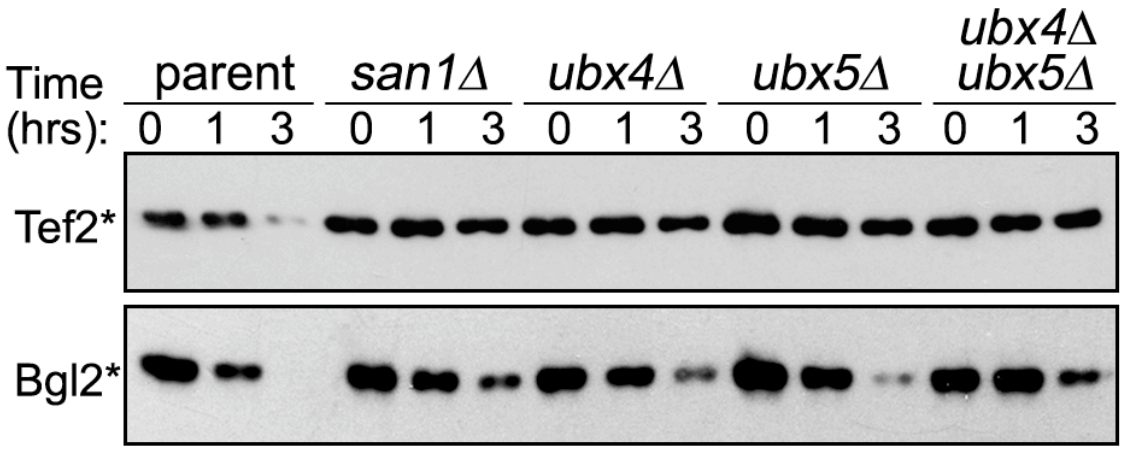

Figure 3.10: Ubx4 and Ubx5 operate in the same pathway. Cycloheximide-chase degradation assays were performed to assess the stability of GFP^{NLS}-Tef2* and GFP^{NLS}-Bgl2* in parent, *san1*Δ, *ubx4*Δ, *ubx5*Δ, and *ubx4*Δ*ubx5*Δ cells. San1 substrate expression was induced by addition of galactose for 2 hours prior to cycloheximide addition. Time after cycloheximide addition is indicated above each lane. Anti-GFP antibodies were used to detect each substrate.

Ubx4 and Ubx5 function in a post-ubiquitination step

Since I found enhanced ubiquitination of substrates in the absence of Cdc48 function (Figure 2.4), I wanted to see if GFP^{NLS}-Tef2* ubiquitination was similarly increased in *ubx4*Δ or *ubx5*Δ cells. Ubx4 and Ubx5 are cofactors for Cdc48 that are required for GFP^{NLS}-Tef2* degradation (Figure 3.5, 3.6). In both *ubx4*Δ and *ubx5*Δ cells, we observed a modest increase in GFP^{NLS}-Tef2* ubiquitination, though the increase was not as pronounced as seen in *cdc48-3* cells (Figure 3.11). We also saw an overall increase in the size of the higher molecular weight ubiquitinated GFP^{NLS}-Tef2* conjugates in both *ubx4*Δ and *ubx5*Δ cells, but the increase was less than that observed in *cdc48-3* cells (Figure 3.11). These data indicate that Cdc48 and its cofactors act downstream of San1 in a post-ubiquitination step.

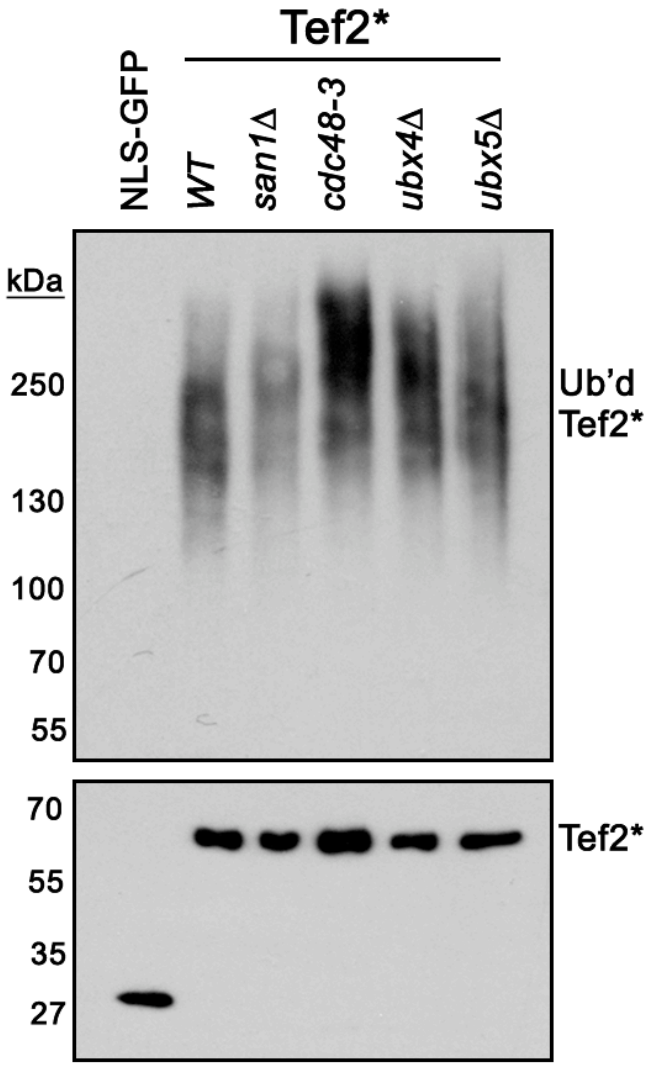

Figure 3.11: Ubx4 and Ubx5 function in a post-ubiquitination step.
Ubiquitination assays were performed to examine levels of ubiquitinated GFP^{NLS}-Tef2* in parent, *ubx4*Δ, and *ubx5*Δ cells expressing 3HA-ubiquitin. GFP-Tef2* expression was induced by addition of galactose for 2 hours in log phase. Cells were shifted to 37ºC 1 hour prior to lysis. GFP^{NLS}-Tef2* or GFP^{NLS} alone was immunoprecipitated from cell lysates. Blots of the immunoprecipitates were probed with anti-HA antibodies to detect ubiquitin (top panel) or anti-GFP antibodies to assess GFP^{NLS}-Tef2* or GFP^{NLS} levels (bottom panel).

Multiple UBX proteins function in the San1 pathway

I found that Ubx1, Ubx4, and Ubx5 are all involved in the degradation of Cdc48-dependent, insoluble San1 substrates (Figures 3.4, 3.5, 3.6). The same three UBX proteins were also found to coordinate Cdc48-dependent degradation of Rpb1, the largest subunit of RNA polymerase II, to execute the DNA damage response following UV irradiation (Verma et al., 2011). From these studies it was suggested that Ubx4 and Ubx5 function in parallel pathways, and our data exploring the relationship between Ubx4 and Ubx5 in San1-mediated degradation suggest that they might be functioning sequentially. I also provide evidence that Ubx1 and Ubx5 may be functioning in the same degradation pathway. In terms of San1-mediated nuclear PQC degradation, it could be that each UBX protein has distinct and separate functions in helping Cdc48 maintain protein solubility or disaggregation, similar to how the AAA-ATPase chaperone Hsp104 uses Hsp26, Hsp42, and Hsp70 for disassembly of protein aggregates (Cashikar et al., 2005; Duennwald et al., 2012; Glover and Lindquist, 1998; Haslbeck et al., 2005; Walter et al., 2011). Exactly how each UBX protein is functioning mechanistically to facilitate nuclear PQC degradation will be an important topic to explore in future studies.

CHAPTER IV: CHAPERONE ROLE AND SUBSTRATE SOLUBILITY IN SAN1-MEDIATED DEGRADATION

Introduction

So far, I have discussed the components that function downstream of San1 ubiquitination, identifying the AAA-ATPase Cdc48 and the adaptors Npl4, Ubx1, Ubx4, and Ubx5 as important players in nuclear PQC degradation. However, in many ubiquitin-mediated degradation pathways, protein chaperones are known to perform a key role prior to or concurrently with the action of E3s. In this chapter, I will highlight our recent findings on chaperone involvement in the San1 pathway for the destruction of misfolded proteins in the nucleus.

One of the outstanding questions in the PQC field is how repair and degradation systems collectively facilitate optimal protein homeostasis. In many cellular compartments, it has been demonstrated that specific chaperones are essential for the degradation of misfolded proteins. For example, the E3 CHIP cooperates with Hsp70 chaperones to coordinate destruction of Hsp70-bound client proteins for ERAD in mammals (Ballinger et al., 1999; Jiang et al., 2001; Murata et al., 2001). In yeast, the ER-membrane ligase Hrd1 partners with Hsp70 chaperone Kar2/BiP to target misfolded proteins in the ER lumen for ubiquitination and subsequent proteasome-dependent destruction (Brodsky et al., 1999; Denic et al., 2006; Huyer et al., 2004; Nishikawa et al., 2001; Taxis et al., 2003). An additional ER-membrane E3, Doa10, requires cytosolic Hsp70 and Hsp40 chaperones for the proteolysis of cytoplasmic ERAD substrates (Huyer et

al., 2004; Metzger et al., 2008; Nakatsukasa et al., 2008). Ubr1, a E3 that localizes to the cytoplasm and nucleus, also partners with Hsp40 and Hsp70 chaperones to mediate cytosolic quality control degradation (Eisele and Wolf, 2008; Heck et al., 2010; Nillegoda et al., 2010; Park et al., 2007). Taken together, chaperones are very intimately involved in ubiquitin-mediated proteolysis.

Although protein chaperones have been implicated in the degradation of misfolded substrates in the ER and cytoplasm, their mechanistic action in these pathways is not known. One hypothesis is that chaperones could be directly involved in PQC degradation by mediating interactions between the ligase and substrate. Alternatively, chaperones might be required to maintain substrate solubility to allow for recognition of substrates by E3s. Furthermore, they could be performing additional yet-to-be discovered roles in ubiquitin-mediated degradation.

We were interested in exploring the potential involvement of chaperones in the San1 pathway for nuclear PQC degradation. Our previous studies indicated that San1 is capable of directly ubiquitinating misfolded proteins *in vitro*, suggesting that it does not require the aid of molecular chaperones for substrate recognition (Rosenbaum et al., 2011). However, two recent papers proposed the contrary from *in vivo* studies. It was demonstrated that San1 requires Hsp70 chaperones (Ssa1/Ssa2) and an Hsp110 chaperone (Sse1) for misfolded substrates that need to be transported from the cytoplasm into the nucleus (Heck et al., 2010; Prasad et al., 2010). We therefore wanted to determine if there are

universal *in vivo* requirements for Ssa1/Ssa2 and additional nuclear chaperones in the San1 degradation pathway.

Requirement for Hsp70 chaperones Ssa1/Ssa2 in San1-mediated degradation correlates with substrate insolubility

Previous studies have shown that Ssa1/Ssa2 are required for the degradation of ΔssCPY* and Δ2GFP which are targeted by San1 for ubiquitination in the nucleus (Heck et al., 2010; Prasad et al., 2010). Intriguingly, these substrates appeared in the nucleus despite not containing canonical nuclear localization signals (NLS). In order to determine whether Ssa1/Ssa1 are universally required for San1-mediated degradation, Eric Fredrickson selected representative examples from distinct classes of San1 substrates, including missense point mutants (Gardner et al., 2005) and truncated proteins (Rosenbaum et al., 2011), and tested for dependency on Ssa1/Ssa2 for their degradation. Furthermore, he compared Ssa1/Ssa2 involvement in the degradation of these substrates to a known Ssa1/Ssa2 substrate, Δ2GFP (Prasad et al., 2010).

Eric discovered that there are differential requirements for Ssa1/Ssa2 in the San1 degradation pathway. In *ssa1*Δ*ssa2*Δ cells, we observed that the San1 substrate Δ2GFP was significantly stabilized, as previously reported (Prasad et al., 2010). When he examined the degradation of GAD-Ura4*, he also found significant stabilization of this +NLS substrate in *ssa1*Δ*ssa2*Δ cells (Figure 4.1). However, the +NLS proteins GAD-Cdc68-1 and GAD-Cdc13-1, were not

stabilized to any observable extent in *ssa1*Δ*ssa2*Δ cells (Figure 4.1). Taken together, our data indicated that the requirement for Hsp70 chaperones Ssa1/Ssa2 is not universal and depends upon the substrate.

Differential solubility of substrates correlates with Ssa1/Ssa2 dependency

We next aimed to elucidate what characteristic of the substrates might require the chaperone function of Ssa1/Ssa2. Our previous data revealed that San1 can ubiquitinate denatured luciferase *in vitro*, however was incapable of ubiquitinating higher molecular forms of denatured luciferase that were most likely aggregates (Rosenbaum et al., 2011). Since we determined that exposed hydrophobicity is the key feature that San1 recognizes in its misfolded substrates (Fredrickson et al., 2011), burial of hydrophobic regions within an aggregate would render substrates inaccessible to San1. Because a major function of molecular chaperones is to maintain protein solubility, we predicted Ssa1/Ssa2 could be selectively targeting insoluble, aggregation-prone misfolded proteins to facilitate San1-mediated degradation.

We tested our hypothesis by exploring how each San1 substrate partitioned between soluble supernatant and insoluble pellet fractions in parent and *ssa1*Δ*ssa2*Δ cells. Eric found that substrates that required Ssa1/Ssa2 to be degraded, Δ2GFP and GAD-Ura4*, had significant portions of their cellular pool partitioning to the insoluble fraction in parent cells. Moreover, even greater levels of Ssa1/Ssa2-dependent substrates partitioned to the insoluble pool in *ssa1*Δ*ssa2*Δ cells. By contrast, substrates that showed no dependency on

Ssa1/Ssa2 for their degradation, GAD-Cdc68-1 and GAD-Cdc13-1, had very little partitioning into the insoluble fraction in either parent or *ssa1*Δ*ssa2*Δ cells (Figure 4.2). Therefore, we were able to conclude that the requirement for Ssa1/Ssa2 in San1-mediated degradation directly correlated with substrate insolubility.

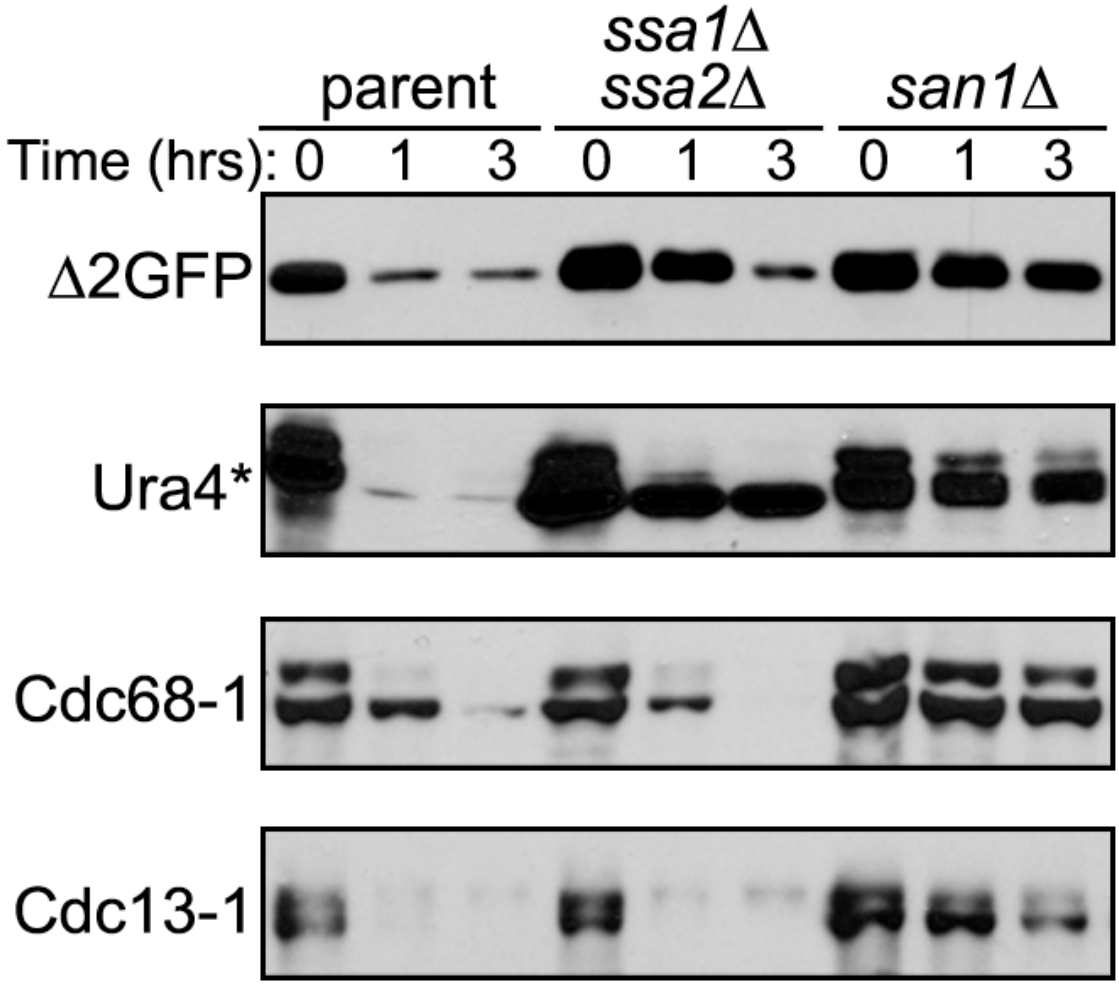

Figure 4.1: The Hsp70 chaperones Ssa1 and Ssa2 are not universally required for San1-mediated degradation. Cycloheximide-chase degradation assays were performed to assess the stability of Δ2GFP, GAD-Ura4*, GAD-Cdc68-1, and GAD-Cdc13-1 in parent cells, *ssa1*Δ*ssa2*Δ cells, and *san1*Δ cells. Time after cycloheximide addition is indicated above the blots. Anti-HA (Δ2GFP) or anti-GAD antibodies (GAD-Ura4*, GAD-Cdc68-1, and GAD-Cdc13-1) were used to detect each appropriate substrate.

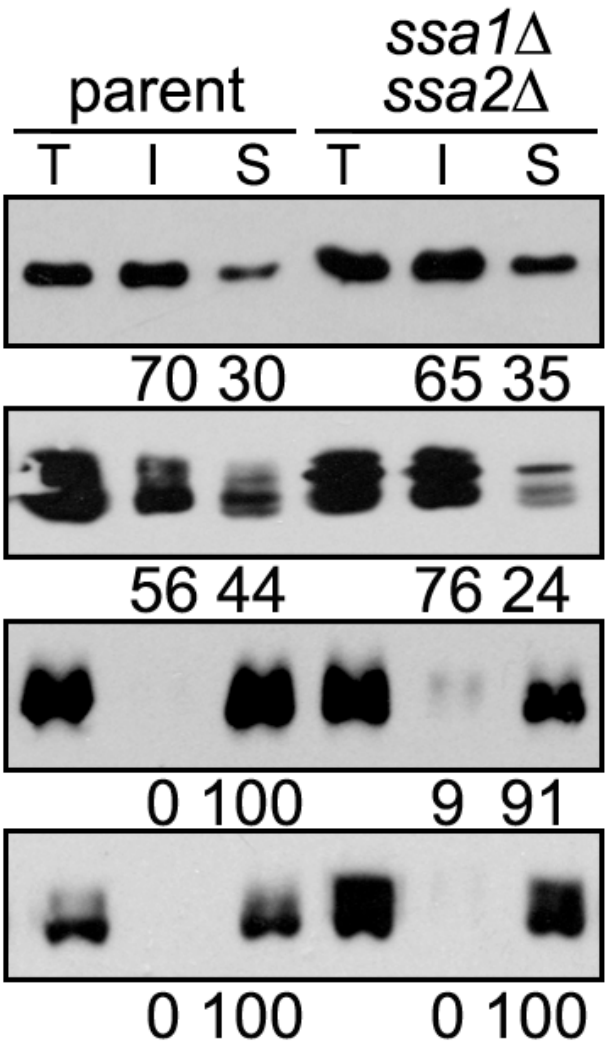

Figure 4.2: Differential solubility of substrates correlates with Ssa1/Ssa2 dependency. Solubility assays were performed to determine how Δ2GFP, GAD-Ura4*, GAD-Cdc68-1, and GAD-Cdc13-1 partition between the insoluble pellet fraction (I) and the soluble supernatant fraction (S). Total lysate (T) indicates the total amount of Δ2GFP, GAD-Ura4*, GAD-Cdc68-1, or GAD-Cdc13-1 in cell lysates. Anti-HA or anti-GAD antibodies were used to detect each appropriate substrate. Numbers below each blot indicate the percentage of substrate in each fraction. Relative levels of the insoluble and soluble fractions were determined using ImageJ.

Small heat shock proteins

In addition to Hsp70 proteins, we also explored the potential involvement of other classes of molecular chaperones in San1-mediated degradation. Intriguingly, we previously revealed that numerous heat shock proteins are up-regulated in the absence of San1 by comparing transcript microarray profiles of parent and *san1*Δ cells (Gardner et al., 2005). One of the most highly up-regulated genes was *HSP26*, which encodes a small heat shock protein known to suppress aggregation of cytosolic proteins (Haslbeck et al., 2004). Hsp26 accumulates in the nucleus during heat shock (Rossi and Lindquist, 1989), however, its nuclear functions remain poorly understood. An additional small heat shock protein whose expression was significantly increased in the absence of San1 was *HSP42* (Gardner et al., 2005). Hsp42 has been found to share approximately 90% substrate overlap with Hsp26 (Haslbeck et al., 2004). Thus, we were interested in determining if either Hsp26 or Hsp42 played a role in the destruction of misfolded nuclear proteins.

Eric first examined the degradation of San1 substrates that showed significant Ssa1/Ssa2 dependency in *hsp26*Δ and *hsp42*Δ cells. None of the substrates he tested displayed any dependency on either Hsp26 or Hsp42, as indicated by the lack of stabilization in *hsp26*Δ and *hsp42*Δ cells. (Figure 4.3, 4.4). I also explored the potential involvement of Hsp26 and Hsp42 in the degradation of additional San1 substrates, including known Hsp70 substrates, ΔssCPY* (Heck et al., 2010) and VHL (McClellan et al., 2005). VHL was degraded independently of Hsp26 and Hsp42 (Figure 4.5). Interestingly,

∆ssCPY* was stabilized in *hsp26*∆ cells nearly to the same extent as in *san1*∆ cells (Figure 4.5). I also examined the stability of ∆ssCPY* in *san1*∆*hsp26*∆ cells, however I did not observe enhanced stability in the double mutant compared to the single deletion mutants. This suggests that San1 and Hsp26 may be operating in the same cellular pathway (Figure 4.6). Since ∆ssCPY* lacks an NLS yet is degraded by San1 in the nucleus, we were interested in determining whether Hsp26 was involved in facilitating nuclear import of substrates that originate in the cytosol. To test our hypothesis, I assessed the requirement for Hsp26 in the degradation of truncated proteins that lack an NLS, yet are targeted by San1 for destruction in the nucleus. In no case did I find Hsp26 involvement in the degradation of any additional substrates tested (Figure 4.7).

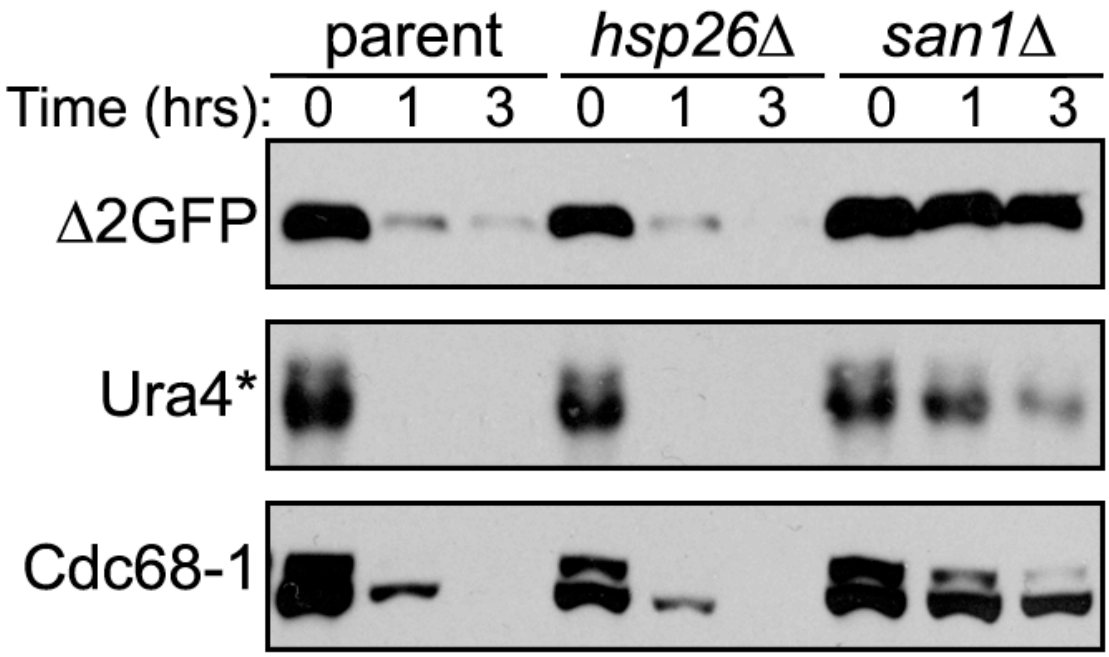

Figure 4.3: Hsp26 is not universally required for San1-mediated degradation. Cycloheximide-chase degradation assays were performed to assess the stability of Δ2GFP, GAD-Ura4*, and GAD-Cdc68-1 in parent, *hsp26*Δ, *san1*Δ cells. Time after cycloheximide addition is indicated above the blots. Anti-HA or anti-GAD antibodies were used to detect each appropriate substrate.

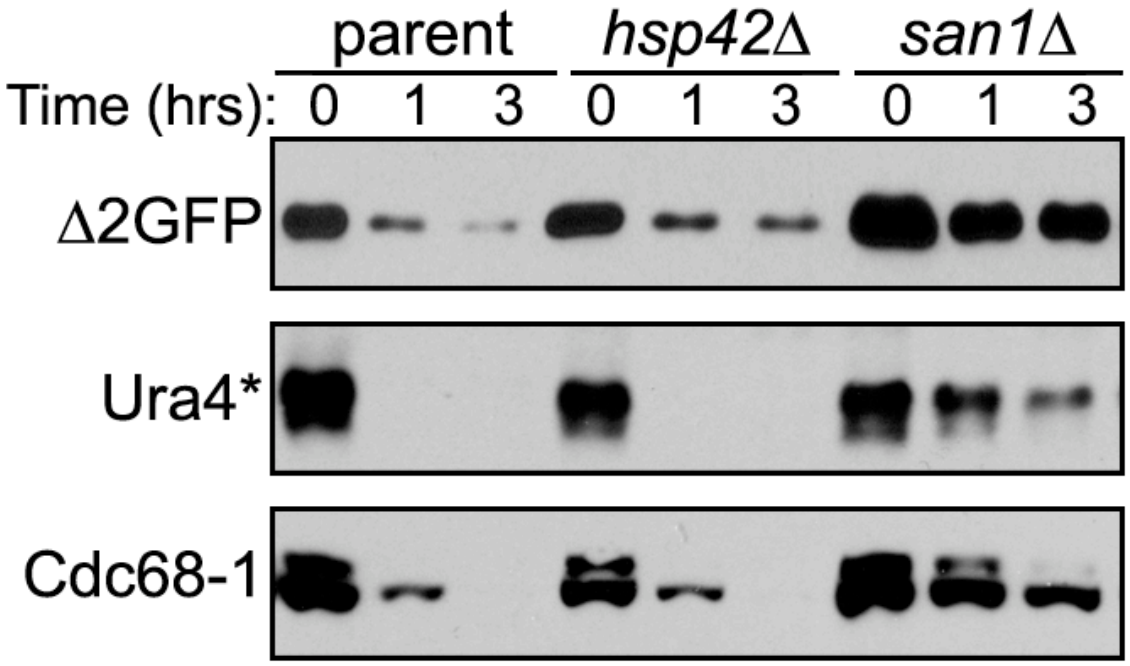

Figure 4.4: Hsp42 is not required for San1-mediated degradation.
Cycloheximide-chase degradation assays were performed to assess the stability of Δ2GFP, GAD-Ura4*, and GAD-Cdc68-1 in parent, *hsp42*Δ, *san1*Δ cells. Time after cycloheximide addition is indicated above the blots. Anti-HA or anti-GAD antibodies were used to detect each appropriate substrate.

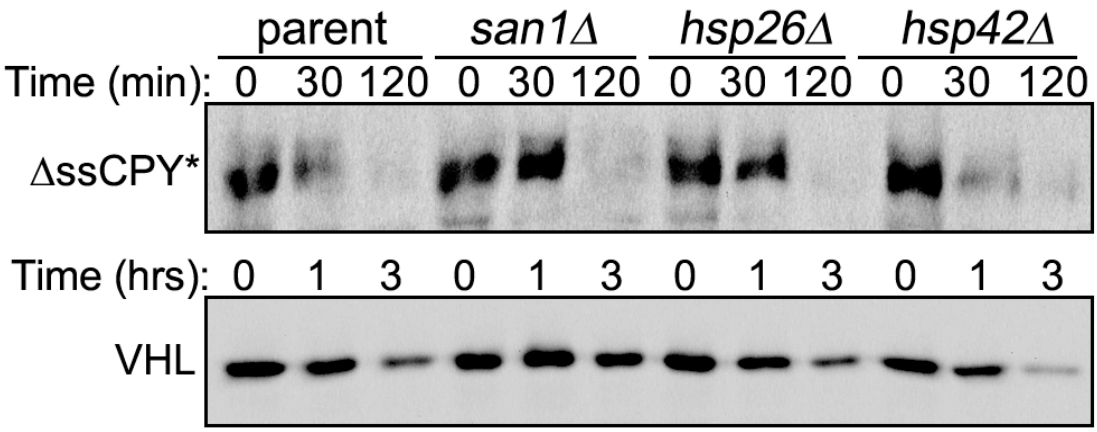

Figure 4.5: Hsp26 is involved in the degradation of ΔssCPY*. Cycloheximide-chase degradation assays were performed to assess the stability of ΔssCPY*-GFP and GFP-VHL in parent, *san1Δ, hsp26Δ,* and *hsp42Δ* cells. Time after cycloheximide addition is indicated above the blots. Anti-GFP antibodies were used to detect each substrate.

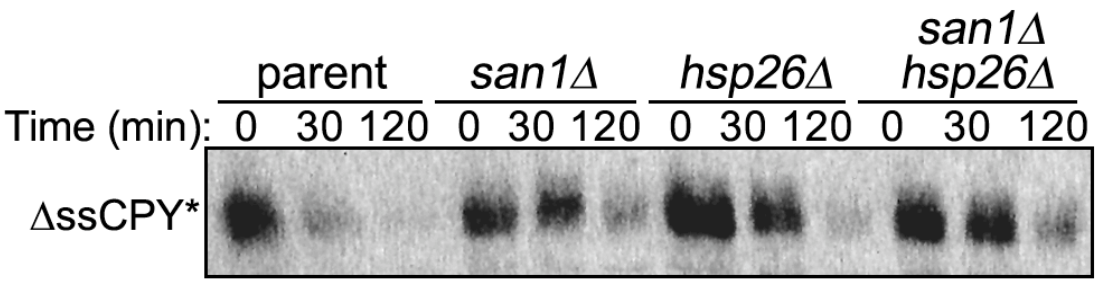

Figure 4.6: San1 and Hsp26 operate in the same pathway for ΔssCPY* degradation. Cycloheximide-chase degradation assays were performed to assess the stability of ΔssCPY*-GFP in parent, *san1Δ, hsp26Δ,* and *san1Δhsp26Δ* cells. Time after cycloheximide addition is indicated above the blots. Anti-GFP antibodies were used to detect substrate.

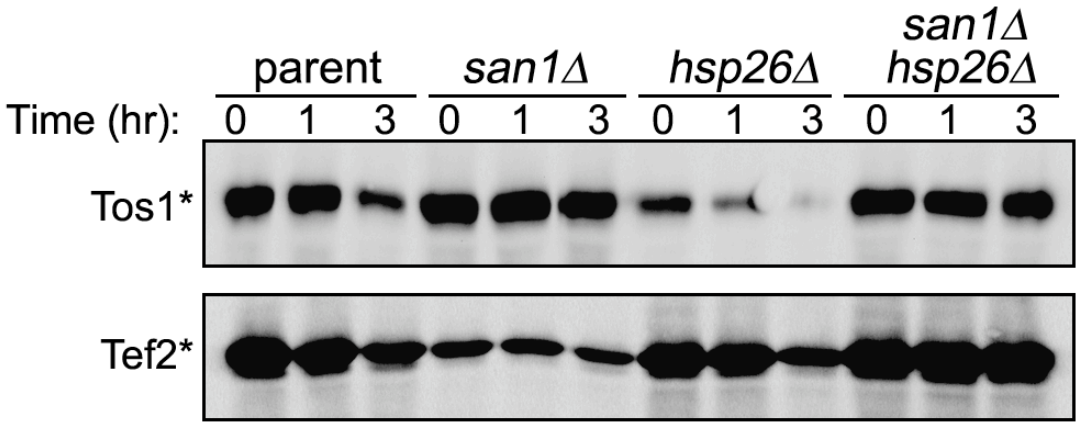

Figure 4.7: Hsp26 is not involved in the degradation of additional –NLS San1 substrates. Cycloheximide-chase degradation assays were performed to assess the stability of GFP-Tos1* and GFP-Tef2* in parent, *san1*Δ*, hsp26*Δ*,* and *san1*Δ*hsp26*Δ cells. Time after cycloheximide addition is indicated above the blots. Anti-GFP antibodies were used to detect substrate.

San1 recognition of hydrophobicity correlates with substrate insolubility

Our data suggests substrate insolubility is a critical factor for Cdc48 and chaperone recruitment in San1-mediated degradation. In terms of San1 recognition of substrates, we previously revealed exposed hydrophobicity as the key feature that determines San1 dependency. To clearly delineate this principle, we showed that San1 recognizes short hydrophobic peptides as degrons when fused to reporter proteins (Fredrickson et al., 2011). Using these peptides, we next wanted to explore the biochemical parameters of the exposed hydrophobicity that leads to their San1 recognition. We previously determined that a minimum of five contiguous hydrophobic residues in the peptide is required for San1-mediated degradation (Fredrickson et al., 2011). We wanted to further elucidate the biochemical nature of this window of hydrophobicity.

Eric examined *in vivo* solubility of GFP^{NLS}-peptide fusions containing 3, 4, 5, 6, or 7 contiguous hydrophobic residues. He found that the threshold for San1-mediated degradation, ≥5 contiguous hydrophobic residues, correlated with the GFP^{NLS}-peptide fusions partitioning to the insoluble fraction. The GFP^{NLS}-peptide fusions containing ≤4 continuous hydrophobic residues, however, were predominantly soluble (Figure 4.9).

We surmised that the GFP^{NLS}-peptide fusions present in the insoluble fraction are likely part of large inclusions since this fraction represents the cellular debris that pellets at 12,800 x g (See Appendix II). Therefore, I examined whether the GFP^{NLS}-peptide fusions in the soluble fraction formed high molecular mass species typical of aggregates using nondenaturing PAGE (Jung et al.,

2004; Lefebvre et al., 2004). Parallel to the solubility assays, I found that the GFP^{NLS}-peptide fusions with ≥5 contiguous hydrophobic residues formed higher molecular mass species compared with GFP^{NLS}-peptide fusions with containing ≤4 continuous hydrophobic residues that ran as monomers (Figure 4.10). These higher molecular weight species were sensitive to the addition of SDS to the loading buffer, indicating that they are likely not SDS-insensitive amyloids (Kryndushkin et al., 2003). Taken together, our data suggests that San1 recognizes exposed hydrophobicity that crosses a particular threshold of insolubility correlated with aggregation.

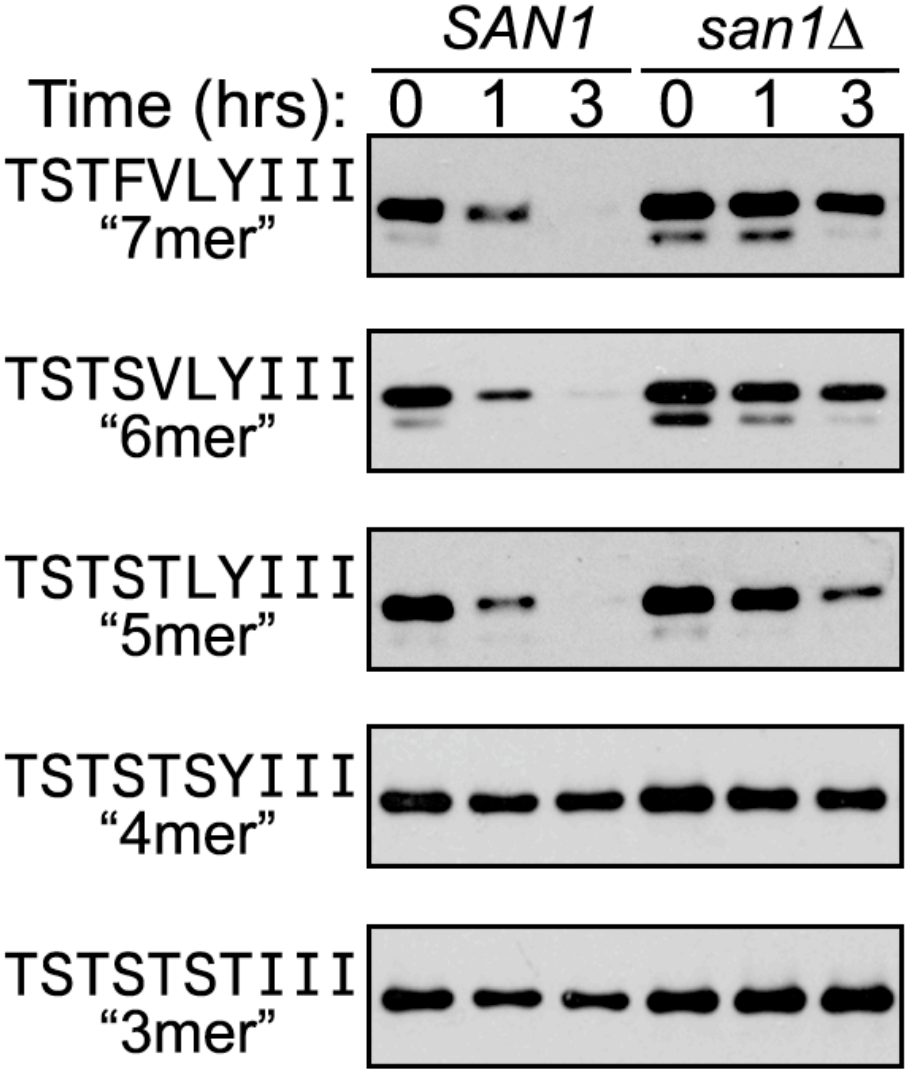

Figure 4.8: Five contiguous hydrophobic residues in the peptide are required for San1-mediated degradation. Cycloheximide-chase degradation assays were performed to assess the stability of GFP^{NLS}-peptide fusions containing 3-7 contiguous hydrophobic residues in the peptide degron in parent and *san1*Δ cells. Time after cycloheximide addition is indicated above the blots. Anti-GFP antibodies were used to detect substrate.

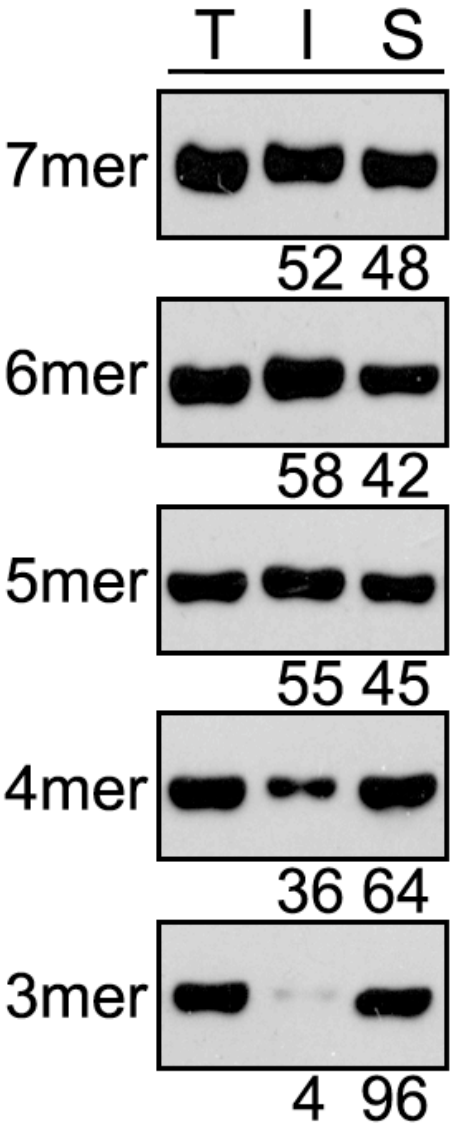

Figure 4.9: San1-mediated degradation correlates with substrate insolubility. Sedimentation assays were performed to determine how the indicated GFP^{NLS}-peptide fusion partitions between the insoluble pellet fraction (I) and the soluble supernatant fraction (S) in parent and *san1*Δ cells. Total lysate (T) indicates the total amount of GFP^{NLS}-peptide fusion in cell lysates. Anti-GFP antibodies were used to detect each substrate. Percentage of protein in the insoluble versus soluble fractions is listed below each appropriate lane. Relative levels of the insoluble and soluble fractions were determined using ImageJ.

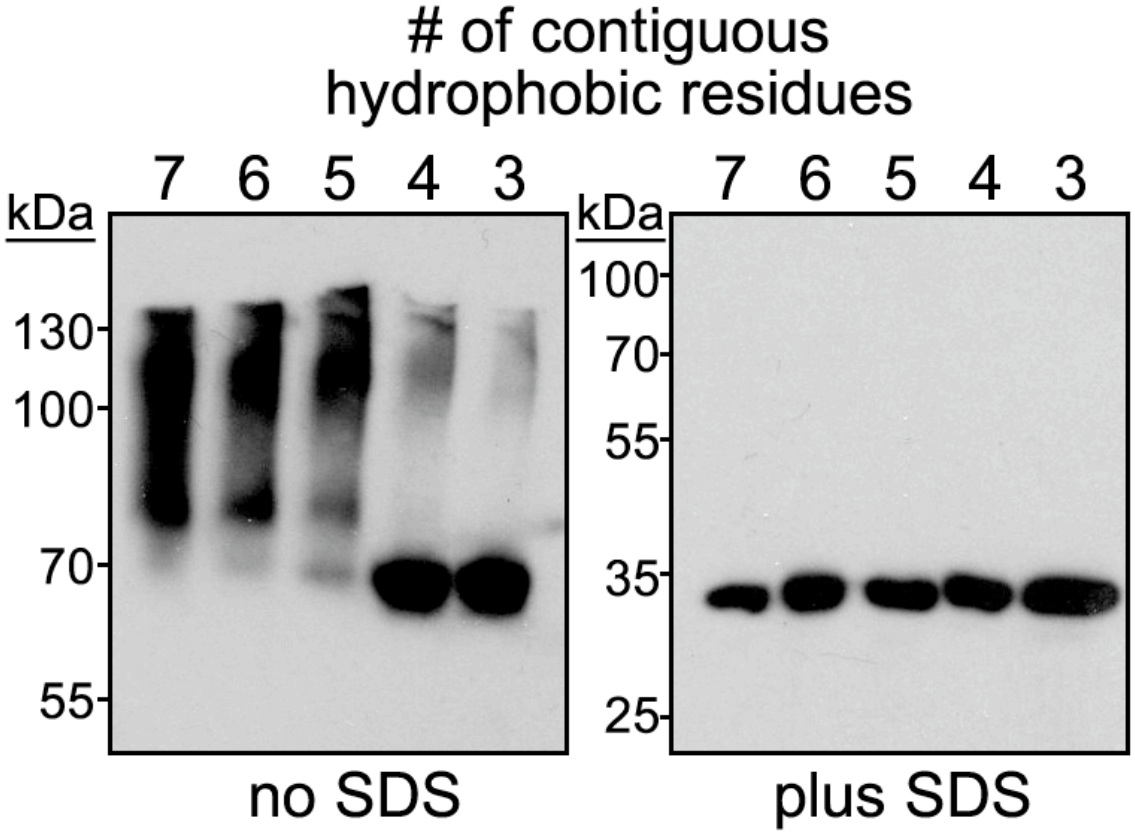

Figure 4.10: Insoluble GFP^{NLS}-peptide fusions form high-molecular weight species. Nondenaturing polyacrylamide gel electrophoresis of GFP^{NLS}-peptide fusions containing 3-7 contiguous hydrophobic residues in the peptide degron was performed to determine if substrates form high-molecular weight species. Soluble fractions were isolated and run on a nondenaturing gel without or with SDS in the loading buffer. Anti-GFP antibodies were used to detect each substrate.

CHAPTER V: CONCLUSIONS

The work in this dissertation unveils several new components that protect the nuclear environment from misfolded proteins. Although Cdc48 had been well established for facilitating quality control degradation in additional cellular compartments, as well as nuclear chromatin-associated processes, its role in the turnover of misfolded proteins in the nucleus had not been defined. I found that Cdc48 is involved in the degradation of some misfolded nuclear proteins, yet intriguingly, it is not required for the degradation of all San1 substrates. I next revealed that solubility is the key determinant for Cdc48 dependency: the more insoluble the substrate the greater the need for Cdc48 in its destruction. Since we observed greater levels of ubiquitinated substrate in *cdc48* mutant cells, we postulated that Cdc48 functions after the action of San1 ubiquitination, upstream of the proteasome. Furthermore, loss of Cdc48 function resulted in a number of adverse cellular consequences when substrates accumulated in the nucleus, including enhanced inclusion formation and cell death. Given that mutations in p97 are correlated with neurodegenerative aggregation disorders such as inclusion body myopathy associated with Paget's disease of bone and frontotemporal dementia (IBMPFD) and familial amyotrophic lateral sclerosis (ALS), it could be that Cdc48/p97 is required to maintain substrate solubility subsequent to ubiquitination en route to the proteasome in order to prevent toxic aggregation from occurring.

Although we clearly illustrate a vital function of Cdc48 in a subset of San1 substrates, we have not resolved how Cdc48 is recruited to insoluble misfolded proteins. Our data indicated that multiple Cdc48 cofactors are involved in San1-mediated degradation, including Npl4, Ubx1, Ubx4, and Ubx5. How each adaptor is functioning mechanistically to aid Cdc48 in nuclear quality control degradation will be an important topic to address in future studies. Ubx1 and Ubx5 each contain a UBA domain that enable them to interact with ubiquitinated proteins *in vivo* (Schuberth et al., 2004). Thus, it is possible that UBA domain-containing adaptors could mediate the interaction between Cdc48 and substrates. Furthermore, we provide evidence that the nuclear UBX domain proteins are operating in the same cellular pathway, however, it remains unclear whether they are associating with Cdc48 simultaneously to form a functional complex, or if they are being recruited to Cdc48 sequentially to mediate distinct steps within the pathway.

A significant theme emerging from our collective studies is that substrate solubility plays a crucial role in determining the path a misfolded nuclear protein will take to destruction. Not only do insoluble proteins require Cdc48 to be degraded, we also demonstrate that Hsp70 chaperones are involved in the degradation of insoluble substrates in the nucleus. Based on our data, it is possible that Ssa1/Ssa2 function to maintain a soluble state of the misfolded protein upstream of San1, and subsequent to ubiquitination, Cdc48 is then recruited to the ubiquitinated substrate to facilitate recognition and degradation

by the proteasome. The precise interplay among chaperones, San1, Cdc48, and the proteasome remains to be elucidated.

Since we revealed that numerous components are required for efficient degradation of insoluble substrates, it will be important to explore whether the accumulation of aggregation-prone misfolded proteins in the nucleus triggers a stress response, similar to the unfolded protein response (UPR) of the ER. Such a signaling cascade might direct localization or up-regulate expression of nuclear quality control regulators so that the nucleus is poised to eliminate potentially harmful misfolded proteins. Future studies should be aimed at determining if expression of insoluble misfolded proteins in the nucleus leads to transcriptional reprogramming in order to facilitate the San1 degradation pathway.

APPENDIX I: STRAINS AND PLASMIDS

Yeast strains

Strain Name	Genotype	Parent	Reference
BY4741	*his3-1, leu2Δ0, met15Δ0, ura3Δ0*		(Brachmann et al., 1998)
RGY506	*san1Δ::KanMX*	BY4741	(Gardner et al., 2005)
RGY4022	*met15Δ0, his3Δ1, ura3Δ0, lys2Δ0, leu2Δ0*		
RGY4025	*san1Δ::KanMX*	RGY4022	
RGY4075	*hsp26Δ::NatMX*	RGY4022	
RGY4078	*san1Δ::KanMX, hsp26Δ::NatMX*	RGY4022	
RGY4081	*hsp42Δ::NatMX*	RGY4022	
RGY4405	*met15Δ0, his3Δ1, ura3Δ0, lys2Δ0, leu2Δ0*		
RGY4407	*san1Δ::KanMX*	RGY4405	
RGY4409	*ubx1Δ::NatMX*	RGY4405	
RGY4411	*san1Δ::KanMX, ubx1Δ::NatMX*	RGY4405	
RGY4414	*met15Δ0, his3Δ1, ura3Δ0, lys2Δ0, leu2Δ0*		
RGY4416	*san1Δ::KanMX*	RGY4414	
RGY4418	*ubx5Δ::NatMX*	RGY4414	
RGY4420	*san1Δ::KanMX, ubx5Δ::NatMX*	RGY4414	
RGY4461	*cdc48-3*	BY4741	
RGY4463	*san1Δ::KanMX, cdc48-3*	BY4741	
RGY5071	*met15Δ0, his3Δ1, ura3Δ0, leu2Δ0*		
RGY5073	*san1Δ::KanMX*	RGY5071	
RGY5075	*ubx2Δ::NatMX*	RGY5071	
RGY5077	*san1Δ::KanMX, ubx2Δ::NatMX*	RGY5071	
RGY5083	*met15Δ0/met15Δ0, his3Δ1/his3Δ1, ura3Δ0/ura3Δ0, LYS2/lys2Δ0, leu2Δ0/leu2Δ0, SAN1/san1Δ::KanMX,*		

	UBX1/ubx1Δ::URA3, UBX4/ubx4Δ::NatMX		
RGY5113	*san1Δ::NatMX*	W303a	
RGY5158	*met15Δ0, his3Δ1, ura3Δ0, leu2Δ0*		
RGY5160	*san1Δ::KanMX*	RGY5158	
RGY5162	*ubx4Δ::NatMX, lys2Δ0*	RGY5158	
RGY5164	*san1Δ::KanMX, ubx4Δ::NatMX, lys2Δ0*	RGY5158	
RGY5166	*met15Δ0, his3Δ1, ura3Δ0, leu2Δ0*		
RGY5168	*san1Δ::KanMX*	RGY5166	
RGY5170	*ubx4Δ::NatMX, lys2Δ0*	RGY5166	
RGY5172	*ubx5Δ::URA3*	RGY5166	
RGY5174	*ubx4Δ::NatMX, ubx5Δ::URA3*	RGY5166	
RGY5176	*pdr5Δ::KanMX,* P_{TDH3}*-3xHA-Ub::URA3*	BY4741	
RGY5177	*san1Δ::NatMX*	RGY5176	
RGY5255	*san1Δ::URA3*	RHY765	
RGY5257	*san1Δ::URA3*	RHY2689	
RGY5325	*cdc48-3*	RGY5176	
RGY5503	*vms1Δ::NatMX*	BY4741	
RGY5551	*met15Δ0, his3Δ1, ura3Δ0, leu2Δ0*		
RGY5552	*san1Δ::KanMX*	RGY5551	
RGY5553	*ubx1Δ::URA3*	RGY5551	
RGY5554	*ubx5Δ::NatMX, lys2Δ0*	RGY5551	
RGY5555	*ubx1Δ::URA3, ubx5Δ::NatMX*	RGY5551	
RGY5569	P_{TDH3}*-3xHA-Ub::URA3*	RGY5162	
RGY5570	P_{TDH3}*-3xHA-Ub::URA3*	RGY4418	
RGY5624	*CDC48-mCherry::HIS3*	BY4741	
RHY2679	*ufd1-1, ura3-52, leu2-3,112, ade1-100, his4-519*		(Johnson et al., 1995)
RHY2680	*ura3-52, leu2-3,112, ade1-100, his4-519*		(Johnson et al., 1995)

RHY726	*npl4-1, ura3-52, leu2Δ1*		(DeHoratius and Silver, 1996)
RHY765	*his3Δ200, ura3-52, leu2Δ1*		(DeHoratius and Silver, 1996)
RPY283	*ssa1Δ::KanMX, ssa2Δ::KanMX*	W303a	(Prasad et al., 2010)
W303a	*ade2-1 his3-11 ura3-1 trp1-1 leu2-3 can1-100*		(Prasad et al., 2010)

Plasmids

Plasmid Name	Encoded Protein	Vector	Reference
pRG1189	GAD-Tef2*	pRS425	(Rosenbaum et al., 2011)
pRG1190	GAD-Bgl2*	pRS425	(Rosenbaum et al., 2011)
pRG1289	GFP^{NLS}-Tef2*	pRS425	(Rosenbaum et al., 2011)
pRG1290	GFP^{NLS}-Bgl2*	pRS425	(Rosenbaum et al., 2011)
pRG1291	GFP^{NLS}-Peptide 6	pRS425	(Fredrickson et al., 2011)
pRG1395	ΔssCPY*-GFP	pRS425	
pRG2054	GAD-Cdc68-1^{NTD}	pRS425	(Rosenbaum et al., 2011)
pRG2056	GAD-Cdc13-1^{NTD}	pRS425	(Rosenbaum et al., 2011)
pRG2304	GFP^{NLS}-Peptide I	pRS425	(Fredrickson et al., 2011)
pRG2342	GFP^{NLS}	pRS425	(Fredrickson et al., 2011)
pRG3025	GFP-VHL	pRS425	
pRG3195	GAD-Ura4*	pRS426	
pRG3630	GAD-Cdc68-1	pRS426	
pRG3668	GAD-Cdc13-1	pRS426	
pRG3770	GFP^{NLS}-Cdc13-1	pRS425	(Rosenbaum et al., 2011)
pRG3771	GFP^{NLS}-Cdc68-1	pRS425	(Rosenbaum et al., 2011)
pRG3789	GFP^{NLS}-TSTFVLYIII	pRS425	(Fredrickson et al., 2013)
pRG3790	GFP^{NLS}-TSTSVLYIII	pRS425	(Fredrickson et al., 2013)

pRG3791	GFP^{NLS}-TSTSTLYIII	pRS425	(Fredrickson et al., 2013)
pRG3792	GFP^{NLS}-TSTSTSYIII	pRS425	(Fredrickson et al., 2013)
pRG3793	GFP^{NLS}-TSTSTSTIII	pRS425	(Fredrickson et al., 2013)
pRG4012	GAD-Δ2GFP	pRS426	

APPENDIX II: MATERIALS AND METHODS

Yeast strains

Yeast strains and plasmids are listed in Appendix I. Standard yeast genetic methods were used in these studies (Guthrie and Fink, 1991). Plasmids were constructed using standard cloning protocols. Oligonucleotide sequences and plasmid construction details will be provided upon request.

Cycloheximide-chase degradation assays

Cycloheximide-chase degradation assays were performed similarly to previously described (Fredrickson *et al.*, 2011). Cells were grown in liquid synthetic media with 3% raffinose to ~1x10^7 cells/ml. Galactose was added to 3% and the cells were incubated 2 hours thereafter. Cycloheximide was added to 50µg/ml and the cells further incubated for 0-3 hours. Cells were lysed at the appropriate time point in 200µl SUMEB buffer (8M Urea, 1% SDS, 10mM MOPS, pH6.8, 10mM EDTA, 1mM PMSF, 0.01% bromophenol blue) by vortexing with 100µL of 0.5mm acid-washed glass beads (Biospec Products). Proteins were resolved on 8% or 16% SDS-PAGE gels, transferred to nitrocellulose, and immunoblotted with anti-GFP antibodies (Sigma) or anti-Gal4AD (GAD) antibodies (Millipore).

Ubiquitination assays

Cells expressing 3HA-ubiquitin were grown in liquid synthetic media with 3% raffinose to ~1x10^7 cells/ml. Galactose was added to 3% and the cells were incubated 2 hours thereafter. Harvested cells were lysed in 200µL SUME buffer (8M Urea, 1% SDS, 10mM MOPS, pH6.8, 10mM EDTA, 1mM PMSF) by

vortexing with 100µL of 0.5mm acid-washed glass beads. Lysates were clarified by centrifugation, and IP buffer (15 mM Na_2HPO_4, 150 mM NaCl, 2% Triton X-100, 0.1% SDS, 0.5% deoxycholate, 10 mM EDTA, pH7.5) was added to each sample to a final volume of 1mL. Anti-GFP antibodies (Sigma) conjugated to Protein A Dynabeads (Dynal) were added to the lysates and incubated overnight at 4˚C. The beads were washed once in IP buffer, and twice in IP wash buffer (50 mM NaCl, 10 mM Tris-HCl, pH7.5). Samples were divided in half and immunoprecipitated proteins were eluted in either SUMEB buffer (for lysate blot) or 100mM acetic acid (for ubiquitin blot), which was subsequently neutralized 1:1 in SUTEB buffer (8M Urea, 1% SDS, 100mM unbuffered Tris-HCl, 10mM EDTA, 0.01% bromophenol blue). All samples were incubated at 65˚C for 10 minutes and then clarified for 5 minutes by centrifugation at 12,800x g. Proteins were resolved on 4-12% or 8-16% SDS-PAGE gels, transferred to nitrocellulose, and immunoblotted with anti-GFP antibodies (Abcam) or anti-HA antibodies (Sigma).

Sedimentation assays

Sedimentation assays were adapted from a previously described protocol (Theodoraki *et al.*, 2012). Cells were grown in liquid synthetic media with 3% raffinose to ~$1x10^7$ cells/ml. Galactose was added to 3% and the cells were incubated 2 hours thereafter. 5ml of cells were harvested and lysed in Lysis buffer (100 mM Tris pH7.5, 200mM NaCl, 1mM EDTA, 1mM DTT, 5% glycerol, and 0.1% Nonidet P40) + PMSF by vortexing 5 minutes at 4˚C with 100µl of 0.5mm acid-washed glass beads. To remove unlysed cells, lysates were centrifuged at 700x g for 1 minute at 4˚C. 50µl lysate, representing the “total

lysate", was removed and added to 50µl SUMEB. 100µL remaining lysate was centrifuged at 12,800x g for 15 minutes at 4˚C. 100µl supernatant, representing the "soluble fraction", was added to 100µl SUMEB. The pellet, representing the "insoluble fraction", was resuspended in 100µl Lysis buffer and 100µl SUMEB. All samples were incubated at 65˚C for 10 minutes and then clarified for 5 minutes by centrifugation at 12,800x g. Proteins were resolved on 8 or 16% SDS-PAGE gels, transferred to nitrocellulose, and immunoblotted with anti-GFP (Sigma) or anti-Gal4AD (GAD) antibodies (Millipore).

Microscopy

Cells were grown in 3% raffinose media to ~ $0.5x10^7$ cells/ml. Galactose was added to 3% and the cells incubated 6 hours. Cells were harvested, fixed in 4% paraformaldehyde in 0.1 M sucrose for 15 minutes, washed in wash buffer (1.2 M sorbitol, 0.4 M KPO_4), stained with DAPI for 10 minutes in wash buffer plus 2% Triton X-100, and washed two times in wash buffer. Cells were imaged on a Nikon Eclipse 90i with a 100X objective, filters for GFP (HC HiSN Zero Shift filter set with excitation wavelength (450–490 nm), dichroic mirror (495 nm), and emission filter (500–550 nm)) or DAPI (HC HiSN Zero Shift filter set with excitation wavelength (325-375 nm), dichroic mirror (400 nm), and emission filter (435-485 nm)), and a Photometrics Cool Snap HQ2 cooled CCD camera with NIS-Elements acquisition software.

Non-denaturing polyacrylamide gel electrophoresis

The soluble fractions generated from sedimentation assays, with or without SDS (final concentration of 2%) added to the loading buffer, were loaded onto 8-16% Tris-Glycine PAGE gels (Lonza Rockland Inc). Running buffer was 25mM Tris and 192mM glycine. Gels were run at 4ºC. Proteins were transferred to nitrocellulose and immnobotted with anti-GFP antibodies (Sigma).

Image processing

All western blots were scanned using an Epson Perfection V350 Photo scanner at 300 dpi. All images were processed with a Mac iMac or Pro computer (Apple) using Photoshop CS (Adobe) and quantified using ImageJ 1.36b.

REFERENCES

Alberts, S.M., Sonntag, C., Schafer, A., and Wolf, D.H. (2009). Ubx4 modulates cdc48 activity and influences degradation of misfolded proteins of the endoplasmic reticulum. J Biol Chem *284*, 16082-16089.

Baek, G.H., Cheng, H., Kim, I., and Rao, H. (2012). The cdc48 protein and its cofactor vms1 are involved in cdc13 protein degradation. J Biol Chem *287*, 26788-26795.

Ballinger, C.A., Connell, P., Wu, Y., Hu, Z., Thompson, L.J., Yin, L.Y., and Patterson, C. (1999). Identification of CHIP, a novel tetratricopeptide repeat-containing protein that interacts with heat shock proteins and negatively regulates chaperone functions. Mol Cell Biol *19*, 4535-4545.

Bays, N.W., Wilhovsky, S.K., Goradia, A., Hodgkiss-Harlow, K., and Hampton, R.Y. (2001). HRD4/NPL4 is required for the proteasomal processing of ubiquitinated ER proteins. Mol Biol Cell *12*, 4114-4128.

Brachmann, C.B., Davies, A., Cost, G.J., Caputo, E., Li, J., Hieter, P., and Boeke, J.D. (1998). Designer deletion strains derived from Saccharomyces cerevisiae S288C: a useful set of strains and plasmids for PCR-mediated gene disruption and other applications. Yeast *14*, 115-132.

Braun, S., Matuschewski, K., Rape, M., Thoms, S., and Jentsch, S. (2002). Role of the ubiquitin-selective CDC48(UFD1/NPL4)chaperone (segregase) in ERAD of OLE1 and other substrates. EMBO J *21*, 615-621.

Brodsky, J.L., Werner, E.D., Dubas, M.E., Goeckeler, J.L., Kruse, K.B., and McCracken, A.A. (1999). The requirement for molecular chaperones during endoplasmic reticulum-associated protein degradation demonstrates that protein export and import are mechanistically distinct. J Biol Chem *274*, 3453-3460.

Cashikar, A.G., Duennwald, M., and Lindquist, S.L. (2005). A chaperone pathway in protein disaggregation. Hsp26 alters the nature of protein aggregates to facilitate reactivation by Hsp104. J Biol Chem *280*, 23869-23875.

D'Angelo, M.A., Raices, M., Panowski, S.H., and Hetzer, M.W. (2009). Age-dependent deterioration of nuclear pore complexes causes a loss of nuclear integrity in postmitotic cells. Cell *136*, 284-295.

Dantuma, N.P., and Hoppe, T. (2012). Growing sphere of influence: Cdc48/p97 orchestrates ubiquitin-dependent extraction from chromatin. Trends Cell Biol *22*, 483-491.

DeHoratius, C., and Silver, P.A. (1996). Nuclear transport defects and nuclear envelope alterations are associated with mutation of the Saccharomyces cerevisiae NPL4 gene. Mol Biol Cell *7*, 1835-1855.

Denic, V., Quan, E.M., and Weissman, J.S. (2006). A luminal surveillance complex that selects misfolded glycoproteins for ER-associated degradation. Cell *126*, 349-359.

Dittmer, T.A., and Misteli, T. (2011). The lamin protein family. Genome Biol *12*, 222.

Duennwald, M.L., Echeverria, A., and Shorter, J. (2012). Small heat shock proteins potentiate amyloid dissolution by protein disaggregases from yeast and humans. PLoS Biol *10*, e1001346.

Dyson, H.J., and Wright, P.E. (2005). Intrinsically unstructured proteins and their functions. Nat Rev Mol Cell Biol *6*, 197-208.

Eisele, F., and Wolf, D.H. (2008). Degradation of misfolded protein in the cytoplasm is mediated by the ubiquitin ligase Ubr1. FEBS Lett *582*, 4143-4146.

Elkabetz, Y., Shapira, I., Rabinovich, E., and Bar-Nun, S. (2004). Distinct steps in dislocation of luminal endoplasmic reticulum-associated degradation substrates: roles of endoplamic reticulum-bound p97/Cdc48p and proteasome. J Biol Chem *279*, 3980-3989.

Evans, D.R., Brewster, N.K., Xu, Q., Rowley, A., Altheim, B.A., Johnston, G.C., and Singer, R.A. (1998). The yeast protein complex containing cdc68 and pob3 mediates core-promoter repression through the cdc68 N-terminal domain. Genetics *150*, 1393-1405.

Finley, D., Ulrich, H.D., Sommer, T., and Kaiser, P. (2012). The ubiquitin-proteasome system of Saccharomyces cerevisiae. Genetics *192*, 319-360.

Franz, A., Orth, M., Pirson, P.A., Sonneville, R., Blow, J.J., Gartner, A., Stemmann, O., and Hoppe, T. (2011). CDC-48/p97 coordinates CDT-1 degradation with GINS chromatin dissociation to ensure faithful DNA replication. Mol Cell *44*, 85-96.

Fredrickson, E.K., Gallagher, P.S., Clowes Candadai, S.V., and Gardner, R.G. (2013). Substrate recognition in nuclear protein quality control degradation is governed by exposed hydrophobicity that correlates with aggregation and insolubility. J Biol Chem *288*, 6130-6139.

Fredrickson, E.K., Rosenbaum, J.C., Locke, M.N., Milac, T.I., and Gardner, R.G. (2011). Exposed hydrophobicity is a key determinant of nuclear quality control degradation. Mol Biol Cell *22*, 2384-2395.

Frohlich, K.U., Fries, H.W., Rudiger, M., Erdmann, R., Botstein, D., and Mecke, D. (1991). Yeast cell cycle protein CDC48p shows full-length homology to the mammalian protein VCP and is a member of a protein family involved in secretion, peroxisome formation, and gene expression. J Cell Biol *114*, 443-453.

Gall, J.G., Bellini, M., Wu, Z., and Murphy, C. (1999). Assembly of the nuclear transcription and processing machinery: Cajal bodies (coiled bodies) and transcriptosomes. Mol Biol Cell *10*, 4385-4402.

Gardner, R.G., Nelson, Z.W., and Gottschling, D.E. (2005). Degradation-mediated protein quality control in the nucleus. Cell *120*, 803-815.

Gasch, A.P., Spellman, P.T., Kao, C.M., Carmel-Harel, O., Eisen, M.B., Storz, G., Botstein, D., and Brown, P.O. (2000). Genomic expression programs in the response of yeast cells to environmental changes. Mol Biol Cell *11*, 4241-4257.

Glickman, M.H., and Ciechanover, A. (2002). The ubiquitin-proteasome proteolytic pathway: destruction for the sake of construction. Physiol Rev *82*, 373-428.

Glover, J.R., and Lindquist, S. (1998). Hsp104, Hsp70, and Hsp40: a novel chaperone system that rescues previously aggregated proteins. Cell *94*, 73-82.

Goldberg, A.L. (2003). Protein degradation and protection against misfolded or damaged proteins. Nature *426*, 895-899.

Goldstein, G., Scheid, M., Hammerling, U., Schlesinger, D.H., Niall, H.D., and Boyse, E.A. (1975). Isolation of a polypeptide that has lymphocyte-differentiating properties and is probably represented universally in living cells. Proc Natl Acad Sci U S A *72*, 11-15.

Guerriero, C.J., Weiberth, K.F., and Brodsky, J.L. (2013). Hsp70 Targets a Cytoplasmic Quality Control Substrate to the San1p Ubiquitin Ligase. Journal of Biological Chemistry *in press*.

Guthrie, C., and Fink, G.R. (1991). Guide to yeast genetics and molecular biology. Methods Enzymol *194*, 1-863.

Hampton, R.Y. (2002). ER-associated degradation in protein quality control and cellular regulation. Curr Opin Cell Biol *14*, 476-482.

Haslbeck, M., Braun, N., Stromer, T., Richter, B., Model, N., Weinkauf, S., and Buchner, J. (2004). Hsp42 is the general small heat shock protein in the cytosol of Saccharomyces cerevisiae. EMBO J *23*, 638-649.

Haslbeck, M., Miess, A., Stromer, T., Walter, S., and Buchner, J. (2005). Disassembling protein aggregates in the yeast cytosol. The cooperation of Hsp26 with Ssa1 and Hsp104. J Biol Chem *280*, 23861-23868.

Heck, J.W., Cheung, S.K., and Hampton, R.Y. (2010). Cytoplasmic protein quality control degradation mediated by parallel actions of the E3 ubiquitin ligases Ubr1 and San1. Proc Natl Acad Sci U S A *107*, 1106-1111.

Heo, J.M., Livnat-Levanon, N., Taylor, E.B., Jones, K.T., Dephoure, N., Ring, J., Xie, J., Brodsky, J.L., Madeo, F., Gygi, S.P.*, et al.* (2010). A stress-responsive system for mitochondrial protein degradation. Mol Cell *40*, 465-480.

Hirabayashi, M., Inoue, K., Tanaka, K., Nakadate, K., Ohsawa, Y., Kamei, Y., Popiel, A.H., Sinohara, A., Iwamatsu, A., Kimura, Y.*, et al.* (2001). VCP/p97 in abnormal protein aggregates, cytoplasmic vacuoles, and cell death, phenotypes relevant to neurodegeneration. Cell Death Differ *8*, 977-984.

Holmberg, C.I., Staniszewski, K.E., Mensah, K.N., Matouschek, A., and Morimoto, R.I. (2004). Inefficient degradation of truncated polyglutamine proteins by the proteasome. EMBO J *23*, 4307-4318.

Hubbers, C.U., Clemen, C.S., Kesper, K., Boddrich, A., Hofmann, A., Kamarainen, O., Tolksdorf, K., Stumpf, M., Reichelt, J., Roth, U.*, et al.* (2007). Pathological consequences of VCP mutations on human striated muscle. Brain *130*, 381-393.

Huyer, G., Piluek, W.F., Fansler, Z., Kreft, S.G., Hochstrasser, M., Brodsky, J.L., and Michaelis, S. (2004). Distinct machinery is required in Saccharomyces cerevisiae for the endoplasmic reticulum-associated degradation of a multispanning membrane protein and a soluble luminal protein. J Biol Chem *279*, 38369-38378.

Ishigaki, S., Hishikawa, N., Niwa, J., Iemura, S., Natsume, T., Hori, S., Kakizuka, A., Tanaka, K., and Sobue, G. (2004). Physical and functional interaction between Dorfin and Valosin-containing protein that are colocalized in ubiquitylated inclusions in neurodegenerative disorders. J Biol Chem *279*, 51376-51385.

Janiesch, P.C., Kim, J., Mouysset, J., Barikbin, R., Lochmuller, H., Cassata, G., Krause, S., and Hoppe, T. (2007). The ubiquitin-selective chaperone CDC-48/p97 links myosin assembly to human myopathy. Nat Cell Biol *9*, 379-390.

Jarosch, E., Taxis, C., Volkwein, C., Bordallo, J., Finley, D., Wolf, D.H., and Sommer, T. (2002). Protein dislocation from the ER requires polyubiquitination and the AAA-ATPase Cdc48. Nat Cell Biol *4*, 134-139.

Jentsch, S., and Rumpf, S. (2007). Cdc48 (p97): a "molecular gearbox" in the ubiquitin pathway? Trends Biochem Sci *32*, 6-11.

Jiang, J., Ballinger, C.A., Wu, Y., Dai, Q., Cyr, D.M., Hohfeld, J., and Patterson, C. (2001). CHIP is a U-box-dependent E3 ubiquitin ligase: identification of Hsc70 as a target for ubiquitylation. J Biol Chem *276*, 42938-42944.

Johnson, E.S., Ma, P.C., Ota, I.M., and Varshavsky, A. (1995). A proteolytic pathway that recognizes ubiquitin as a degradation signal. J Biol Chem *270*, 17442-17456.

Johnson, J.O., Mandrioli, J., Benatar, M., Abramzon, Y., Van Deerlin, V.M., Trojanowski, J.Q., Gibbs, J.R., Brunetti, M., Gronka, S., Wuu, J.*, et al.* (2010). Exome sequencing reveals VCP mutations as a cause of familial ALS. Neuron *68*, 857-864.

Ju, J.S., Miller, S.E., Hanson, P.I., and Weihl, C.C. (2008). Impaired protein aggregate handling and clearance underlie the pathogenesis of p97/VCP-associated disease. J Biol Chem *283*, 30289-30299.

Jung, C.H., Na, Y.R., and Im, H. (2004). Retarded protein folding of deficient human alpha 1-antitrypsin D256V and L41P variants. Protein Sci *13*, 694-702.

Kobayashi, T., Manno, A., and Kakizuka, A. (2007). Involvement of valosin-containing protein (VCP)/p97 in the formation and clearance of abnormal protein aggregates. Genes Cells *12*, 889-901.

Kryndushkin, D.S., Alexandrov, I.M., Ter-Avanesyan, M.D., and Kushnirov, V.V. (2003). Yeast [PSI+] prion aggregates are formed by small Sup35 polymers fragmented by Hsp104. J Biol Chem *278*, 49636-49643.

Lague, M.N., Romieu-Mourez, R., Bonneil, E., Boyer, A., Pouletty, N., Mes-Masson, A.M., Thibault, P., Nadeau, M.E., and Boerboom, D. (2012). Proteomic Profiling of a Mouse Model for Ovarian Granulosa Cell Tumor Identifies VCP as a Highly Sensitive Serum Tumor Marker in Several Human Cancers. PLoS One *7*, e42470.

Lefebvre, B.G., Comolli, N.K., Gage, M.J., and Robinson, A.S. (2004). Pressure dissociation studies provide insight into oligomerization competence of temperature-sensitive folding mutants of P22 tailspike. Protein Sci *13*, 1538-1546.

Lindquist, S., and Kim, G. (1996). Heat-shock protein 104 expression is sufficient for thermotolerance in yeast. Proc Natl Acad Sci U S A *93*, 5301-5306.

Matsumoto, M.L., Wickliffe, K.E., Dong, K.C., Yu, C., Bosanac, I., Bustos, D., Phu, L., Kirkpatrick, D.S., Hymowitz, S.G., Rape, M.*, et al.* (2010). K11-linked polyubiquitination in cell cycle control revealed by a K11 linkage-specific antibody. Mol Cell *39*, 477-484.

McClellan, A.J., Scott, M.D., and Frydman, J. (2005). Folding and quality control of the VHL tumor suppressor proceed through distinct chaperone pathways. Cell *121*, 739-748.

Meerang, M., Ritz, D., Paliwal, S., Garajova, Z., Bosshard, M., Mailand, N., Janscak, P., Hubscher, U., Meyer, H., and Ramadan, K. (2011). The ubiquitin-selective segregase VCP/p97 orchestrates the response to DNA double-strand breaks. Nat Cell Biol *13*, 1376-1382.

Metzger, M.B., Maurer, M.J., Dancy, B.M., and Michaelis, S. (2008). Degradation of a cytosolic protein requires endoplasmic reticulum-associated degradation machinery. J Biol Chem *283*, 32302-32316.

Meyer, H., Bug, M., and Bremer, S. (2012). Emerging functions of the VCP/p97 AAA-ATPase in the ubiquitin system. Nat Cell Biol *14*, 117-123.

Mizuno, Y., Hori, S., Kakizuka, A., and Okamoto, K. (2003). Vacuole-creating protein in neurodegenerative diseases in humans. Neurosci Lett *343*, 77-80.

Moir, D., Stewart, S.E., Osmond, B.C., and Botstein, D. (1982). Cold-sensitive cell-division-cycle mutants of yeast: isolation, properties, and pseudoreversion studies. Genetics *100*, 547-563.

Murata, S., Minami, Y., Minami, M., Chiba, T., and Tanaka, K. (2001). CHIP is a chaperone-dependent E3 ligase that ubiquitylates unfolded protein. EMBO Rep *2*, 1133-1138.

Nakatsukasa, K., Huyer, G., Michaelis, S., and Brodsky, J.L. (2008). Dissecting the ER-associated degradation of a misfolded polytopic membrane protein. Cell *132*, 101-112.

Nalbandian, A., Donkervoort, S., Dec, E., Badadani, M., Katheria, V., Rana, P., Nguyen, C., Mukherjee, J., Caiozzo, V., Martin, B.*, et al.* (2012). The multiple faces of valosin-containing protein-associated diseases: inclusion body myopathy with Paget's disease of bone, frontotemporal dementia, and amyotrophic lateral sclerosis. J Mol Neurosci *45*, 522-531.

Neuber, O., Jarosch, E., Volkwein, C., Walter, J., and Sommer, T. (2005). Ubx2 links the Cdc48 complex to ER-associated protein degradation. Nat Cell Biol *7*, 993-998.

Newnam, G.P., Wegrzyn, R.D., Lindquist, S.L., and Chernoff, Y.O. (1999). Antagonistic interactions between yeast chaperones Hsp104 and Hsp70 in prion curing. Mol Cell Biol *19*, 1325-1333.

Nillegoda, N.B., Theodoraki, M.A., Mandal, A.K., Mayo, K.J., Ren, H.Y., Sultana, R., Wu, K., Johnson, J., Cyr, D.M., and Caplan, A.J. (2010). Ubr1 and Ubr2 Function in a Quality Control Pathway for Degradation of Unfolded Cytosolic Proteins. Mol Biol Cell *21*, 2102-2116.

Nishikawa, S.I., Fewell, S.W., Kato, Y., Brodsky, J.L., and Endo, T. (2001). Molecular chaperones in the yeast endoplasmic reticulum maintain the solubility of proteins for retrotranslocation and degradation. J Cell Biol *153*, 1061-1070.

Nugent, C.I., Hughes, T.R., Lue, N.F., and Lundblad, V. (1996). Cdc13p: a single-strand telomeric DNA-binding protein with a dual role in yeast telomere maintenance. Science *274*, 249-252.

Park, S.H., Bolender, N., Eisele, F., Kostova, Z., Takeuchi, J., Coffino, P., and Wolf, D.H. (2007). The cytoplasmic Hsp70 chaperone machinery subjects misfolded and endoplasmic reticulum import-incompetent proteins to degradation via the ubiquitin-proteasome system. Mol Biol Cell *18*, 153-165.

Prasad, R., Kawaguchi, S., and Ng, D.T. (2010). A nucleus-based quality control mechanism for cytosolic proteins. Mol Biol Cell *21*, 2117-2127.

Prasad, R., Kawaguchi, S., and Ng, D.T. (2012). Biosynthetic mode can determine the mechanism of protein quality control. Biochem Biophys Res Commun *425*, 689-695.

Rabinovich, E., Kerem, A., Frohlich, K.U., Diamant, N., and Bar-Nun, S. (2002). AAA-ATPase p97/Cdc48p, a cytosolic chaperone required for endoplasmic reticulum-associated protein degradation. Mol Cell Biol *22*, 626-634.

Ravid, T., Kreft, S.G., and Hochstrasser, M. (2006). Membrane and soluble substrates of the Doa10 ubiquitin ligase are degraded by distinct pathways. EMBO J *25*, 533-543.

Richly, H., Rape, M., Braun, S., Rumpf, S., Hoege, C., and Jentsch, S. (2005). A series of ubiquitin binding factors connects CDC48/p97 to substrate multiubiquitylation and proteasomal targeting. Cell *120*, 73-84.

Rosenbaum, J.C., Fredrickson, E.K., Oeser, M.L., Garrett-Engele, C.M., Locke, M.N., Richardson, L.A., Nelson, Z.W., Hetrick, E.D., Milac, T.I., Gottschling, D.E., and Gardner, R.G. (2011). Disorder targets misorder in nuclear quality control degradation: a disordered ubiquitin ligase directly recognizes its misfolded substrates. Mol Cell *41*, 93-106.

Rossi, J.M., and Lindquist, S. (1989). The intracellular location of yeast heat-shock protein 26 varies with metabolism. J Cell Biol *108*, 425-439.

Santner, A.A., Croy, C.H., Vasanwala, F.H., Uversky, V.N., Van, Y.Y., and Dunker, A.K. (2012). Sweeping away protein aggregation with entropic bristles: intrinsically disordered protein fusions enhance soluble expression. Biochemistry *51*, 7250-7262.

Schnell, R., D'Ari, L., Foss, M., Goodman, D., and Rine, J. (1989). Genetic and molecular characterization of suppressors of SIR4 mutations in Saccharomyces cerevisiae. Genetics *122*, 29-46.

Schubert, U., Antón, L.C., Gibbs, J., Norbury, C.C., Yewdell, J.W., and Bennink, J.R. (2000). Rapid degradation of a large fraction of newly synthesized proteins by proteasomes [see comments]. Nature *404*, 770-774.

Schuberth, C., and Buchberger, A. (2005). Membrane-bound Ubx2 recruits Cdc48 to ubiquitin ligases and their substrates to ensure efficient ER-associated protein degradation. Nat Cell Biol *7*, 999-1006.

Schuberth, C., and Buchberger, A. (2008). UBX domain proteins: major regulators of the AAA ATPase Cdc48/p97. Cell Mol Life Sci *65*, 2360-2371.

Schuberth, C., Richly, H., Rumpf, S., and Buchberger, A. (2004). Shp1 and Ubx2 are adaptors of Cdc48 involved in ubiquitin-dependent protein degradation. EMBO Rep *5*, 818-824.

Shulga, N., and Goldfarb, D.S. (2003). Binding dynamics of structural nucleoporins govern nuclear pore complex permeability and may mediate channel gating. Mol Cell Biol *23*, 534-542.

Shulga, N., Mosammaparast, N., Wozniak, R., and Goldfarb, D.S. (2000). Yeast nucleoporins involved in passive nuclear envelope permeability. J Cell Biol *149*, 1027-1038.

Snyder, H., Mensah, K., Theisler, C., Lee, J., Matouschek, A., and Wolozin, B. (2003). Aggregated and monomeric alpha-synuclein bind to the S6' proteasomal protein and inhibit proteasomal function. J Biol Chem *278*, 11753-11759.

Song, C., Wang, Q., and Li, C.C. (2007). Characterization of the aggregation-prevention activity of p97/valosin-containing protein. Biochemistry *46*, 14889-14898.

Spence, J., Sadis, S., Haas, A.L., and Finley, D. (1995). A ubiquitin mutant with specific defects in DNA repair and multiubiquitination. Mol Cell Biol *15*, 1265-1273.

Stirling, P.C., Lundin, V.F., and Leroux, M.R. (2003). Getting a grip on non-native proteins. EMBO Rep *4*, 565-570.

Taxis, C., Hitt, R., Park, S.H., Deak, P.M., Kostova, Z., and Wolf, D.H. (2003). Use of modular substrates demonstrates mechanistic diversity and reveals differences in chaperone requirement of ERAD. J Biol Chem *278*, 35903-35913.

Taylor, E.B., and Rutter, J. (2011). Mitochondrial quality control by the ubiquitin-proteasome system. Biochem Soc Trans *39*, 1509-1513.

Theodoraki, M.A., Nillegoda, N.B., Saini, J., and Caplan, A.J. (2012). A network of ubiquitin ligases is important for the dynamics of misfolded protein aggregates in yeast. J Biol Chem *287*, 23911-23922.

Thrower, J.S., Hoffman, L., Rechsteiner, M., and Pickart, C.M. (2000). Recognition of the polyubiquitin proteolytic signal. EMBO J *19*, 94-102.

Tompa, P. (2002). Intrinsically unstructured proteins. Trends Biochem Sci *27*, 527-533.

Verhoef, L.G., Lindsten, K., Masucci, M.G., and Dantuma, N.P. (2002). Aggregate formation inhibits proteasomal degradation of polyglutamine proteins. Hum Mol Genet *11*, 2689-2700.

Verma, R., Oania, R., Fang, R., Smith, G.T., and Deshaies, R.J. (2011). Cdc48/p97 mediates UV-dependent turnover of RNA Pol II. Mol Cell *41*, 82-92.

Waldo, G.S., Standish, B.M., Berendzen, J., and Terwilliger, T.C. (1999). Rapid protein-folding assay using green fluorescent protein. Nat Biotechnol *17*, 691-695.

Walter, G.M., Smith, M.C., Wisen, S., Basrur, V., Elenitoba-Johnson, K.S., Duennwald, M.L., Kumar, A., and Gestwicki, J.E. (2011). Ordered assembly of heat shock proteins, Hsp26, Hsp70, Hsp90, and Hsp104, on expanded polyglutamine fragments revealed by chemical probes. J Biol Chem *286*, 40486-40493.

Wang, S.S., Wu, J.W., Yamamoto, S., and Liu, H.S. (2008). Diseases of protein aggregation and the hunt for potential pharmacological agents. Biotechnol J *3*, 165-192.

Watts, G.D., Wymer, J., Kovach, M.J., Mehta, S.G., Mumm, S., Darvish, D., Pestronk, A., Whyte, M.P., and Kimonis, V.E. (2004). Inclusion body myopathy associated with Paget disease of bone and frontotemporal dementia is caused by mutant valosin-containing protein. Nat Genet *36*, 377-381.

Weihl, C.C., Dalal, S., Pestronk, A., and Hanson, P.I. (2006). Inclusion body myopathy-associated mutations in p97/VCP impair endoplasmic reticulum-associated degradation. Hum Mol Genet *15*, 189-199.

Weihl, C.C., Miller, S.E., Hanson, P.I., and Pestronk, A. (2007). Transgenic expression of inclusion body myopathy associated mutant p97/VCP causes

weakness and ubiquitinated protein inclusions in mice. Hum Mol Genet *16*, 919-928.

Wilcox, A.J., and Laney, J.D. (2009). A ubiquitin-selective AAA-ATPase mediates transcriptional switching by remodelling a repressor-promoter DNA complex. Nat Cell Biol *11*, 1481-1486.

Wojcik, C., and DeMartino, G.N. (2003). Intracellular localization of proteasomes. Int J Biochem Cell Biol *35*, 579-589.

Wolf, D.H., and Stolz, A. (2012). The Cdc48 machine in endoplasmic reticulum associated protein degradation. Biochim Biophys Acta *1823*, 117-124.

Woulfe, J.M. (2007). Abnormalities of the nucleus and nuclear inclusions in neurodegenerative disease: a work in progress. Neuropathol Appl Neurobiol *33*, 2-42.

Xie, K., Lambie, E.J., and Snyder, M. (1993). Nuclear dot antigens may specify transcriptional domains in the nucleus. Mol Cell Biol *13*, 6170-6179.

Xu, Q., Johnston, G.C., and Singer, R.A. (1993). The Saccharomyces cerevisiae Cdc68 transcription activator is antagonized by San1, a protein implicated in transcriptional silencing. Mol Cell Biol *13*, 7553-7565.

Yamamoto, S., Tomita, Y., Hoshida, Y., Sakon, M., Kameyama, M., Imaoka, S., Sekimoto, M., Nakamori, S., Monden, M., and Aozasa, K. (2004). Expression of valosin-containing protein in colorectal carcinomas as a predictor for disease recurrence and prognosis. Clin Cancer Res *10*, 651-657.

Yamamoto, S., Tomita, Y., Uruno, T., Hoshida, Y., Qiu, Y., Iizuka, N., Nakamichi, I., Miyauchi, A., and Aozasa, K. (2005). Increased expression of valosin-containing protein (p97) is correlated with disease recurrence in follicular thyroid cancer. Ann Surg Oncol *12*, 925-934.

Yamanaka, K., Sasagawa, Y., and Ogura, T. (2012). Recent advances in p97/VCP/Cdc48 cellular functions. Biochim Biophys Acta *1823*, 130-137.

Ye, Y. (2006). Diverse functions with a common regulator: ubiquitin takes command of an AAA ATPase. J Struct Biol *156*, 29-40.

Ye, Y., Meyer, H.H., and Rapoport, T.A. (2001). The AAA ATPase Cdc48/p97 and its partners transport proteins from the ER into the cytosol. Nature *414*, 652-656.

Yeung, H.O., Kloppsteck, P., Niwa, H., Isaacson, R.L., Matthews, S., Zhang, X., and Freemont, P.S. (2008). Insights into adaptor binding to the AAA protein p97. Biochem Soc Trans *36*, 62-67.

Zhao, Y., Abreu, E., Kim, J., Stadler, G., Eskiocak, U., Terns, M.P., Terns, R.M., Shay, J.W., and Wright, W.E. (2011). Processive and distributive extension of human telomeres by telomerase under homeostatic and nonequilibrium conditions. Mol Cell *42*, 297-307.

PAMELA S. GALLAGHER

University of Washington • Department of Pharmacology
1959 NE Pacific Street • Seattle, WA • 206.616.1976
pamelag3@u.washington.edu

EDUCATION

University of Washington, Seattle, WA, 2007- present
Doctoral candidate in Pharmacology

Northwestern University, Evanston, IL 2001-2005
B.A. in Psychology and Spanish, June 2005

RESEARCH EXPERIENCE

Doctoral Research: Investigation of protein quality control degradation in the nucleus using *Saccharomyces cerevisiae*, Research advisor: Dr. Richard Gardner.

- Characterizing the role of Cdc48/p97 in regulating quality control degradation of misfolded proteins in the nucleus.
- Determining which cofactors are recruited to the Cdc48 complex to facilitate nuclear protein quality control degradation.

Laboratory rotations:

- Tested for the potential interaction between spinophilin and the α1A-adrenergic receptor, Advisor: Dr. Debra Schwinn.
- Characterized binding and cell migration properties of a novel WIN-binding protein, Advisor: Dr. Nephi Stella.

NIH Postbaccalaureate Intramural Research: National Institute of Mental Health, Bethesda, MD, 2005-2006, Advisor: Dr. Dennis Murphy.

- Characterized behavioral phenotype of the serotonin transporter knockout mouse.
- Studied molecular genetics of the serotonin transporter and its association with obsessive-compulsive disorder.

Undergraduate Research: Northwestern University, Department of Cardiology, Chicago, IL, 2002-2004, Advisor: Dr. Nalini Rajamannan.

- Studied effects of atorvastatin on hypercholesterolemic aortic valves.

Research Internship: Mayo Clinic, Department of Biochemistry and Molecular Biology, Rochester, MN, Summer 2002, Advisor: Dr. Thomas Spelsberg

- Characterized transcriptional regulation of TIEG (TGFß inducible early gene) in development of breast cancer.

PUBLICATIONS

Gallagher PS and Gardner RG. A differential requirement for Cdc48/p97 in nuclear protein quality control degradation correlates with misfolded substrate insolubility. *Manuscript in preparation*.

Fredrickson EK, Clowes Candadai SV, **Gallagher PS**, Gardner RG. Chaperone involvement in nuclear protein quality control degradation depends upon the insolubility and mode of nuclear import of the misfolded substrate. *Manuscript in preparation.*

Fredrickson EK, **Gallagher PS**, Clowes Candadai SV, Gardner RG. Substrate recognition in nuclear protein quality control degradation is governed by exposed hydrophobicity that correlates with aggregation and insolubility. *J Biol Chem*. 2013 Jan 18.

Konopka CA, Locke MN, **Gallagher PS**, Pham N, Hart MP, Walker CJ, Gitler AD, Gardner RG. A yeast model for polyalanine-expansion aggregation and toxicity. *Mol Biol Cell.* 2011 Jun 15;22(12):1971-84.

Fox MA, Jensen CL, **Gallagher PS**, Murphy DL. Receptor mediation of exaggerated responses to serotonin-enhancing drugs in serotonin transporter (SERT)-deficient mice. *Neuropharmacology*. 53:643-56, 2007.

Kalueff AV, Fox MA, **Gallagher PS**, Murphy DL. Hypolocomotion, anxiety and serotonin syndrome-like behavior contribute to the complex phenotype of serotonin transporter knockout mice. *Genes, Brain, and Behavior*. 2007 Jun;6(4):389-400.

Allan V. Kalueff, **Pamela S. Gallagher**, Dennis L. Murphy. Are serotonin transporter knockout mice "depressed"? Hypoactivity but no anhedonia. *Neuroreport*. 2006 Aug 21;17(12):1347-51.

CONFERENCES

FASEB Summer research conference on "Ubiquitin and Cellular Regulation", Saxtons River, VT, 2012, Symposium speaker

Yeast Genetics and Molecular Biology Meeting, Vancouver, BC Canada, 2010

Society for Neuroscience, Washington, DC, 2005

TEACHING EXPERIENCE

Teaching Assistant, Pharmacology 401, 402, University of Washington, 2008-2009

- Planned and led weekly discussion/quiz sections

AWARDS/HONORS

NIH Postbaccalaureate Intramural Research Training Award, 2005-2006